Influence of altered gravity on the oxidative burst in macrophages

Dissertation

zur
Erlangung des Doktorgrades (Dr. rer. nat.)
der
Mathematisch-Naturwissenschaftlichen Fakultät
der
Rheinischen Friedrich-Wilhelms-Universität Bonn

Vorgelegt von
Sonja Brungs
aus
Köln

Bonn, September 2013

Angefertigt mit Genehmigung der Mathematisch-Naturwissenschaftlichen Fakultät der Rheinischen Friedrich-Wilhelms-Universität Bonn.

1. Gutachterin: PD Dr. Ruth Hemmersbach

2. Gutachter: Prof. Dr. Waldemar Kolanus

Tag der Promotion: 20.11.2013

Erscheinungsjahr: 2013

Erklärung

Diese Dissertation wurde im Sinne von § 4 der Promotionsordnung vom 03.06.2011 im Zeitraum April 2010 bis September 2013 von PD Dr. R. Hemmersbach und Prof. Dr. W. Kolanus und betreut.

Eidesstattliche Erklärung

Hiermit versichere ich, dass ich die vorliegende Arbeit ohne unzulässige Hilfe Dritter und ohne Benutzung anderer als der angegebenen Hilfsmittel angefertigt habe; die aus fremden Quellen direkt oder indirekt übernommenen Gedanken sind als solche kenntlich gemacht (gemäß § 6 der Promotionsordnung vom 03.06.2011).

Bonn, den

Sonja Brungs

Ein Teil der vorliegenden Arbeit wird in folgender Originalpublikation veröffentlicht:

Horn, A.; Huber, K. Sromicki, J.; **Brungs, S.**; Layer, L.; von der Wiesche, M..; Hock, B.; Kolanus, W.; Hemmersbach, R.; Ullrich, O.: The oxidative burst reaction in mammalian cells depends on gravity.

Wird in Kürze beim *Journal of Cell Communication and Signaling* eingereicht.

Weitere Publikationen und Preise

Zander, V.; Anken, R.; Pesquet, T.; **Brungs, S.**; Latsch, J. (2013): Short radius centrifuges – A new approach for life sciences experiments under hyper-g conditions for applications in space and beyond. *Recent Patents on Space Technology* 3 (1), 74-81

Brungs, S.; Hauslage, J.; Hilbig, R.; Hemmersbach, R. und Anken, R. (2011): Effects of simulated weightlessness on fish otolith growth: Clinostat versus Rotating-Wall Vessel. *Advances in Space Research* 48, 798-798

ISGP/ESA Young Researcher Award

Life in Space for Life on Earth Symposium Aberdeen, UK, 2012

Rainer-Kowoll-First-Presenter Preis

50. Jahrestagung Deutsche Gesellschaft für Luft- und Raumfahrtmedizin, Bonn, 2012

What we know is a drop. What we don't know is an ocean.

Isaac Newton

Contents

1 Introduction

1.1 Human health during spaceflight

Spaceflight is one of the most intriguing challenges of mankind. Life under these extreme conditions bears risks concerning health. Humans in space are exposed to the microgravity and radiation environment. There is also the hardship of confinement and psychological issues (fig. 1.1).

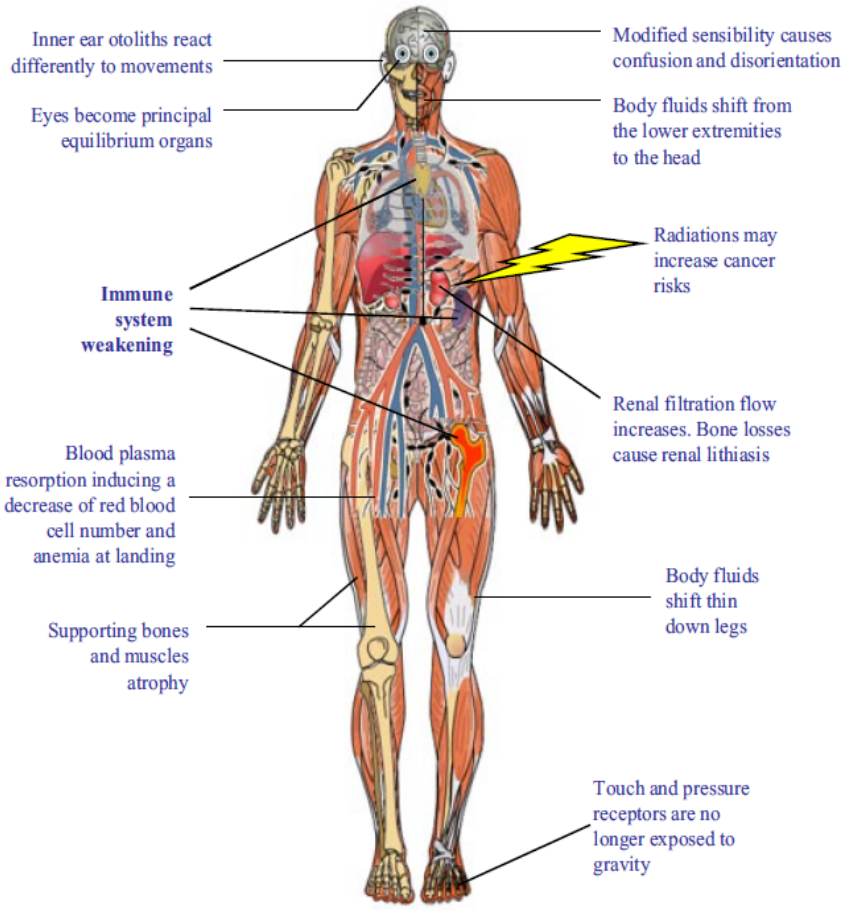

Figure 1.1: **Overview of the physiological problems during spaceflight.** From Gueguinou et al. (2009).

Since the first journeys to space, more than 50 years ago, there is increasing knowledge on the effects of space conditions on the human body (Gerzer et al. 2006).

Clément (2005) gives a good overview of the impact of spaceflight on the human physiology. The immune system is highly impaired during spaceflight. Astronauts suffer from various infectious diseases such as respiratory and urinary tract infections (Ullrich et al. 2011) and a higher susceptibility to the reactivation of persistent viruses e.g. herpes virus (Stowe et al. 2001). In addition, pathogens show a higher virulence when exposed to a microgravity environment. The likelihood of astronauts suffering from infections due to their impaired immune system and/or the increased virulence of microbes on board the International Space Station (ISS) (Nickerson et al. 2004) might be increased.

1.2 Graviperception in cells

The gravitational force of $9.81\mathrm{m/s^2}$ is the oldest environmental factor and life on earth has adapted perfectly to this nearly constant force. Plants as well as animals gain information regarding to their position *via* sensation of the gravitational force. This is especially important when animals make use of direct locomotion to maintain their equilibrium *via* postural control orientation (Anken & Rahmann 2002). Graviperception in animals, plants and cells is accomplished by passively moving mass in the gravitational field. Unicellular organisms like *Paramecium* respond to gravity *via* mechanical loading on the lower cell membrane resulting in an activation of mechanosensitive ion channels (Hemmersbach et al. 2001; Häder 1999), whereas *Loxodos* perceives gravity by displacing heavy bodies (statoliths) connected to force transducing molecules (e.g. cytoskeleton) (Fenchel & Finlay 1986).

However, it is not known if the mammalian cells respond to physical changes passively, or if they are able to actively "sense" gravity as it is well-known for unicellular organisms (Hemmersbach et al. 2001; Gerzer et al. 2006). It is assumed that mammalian cells do not have a gravisensing "body" like statoliths, but instead sense gravity by the whole cell mass. The "tensegrity" model of Ingber (1997b) describes the cell as a "tension-dependent form of architecture" which is highly capable of sensing mechanical stress (or load) *via* alterations in the cytoskeleton tension. The word *tensegrity* derives from *tensional integrity* and describes a form of architecture which remains stable due to the tension of its framework (fig. 1.2). The model of Ingber gives us an idea of how cells might sense gravity. Gravity sensing is not dependent on single molecules. In fact, changes in the tension of the cytoskeleton due to transmitting stress through focal adhesion and integrin signalling transmit extracellular forces to intracellular changes e.g in signalling (Ingber 1991; Alenghat & Ingber 2002; Ingber 1999, 1993). Mechanical stress can lead to changes in their cellular force balance and can, in turn, lead to intracellular biochemical changes, e.g. gen-expression.

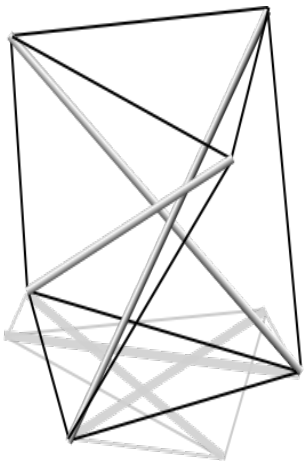

Figure 1.2: **A simple tensegrity exemplar (3-prism).** From wikipedia.

The existence of a form of force perception in cells is a matter of fact, since cells are able to adapt to altered force conditions, e.g. shear stress. Endothelial cells, for example, in the blood are subjected to shear forces *per se* and can respond to differences in occurring forces by modulating gen-expression for adhesion and growth (Chien et al. 1998; Davies 1995). Owan et al. (1997) have shown that bone cells (osteoblast) respond to mechanical loading, e.g. fluid forces by the production of osteopontin which is crucial for bone formation.

Integrins are adhesion molecules which integrate the extracellular matrix with the cytoskeleton of the cell, therefore transducing signals from outside of the cell and so transducing signals inside the cell (for reviews see Giancotti 1999; Gersuk et al. 2006). Furthermore, integrins are known to be involved in mechanotransduction of the cell. Focal adhesion sites or catherins and others, transmit extracellular stress into intracellular signalling response *via* their connection between the extracellular matrix and the actin cytoskeleton (for review see Ingber 1991). Adaptor proteins between integrins and cytoskeleton play a critical role in force transmittance to biochemical reactions. Thus the forces can stretch inactive enzymes, resulting in an active form of the enzyme (Ingber 2006). One example of a linker protein in leukocytes is the mammalian actin binding protein (mABP1) and it is therefore crucial for linking the β_2 integrins to cytoskeleton when shear forces occur (Schymeinsky et al. 2011). Furthermore, mABP1 is a target of the Src and Syk family kinases (Larbolette et al. 1999) and is therefore involved in phagocytosis and oxidative burst which will be introduced in section 1.5.

1.3 Research platforms to study the effects of microgravity

Several platforms are in worldwide use where the conditions of microgravity can be achieved. The ISS provides the ideal environment to study the effect of real microgravity on the hu-

man body as well as other model organisms. In addition, sounding rockets provide several minutes of real microgravity and satellites, e.g. Bion, even several weeks.

1.3.1 Parabolic flights

A parabolic flight provides an excellent platform in which to study real microgravity as well as hypergravity effects in a fast responding model systems since the changes in gravity are consecutive and very rapid. The aircraft A300 zero-g of Novespace (France) flies parabola manoeuvres to achieve a microgravity environment for 22 seconds. Before and after each microgravity phase, a hypergravity phase of 1.8g for 20 seconds takes place (compare fig. 1.3).

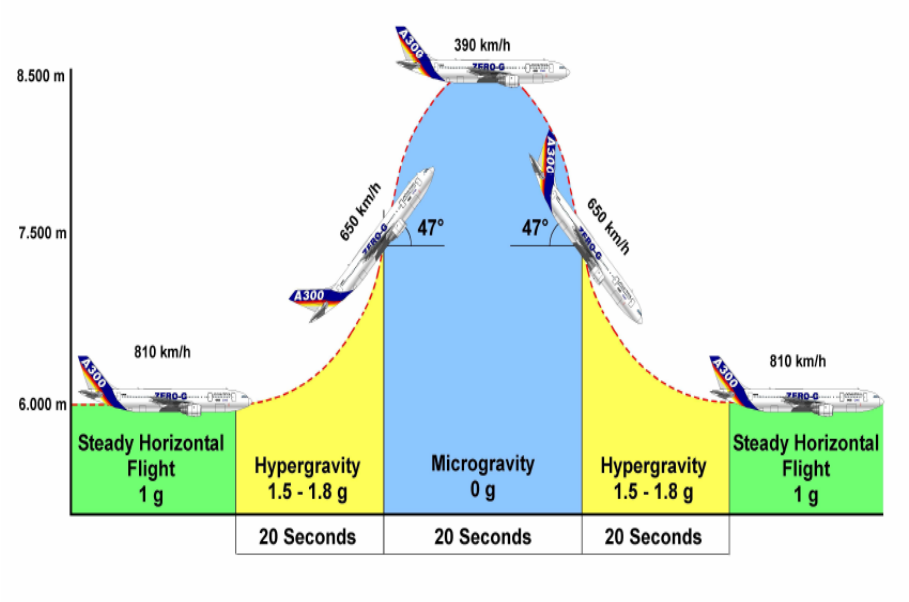

Figure 1.3: **Flight profile of a single parabola manoeuvre.** From www.spaceflight.esa.int.

To achieve this, the aircraft is subjected to a parabola. First, with full thrust in a 47° angle in an upward direction and an increased gravity of 1.8g for 20 seconds. Then, the thrust is reduced to a minimum, where it equals the aerodynamic resistance. The reduction of the jet engine induces the phase of free fall (microgravity). During this phase, the acceleration is reduced to 0.03g and results in a microgravity environment for experiments and passengers on board. After 22 seconds the engine power is increased to start the second 1.8g phase and to redirect the aircraft in the horizontal direction.

CNES, DLR and ESA arrange 6-8 campaigns a year and these consists of 3 flight days with 31 parabolas each, resulting in total 34 minutes of real microgravity per campaign.

Since the flight opportunities are rare and very expensive, many ground-based platforms have gained popularity.

1.3.2 Microgravity simulators

Numerous simulators are used to expose plants, unicellular organisms, aquatic animals and mammalian cells to microgravity. Herranz et al. (2013) have reviewed the terminology and properties of several ground-based facilities used for microgravity simulations. In my study, so-called **Clinostats** are used to simulate the conditions of microgravity in the laboratory. These experimental platforms enable the installation of a sample cuvette with a small diameter (less than 4mm) which is rotated along its horizontal axis with a speed of 60rpm. Within this cuvette, only small centrifugal forces are occurring which nullify the occurring sedimentation force. Cells or small organisms exposed in the Clinostat cuvette will describe small circular paths on which they are "weightless" (compare fig. 1.4). Gravity is still present but, as the cuvette is constantly rotated, the gravity vector is constantly averaged. Therefore, it is assumed that gravity sensing by the organism is abolished similiar to under real microgravity conditions.

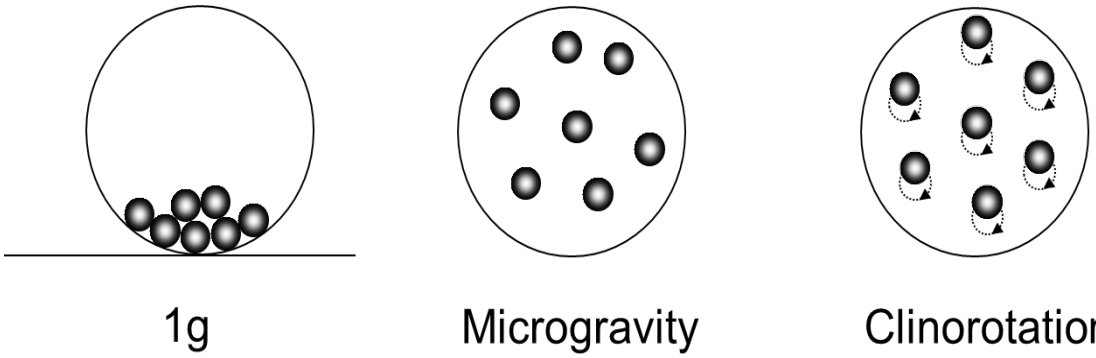

Figure 1.4: **Clinostat principle.**
Cells (in fluid) within the Clinostat cuvette will always sediment under 1g conditions (left). Under real microgravity conditions, the cells will be evenly distributed and weightless (middle). This condition is simulated during clinorotation: Cells are forced to circular paths due to rotation of the cuvette (right). This condition simulates weightlessness as in real microgravity.

1.4 Impaired immunity during spaceflight on the cellular level

Until recently, it had been assumed that a change in immunity derives from psychological stress of the astronauts, rather than space conditions. Nevertheless, immune deficiency can also be observed at the cellular level. Cogoli (1993) had investigated the influence of altered gravity on lymphocytes and showed that T cells respond to diminished gravity (microgravity) with impaired proliferation (upon Con A stimulation). For instance, the adaptive immune and the innate immunity systems display also major injury:

- altered cytokine production in monocytes (Crucian et al. 2011; Kaur et al. 2008) and T cells (Crucian et al. 2008)

- loss of locomotion capability in lymphocytes and monocytes (Sundaresan et al. 2002; Meloni et al. 2006)
- changes in mitogen-activated protein (MAP) kinase and NF-κB signalling in T cells (Paulsen et al. 2010; Ullrich et al. 2008; Wise et al. 2005)
- increased apoptosis in T cells and osteoblasts (Lewis et al. 1998; Schatten et al. 2001; Sarkar et al. 2000)
- reduced tyrosine-phosphorylation in monocytes (Paulsen et al. 2010)

Numerous studies have investigated the effects of microgravity on the cytoskeleton of cells: Schatten et al. (2001), reported an altered microtubule network and several other investigators have reported that the actin cytoskeleton is highly affected by gravity simulators which were used to study the changes in the cytoskeleton (Meloni et al. 2006; Vassy et al. 2003; Papaseit et al. 2000; Buravkova & Romanov 2001). These results demonstrate that the cytoskeleton is greatly influenced by the lack of gravity even within seconds (Sciola et al. 1999) but also show a high adaptation capacity (Eiermann et al. 2013).

So far, several studies point to a high sensitivity of myeloid cells to microgravity. This cell type plays a critical role in the first-line of defence of the innate immune system. Neutrophils and monocytes of spaceflown astronauts display a reduced capability to phagocytise pathogens and to produce reactive oxygen species during oxidative burst (Kaur et al. 2004, 2008). This was assumed to be due to stress related to the duration of spaceflight. Horn (2011) and Huber (2007) were able to show that macrophages respond to microgravity with a reduction in ROS after stimulation with the yeast cell wall component zymosan. Rat macrophages increased their ROS production after zymosan stimulation in hypergravity ($1.8g$) as shown during parabolic flight and centrifugation (Horn 2011). The underlying mechanism to altered gravity remained to be elucidated. It is not clear on which level gravity influences the crucial features of macrophages that lead to the establishment of host-defence. It can be assumed that the failure in phagocytosis, as well as oxidative burst of macrophages, plays a critical role in the immune deficiencies observed in astronauts. The complex features in host-defence of myeloid cells will be described in detail in the following sections.

1.5 Features of the early innate immune response

1.5.1 Recognition of pathogenic patterns

Cells of the myeloid lineage respond mainly to the presence of pathogenic patterns like

fungi, bacteria and viruses as well as dead host cells, by recognition and removal of these. The pathogen-associated molecular patterns (PAMPs) of microbes are recognised by receptors on the cell surface of neutrophils and macrophages. There are a variety of cell surface receptor classes responding to pathogen patterns: Two different pattern recognition receptor types respond to molecular PAMPs: Toll-like receptors and C-Lectin type receptors which will be introduced below.

1.5.1.1 Toll-like receptors

The 11 Toll-like receptors (TLR) found in humans respond to mainly bacterial PAMPs, like lipopeptides, flagellin, lipoteichoic acid but also fungal mannans and viral envelope proteins (Abbas et al. 2010). TLR 4 responds to lipopolysaccharide (LPS) of Gram-negative bacteria. TLR 2 and 6 cooperate and recognise yeast cell walls (e.g. zymosan) (Medzhitov 2001; fig. 1.5). The PAMPs and TLR receptor engagement leads to the activation of TLR receptor adaptor proteins like TOLLIP (Toll-interacting protein), IRAK (IL-1R-associated kinase) and TRAF6 (TNF receptor-associated factor 6) (Medzhitov 2001). Nitric oxide and the activation of nuclear factor kappa B (NF-$\varkappa$B) are signalling steps activated by TLR receptor signalling (Abbas et al. 2010; Medzhitov 2001).

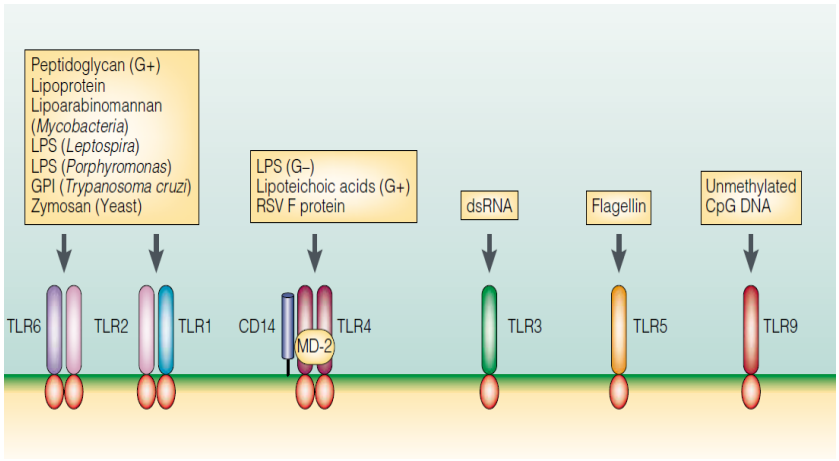

Figure 1.5: **Examples of Toll-like receptors and the corresponding stimuli.** From Medzhitov 2001.

1.5.1.2 Non-TLR pattern recognition receptors

Dectin-1 is not a TLR but is a C-Lectin types surface receptors in macrophages and neutrophils. It recognises β 1,3- and/or β 1,6-linked glucans (Brown & Gordon 2001) like the yeast cell wall component zymosan, alongwith curdlan, a β 1,3-glucan polymer from the bacterium *Alcaligenes faecalis*. Dectin-1 is a immunoreceptor tyrosine-based activation motif (ITAM) and its involvement activates the phosphorylation by Src kinase and docking of the spleen tyrosine kinase Syk. Syk induces ROS production (Underhill et al. 2005), the

activation of the caspase recruitment domain 9 (CARD9), and the assembly with bcl10 and malt1 complex (Gross et al. 2006), inducing the transcription factor NF-κB activation. TLR (Takada et al. 2003) and C-lectin type receptors (e.g. Dectin-1) (Brown & Gordon 2001; Brown et al. 2003; Gantner et al. 2003) bind to fungal surfaces e.g. *Candida albicans*. A yet undefined mechanism results in a cross-talk between both cell surface receptor types and finally an optimal chemokine and cytokine production upon tumor necrosis factor alpha (TNFα) stimulation (Gantner et al. 2003; Ferwerda et al. 2008; Dennehy et al. 2008).

Several **complement receptor** types have phagocytic properties since they serve as a pattern recognition receptor (PRR) recognising different complement factors which are evident in the blood serum and label fungal or bacterial components. Complement receptor 1 (CR1) or CD35 recognises mainly complement factors C3b, but also C4b and iC3b and β-glucan (Ross 1989). CR3 has dual functions as a PRR and a β_2 integrin also known as Mac-1 or CD11a/CD18. CR3 recognises iCb3 complement factor, β-glucans and lipopolysaccharide (Ross 1989) in its PRR function and enables adherence, migration and phagocytosis in leukocytes as an integrin (Ehlers 2000). A mutation in the β subunit leads to the so-called leukocyte adhesion deficiency disease, which is indicated with a loss of migration and disabled wound-healing capability, underlining the importance of the dual function of this receptor (Ehlers 2000).

The Fc parts of immunoglobulin A/G are recognised as a PAMP by a variety of **Fc receptors**. The immunoglobulins enhance the immune response by binding to foreign patterns like bacteria or fungi. Fcγ receptors recognise IgA immunoglobulins and this leads to the activation of kinases Src and the Syk *via* the linking ITAM (Ivashkiv 2009; Ravetch 1997). ITAM based immunoreceptors are also capable of cross-linking: Ivashkiv (2009) reviews the cross-talk of ITAM based receptors with TLR and integrin receptors (CR3; Ehlers 2000; Ortiz-Stern & Rosales 2003) which can dampen or augment each other in order to fine-tune the immune response.

1.5.1.3 Recognition of zymosan

Yeast (*Saccharomyces*) and *Candida* are fungi which are always present in the human body, but can be life-threatening pathogens if the immune system is impaired. To study the pathogen-phagocyte interaction *in vitro* and *in vivo,* zymosan has been widely used for more than 50 years (Underhill 2003; Brown & Gordon 2001). This yeast cell wall component consists of β 1,3-glucan linked to chitin and β 1,6-glucans (Smits et al. 1999), although it does not reflect the whole complexity of fungi (Brown 2005). Nevertheless, a variety of pattern recognition receptors (PRR) of the macrophages cell surface recognise the zymosan: Toll-like receptor (TLR) 2/6 complex, Dectin-1 as well as the complement receptor. Opsonisation of the zymosan particles can increase the number of recognition receptors. Opsonins, like antibodies and complement factors, are present in the blood and bind to different fungal and bacterial patterns. This labelling enables the recognition of the

complement receptor CR1 an CR3 and Fcγ receptors and can therefore induce a stronger immune response to pathogens.

1.5.2 Pattern recognition downstream signalling: activation of the spleen tyrosine kinase Syk

After pathogen-receptor binding, the pathogen is engulfed by the phagocytes, according to distinct activated pathways. Fig. 1.6 shows a simplified overview of the above described PRRs resulting in a recruitment of adapter proteins and Syk kinase as well as production of reactive oxygen species (ROS) in the phagosome upon pathogen stimulation. The 72kDa big spleen tyrosine kinase **Syk** is activated by adapter proteins of PRR on the cell surface by Src kinase and plays a crucial role in different biological functions (Mócsai et al. 2010). Syk is homolog to the ZAP-70 protein which is naturally found in T cells and natural killer cells (Mócsai et al. 2010). Syk is required for adhesion, phagocytosis and ROS production as well as nuclear factor-kappa B (NF-κB) activation in dendritic cells and macrophages (Mócsai et al. 2002; Shi et al. 2006; Underhill et al. 2005; Crowley et al. 1997).

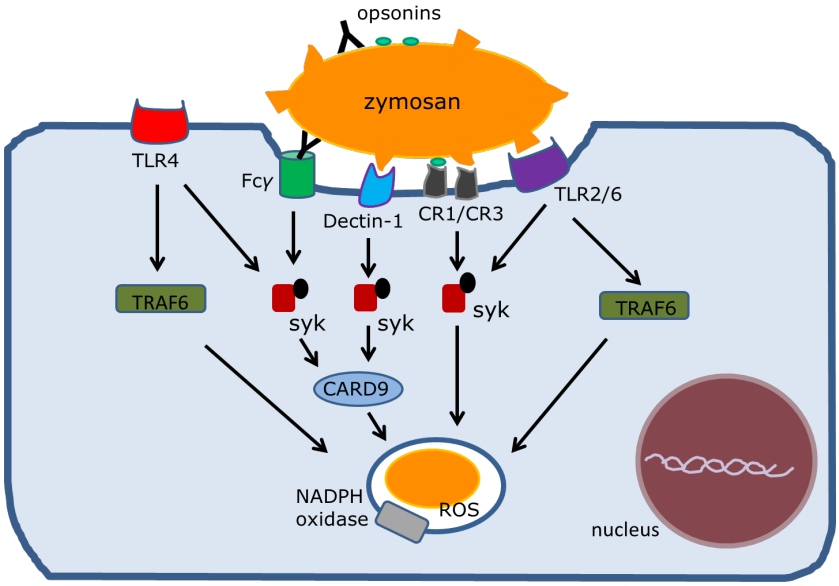

Figure 1.6: **Simplified overview of pattern recognition receptors and signalling.**
Fcγ, Dectin-1, Complement, TLR 4 and TLR2/6 recognise patterns of pathogens and lead to ROS production in the phagosome *via* the activation of adapter proteins (especially Syk).

Syk triggers ROS production upon pattern recognition receptor stimulation by a so far unknown mechanism (Mócsai et al. 2010). Underhill et al. (2005) showed that zymosan is phagocytosed normally in Syk-deficient mice but ROS production is abolished. Furthermore, Syk plays an important role in activation of transcription factors like NF-κB (Gross et al. 2006) and nuclear factor of activated T cells (NFAT) (Goodridge et al. 2007). It has

been shown that Syk functions as a linker protein between ITAM-based receptors (Fcγ) and β_2 integrins (CR3/CD18) *via* the adaptor protein DAP12 (Mócsai et al. 2010) and is therefore important for integrin signalling and migration (Mócsai et al. 2006; Schymeinsky et al. 2006).

However, Syk is also involved in actin assembly after phagocytosis and subsequent activation of ITAM adapter proteins in lymphocytes and macrophages (Cox et al. 1996; Majeed et al. 2001). In bone metabolisms, Syk has recently become a keyplayer in osteoclast signalling. In fact, a DAP2 and Fcγ receptor chain γ are responsible for Syk recruitment and a Syk deficiency shows impaired osteoclast development and function (Mócsai et al. 2004; Zou et al. 2007).

1.5.3 Killing of phagocytosed microbes: Oxidative burst

The engulfment of microbes by monocytes, macrophages and neutrophils is a complex action including the involvement of the above described pattern recognition receptors, followed by a cytoskeleton rearrangement leading to embracement of the particles by forming pseudopodia.

After engulfment of the microbe, lysosomes fuse with the newly formed phagosome and release digestives enzymes for microbe killing (fig. 1.7). Furthermore, the pH is lowered and the release of radicals is managed by the nicotinamide adenine dinucleotide phosphate (NADPH) oxidase. This process is called the oxidative burst and enables killing of engulfed microbes.

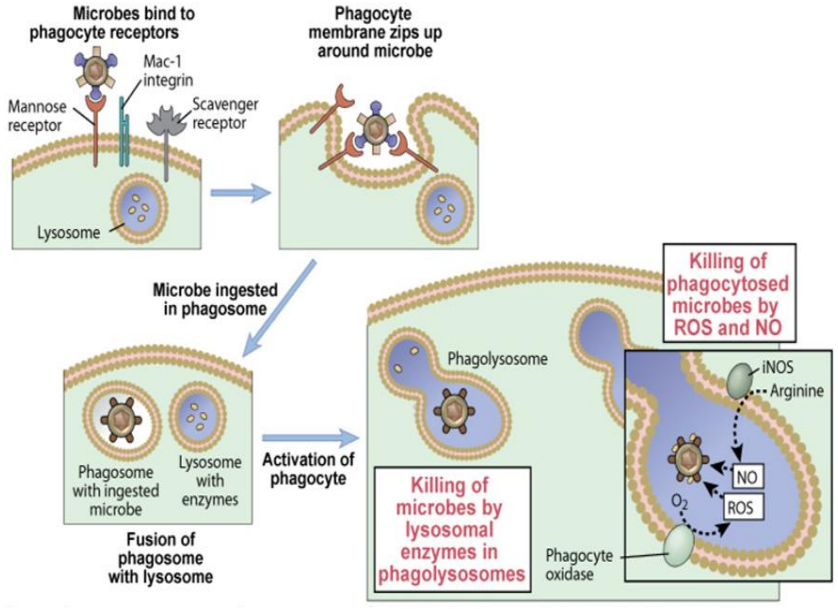

Figure 1.7: **Phagocytosis and oxidative burst.**
Microbes are recognised by the pattern recognition receptors and are engulfed *via* zipping membrane around the microbe. After ingestion of the microbe, lysosomes fuse with the phagosome. Subsequently, the killing of the pathogen is accomplished by lysosomal enzymes and the production of reactive oxygen and nitrogen species. From Abbas et al. (2010).

The NADPH oxidase is a multi-subunit enzyme activated in the cell and phagosome membrane, respectively. A protein complex consisting of subunits gp91phox and p22phox (together known as flavocytochrome b558) is located in the cell membrane prior to phagocytosis. Pattern recognition at the cell surface results in an activation of different kinases phosphorylating the subunits of the NADPH complex in the membrane as well as subunits p67phox, p40phox, p47phox which are present in the cytosol (El-Benna et al. 2005; Babior 1999; Nauseef 2004). The active NADPH oxidase transfers oxygen into superoxide radicals according to the formula:

$$2O_2 + NADPH \longrightarrow 2O_2^- + NADP^+ + H^+$$

Based on the production of superoxide by the NADPH oxidase, enzymatic and non-enzymatic processes produce different radical derivates (El-Benna et al. 2005): Superoxide dismutase (SOD) in the cytosol produces hydrogen peroxide from superoxide:

$$O_2^- + O_2^- + 2H^+ - (SOD) \longrightarrow H_2O_2 + O_2$$

Due to the Haber-Weiss reaction, hydrogen peroxide and superoxide react in the presence of a metal to the hydroxide anion:

$$O_2^- + H_2O_2 \; - (Fe^{++} or \, Cu^{++}) \longrightarrow OH^\bullet + OH^- + O_2$$

The myeloidperoxidase (MPO) catalyses the reaction between hydroxyperoxide and halogens in hypochlorid acid:

$$H_2O_2 + H^+ + Cl^- \ -(MPO) \longrightarrow OCl^- + H_2O$$

Nitric oxide synthase (NOS) enables the reaction between L-arginin and molecular oxygen to L-citrullin and $NO^{\cdot}$:

$$L - arginin + O_2 + NADPH \ -(NOS) \longrightarrow L - citrullin + NO^{\bullet} + NADP^+$$

The formed radicals accomplish microbe killing in the phagosome due to their reactivity but also serve as a second messenger in signalling e.g. activation of NF-κB (Iles & Forman 2002) which is reviewed in Forman & Torres (2001) and Finkel (2003). In fact, the production of oxygen radicals is a double-edged sword, because of a fine balance between the microbe killing and second messenger properties and the oxidative stress to the cells which can be extremely harmful to the host (Martin & Barrett 2002; Babior 2000). Patients suffering from the chronic granulomatous disease lack a functional NADPH oxidase and are not capable of pathogen removal (Holland 2010). Finkel & Holbrook (2000) review work on the role of oxidants and radicals in different diseases and aging.

1.5.4 Inflammatory response: NF-κB activation

The activation of transcription factors modulate immune response leading to inflammation which is a crucial feature of macrophages. After the pattern recognition, engulfment and oxidative burst, the transcription factor NF-κB becomes activated to initiate downstream signalling and inflammatory response. Tripathi & Aggarwal (2006) describe how the activation of this transcription factor takes place. The IκB subunits inhibit the translocation of NF-κB to the nucleus and get phosphorylated upon Dectin and TLR receptor stimulation. Degradation of IκB is accomplished by oxygen radicals as well as phosphorylation by Syk kinase (Takada et al. 2003). After translocation of NF-κB to the nucleus, the transcription of serveral genes starts. Cytokines, chemokines and adhesion molecules are expressed, which are crucial for recruiting neutrophils and modulating the adaptive immune response.

1.6 Aim of this study

The influence of microgravity on the health of astronauts is still not well understood and immune cells respond to microgravity with a diminished activity. Whether macrophages are still capable of accomplishing host defence in space is still unknown. Recently, it was shown that macrophages decrease the amount of oxygen radicals when stimulated with a pathogen analogon in microgravity. So far, impact on downstream signalling remains unidentified. This study was conducted to give further insight on the response of macrophages to altered gravity conditions. Real and simulated microgravity as well as hypergravity were applied to further characterise the oxidative burst capacity of macrophages. The phagocytosis was assessed to disconnect the observed changes in ROS production from the phagocytosis. A fast responding process, like the phosphorylation of the Syk kinase, which is crucial for ROS production as well as other biological functions (e.g. adhesion, osteoclast maturation), was analysed to examine downstream signalling of phagocytosis. Long-term effects, resulting in changed gen-expression, were evaluated by measurement of the translocated transcription factor NF-$\varkappa$B to the nucleus. These investigations should help to evaluate the impairment of phagocytes during spaceflight in respect to long-term spaceflights.

2 Materials and Methods

2.1 Materials

2.1.1 Equipment

2D Pipette-Clinostat	German Aerospace Center
Autoclave	H+P, Varioklav 25T
Centrifuge	Heraeus, Fresco 21 Heraeus, Biofuge Primo R
CO2-Incubator	Labotect C60 Binder 210M/CB
Counting chamber (Neubauer)	Brand
Freezer -80°C	Profiline Taurus
Freezingbox	Nalgene
Gel dryer	Model 583, BioRad
g-sensor Arduino uno with tinker acceleration module	Arduino
Heat block	Eppendorf
Horizontal shaker	WS 5, Edmund Bühler
Infrared imaging system	Odyssey, LI-COR
Laminar flow hood for cell culture	Telstar Bio II-A
Magnetic stirrer	Roth
Microplate reader GloMaxMulti+	Promega
Microscopes	Confocal laser scanning, C80i, Nikon fluorescent microscope Axiovert 10, Zeiss
Multi Sample Incubator Centrifuge (MuSIC)	German Aerospace Center
pH-meter	Schott
Pipette-controller	Pipetus-Akku, Hirschmann Laborgeräte
Pipettes	Eppendorf Reference
PMT-Clinostat	German Aerospace Center
Power supply for electrophoreses	BioRad
Protein-transfer-apparature	BioRad
Short-Arm Human Centrifuge (SAHC)	ESA
Temperature data logger	Roth
Vortex	Roth, Vortex-Genie
Water bath	Köttermann

2.1.2 Consumables

Cell culture dishes (10cm, 6cm)	Greiner Bio-one
Cell culture flasks (175/75 cm^2)	Greiner Bio-one
Cell culture plates (6-well)	Greiner Bio-one and Roth
Cell scraper	TPP
Disposable hypodermic needle, (0.4x20mm)	Sterican, Braun
Filter paper	Whatman Nr. 4 Schleicher & Schuell
Flow cytometry tubes (5ml)	Sarstedt
Microtiter plates (96-well)	Greiner Bio-one and Roth
Needles (0.6mm, 0.4mm, 1.2mm)	Braun
Nitrocellulose membrane	PROTRAN, Schleicher & Schuell
Pipette tips (10µl, 200µl, 1000µl, 5000µl)	Roth and Eppendorf
Pipettes, plastic, sterile (5ml, 10ml, 25ml, 50ml)	Roth and VWR
Polypropylene Reaction tubes (0.5/1.5/2.0ml)	Eppendorf an Roth
Sterile filters (0.2µm/0.45µm)	Schleicher & Schuell
Syringe (1ml, 3ml, 5ml)	Braun

2.1.3 Reagents

2-Mercaptoethanol	Gibco
3-Aminophthalhydrazid (Luminol)	AppliChem
Acrylamide 40%	Roth
Adenosine 5'-triphosphate, [γ-32P], 10mCi/ml	Perkin Elmer
Ammonium persulfate (APS)	Roth
Antibiotic-penicillin-streptomycin	Biochrom
Bicinchoninic acid (BCA) reagent solutions	Pierce
Bovine serum albumin (BSA)	Roth
Boracic acid (H_3BO_3)	Merck
Bromphenolblue	Roth

Calcium chloride ($CaCl_2$)	Merck
Curdlan from *Alcaligenes faecalis*	Wako Chemicals
di-Natriumtetraborat-Decahydrat ($Na_2B_4O_7$x 10 H_2O)	Roth
Dimethylsulfoxid (DMSO)	Sigma
Dithiothreitol (DTT)	Roth
EDTA (ethylene diamine tetraacetic acid)	Roth
EGTA (ethylene glycol tetraacetic acid)	Roth
Ethanol (EtOH)	Roth
Ethanol absolut	Merck
Fetal Calf Serum (FCS)	Biochrom
Ficoll400	GE Healthcare
Fluorescein (FITC)	Fluka
Fluorescence Mounting Medium	Dako
Formaldehyde	Roth
HEPES (4-(2-hydroxyethyl)-1-piperazineethanesulfonic acid)	Roth
Horseradish peroxidase	Merck
Isopropanol	Zefa Z
Igepal	Sigma
Lipopolysaccharide (LPS)	Sigma
Magnesium sulfate ($MgSO_4$)	Fluka
Mannan	Sigma
Methanol (MeOH)	Roth
Milk powder	Roth
Nitroblue-tetrazoliumchloride (NBT)	Fluka
Pam3csk4	Invitrogen
Percoll	Sigma
Phorbol 12-myristat 13-acetat (PMA)	Sigma
Phosphatase inhibitor	PhosStop, Roche
Piceatannol	Sigma
Poly(2´-deoxyinosinic-2´-deoxycytidylic acid) sodium salt (poly-dI-dC)	Sigma
Polymyxin B	Sigma
Potassium chloride (KCl)	Merck
Potassium hydroxide (KOH)	Roth
Protein standard	Precision Plus Protein All Blue standard, BioRad
Proteinase inhibitor	ProteaseComplete, Roche
Sodium carbonate ($Na_2 2CO_3$)	Merck
Sodium chloride (NaCl)	Merck

Sodiumdihydrogenphosphat-Monohydrat ($NaH_2PO_4xH_2O$)	Merck
Sodium dodecyl sulfate (SDS)	Roth
Sodiumhydrogencarbonat ($NaHCO_3$)	Merck
Sodiumhydroxide (NaOH)	Roth
TBE buffer (10x)	Roth
Tetramethylethylenediamine (TEMED)	Roth
Tris-[hydroxymethyl]aminomethan (Tris)	Roth
Triton X-100	Roth
Trypanblue-solution 0.4%	Sigma
Urea	Roth
Zymosan A, from *Saccharomyces cerevisiae*	Sigma

2.1.4 Media, sera and buffers

Donor Horse Serum	Biochrom
Fetal Calf Serum (FCS)	Biochrom
Ham's F-12	Biochrom
Phosphate buffered saline (PBS)	Biochrom
Very low endotoxin Dulbecco's modified Eagle medium (VLE DMEM)	Biochrom

Luminol stock solution

Stock solution 100mM luminol in DMSO, stored at -20°C and diluted 1:10 in borate buffer, pH 9 before use.

Borate buffer

The borate buffer was used to dilute the luminol stock solution.

borate buffer, pH 9
0.2M H_3BO_4
0.02M $Na_2B_4O_7$ x 10 H_2O
A.bidest

Stimulation substances stock solutions

The following substances were used to stimulate the cells and to initiate oxidative burst:

10mg/ml zymosan in PBS

50mg/ml curdlan in 0.1M NaOH

10µg/ml lipopolysaccharide (LPS) in PBS

50mg/ml mannan in PBS

10µg/ml pam3csk4 in PBS

10µM phorbol 12-myristat 13-acetat (PMA) in PBS

Opsonification of zymosan A

After Allen (1986), Huber (2007) and Horn (2011): 250mg/dl zymosan A was boiled for 20min in 0.85% physiologic salt solution. After cooling down to 22°C, the zymosan was centrifuged at 300g for 10min. The pellet was resuspended in 200ml donor horse serum and smoothly shaken for 20min at room temperature. Centrifugation and incubation with horse serum was repeated. The pellet was then washed twice with 500ml of physiological salt solution and the original concentration of 250mg/dl was restored. Aliquots were stored at -20°C until use.

FITC-zymosan

Zymosan A (see above) was incubated in darkness with 0.4 % (w/v) FITC for 30min at 37°C. It was washed 6 times with PBS and the aliquots were stored at -20°C.

NBT-zymosan

Opsonised zymosan (2.5mg/ml) was incubated with 0.2% (w/v) NBT for 2 hours at 37°C prior to use.

Horseradish peroxidase

Horseradish peroxidase (HRP) was used to catalyse the luminol reaction (see section 2.2.2.1). The stock solution was 500 U/ml in PBS and stored at -20°C.

2.1.5 Antibodies

The following primary and secondary antibodies were used for Western blot (WB) against rat antigens, or mouse antigens with rat-cross reactivity.

primary antibody	supplier	dilution
Anti-phospho-Syk (rabbit)	Cell Signalling	1:500 (WB)
Anti-β-actin (rabbit)	Sigma	1:1000 (WB)

secondary antibody	supplier	dilution
Goat-anti-rabbit IRDye800CW	LI-COR	1:5000 (WB)
Goat-anti-mouse IRDye700CW	LI-COR	1:5000 (WB)

2.1.6 Oligonucleotides

DNA oligonucleotides

NF-κB sense: 5'-ATCAGGGACTTTCCGCTGGGGACTTTCC*G*-3'

NF-κB anti-sense: 5'-CGGAAAGTCCCCAGCGGAAAGTCCCTGAT-3'

Oligonucleotides were synthesised by Eurofins MWG Operon.

2.1.7 Cell line

The cell line NR8383 of the American Type Culture Collection (ATCC) was a kind gift of the Karlsruhe Institute of Technology. NR8383 (normal rat, August 3, 1983) was established from *rattus norwegicus* alveolar macrophage cells were obtained by lung lavage. This cell line is mixture of adherent cells and non-adherent cells.

2.2 Methods

2.2.1 Cell culture

2.2.1.1 Cell cultivation

Cell line NR8383

NR8383 cells were cultivated in supplemented Ham's F-12 or VLE DMEM medium at a temperature of 37°C and a 5% CO_2 atmosphere with a relative humidity of 95%. The medium was changed every 2 to 3 days.

Ccell culture medium NR8383
Ham's F-12 or VLE DMEM
10% FCS
1% Antibiotic-penicillin-streptomycin
0.1% 2-Mercaptoethanol

For EMSA experiments (see section 2.2.5) VLE DMEM was used. Furthermore, to avoid any stimulating effects of the used chemicals due to lipopolysaccharide (LPS) contamination, Polymyxin B (a LPS captor) was added to the cell culture medium at the concentration of 500ng/ml. The starving of cells (2% FCS) during the experiments also dimished effects of backround stimulation (Dr. Diana Hippe, personal communication).

2.2.1.2 Freezing of cells

The cells contained in a 175cm² flask were scraped, transferred to a Falcon tube and centrifuged. The pellet was dissolved in 1ml freezing medium and then transferred to an Eppendorf cup and stored in a isopropanol-filled freezing box (Nalgene) at -80°C. After several hours of freezing, the Eppendorf cup was transferred to liquid nitrogen.

freezing medium NR8383
Ham's F-12
20% FCS
8.5% DMSO
0.1 % 2-Marcaptoethanol

2.2.1.3 Thawing of cells

For the thawing procedure, the Eppendorf cups with cells were removed from liquid nitrogen and then transferred directly to a Falcon tube with 20ml of 4°C cold medium. After 10min the cells were centrifuged and dissolved in warm medium and transferred into a cell culture flask.

2.2.1.4 Cell counting

The cell number was calculated using a Neubauer improved chamber (Roth). 20µl of the cell suspension was mixed with 20µl of 0.4% trypanblue solution and 10µl of this mixture was added to the Neubauer chamber. The trypanblue dye only stains the dead cells blue, whereas the viable cells remain unstained. After counting all the cells in 4 squares, the number of viable cells was calculated by applying the formula:

*Number of cells /4 * dilution factor * 10^4 = cell number per ml*

2.2.2 Bioassays for measurement of reactive oxygen species (ROS) and superoxide (0_2^-)

2.2.2.1 Luminol-Assay

This assay was adapted to a 96-well design analogue to the protocol of Horn (2011); Allen (1986) and Huber (2007). Luminol is a cell-permeable substance which is able to detect radicals inside as well as outside of a cell. In the presence of an oxidiser, in this case oxygen ions and peroxides which are generated during oxidative burst, luminol becomes oxidised. This process can be catalysed by the addition of the horseradish peroxidase (HRP). During this reaction, luminol passes a conformation change which in turn leads to the emittance of light. The luminol reaction is well suited to monitor the oxigenation activity of phagocytes (Allen 1986).

For the luminol-assay in a 96-well approach, each well contained 8x10^4 cells in 170µl medium, 50µl luminol (10mM), 10µl HRP (500U/ml) and 2.3µl of a stimulating stock solution for initiation of the oxidative burst. At 37°C, the plate was read at minute intervals in accordance to the absorbance protocol of the GloMax Multi+ microplate reader (Promega). This resulted in an online-kinetic measurement for 60min. Each experiment was performed in triplicates and a solvent (PBS) control was used to observe unstimulated radical production due to stress of the cells.

2.2.2.2 NBT-Assay

This assay was adapted to Sierra et al. (2005), Huber (2007) and Horn (2011). Nitroblue-tetrazoliumchloride (NBT) was coupled to opsonised zymosan particles. During the phagocytosis of the NBT-zymosan particles the intracellular radical superoxide reduces the NBT, which in turn falls out as blue substance formazan. The amount of superoxide corresponds to the blue colour shift, which was detected in a microplate reader (Promega). Opsonised zymosan (2.5mg/ml) was incubated with 0.2% (w/v) NBT for 2 hours at 37°C. 150µl NBT-zymosan was added to 100µl of cells suspension (with a concentration of 2.5 x 10^5cells per ml). A non-phagocytosis control was performed with NBT-PBS. Cells were exposed to hypergravity (see section 2.3) and allowed to phagocytose the NBT-zymosan particles. The phagocytosis was stopped by adding 1ml of ice-cold PBS and placing the samples on ice. After centrifugation for 2min at 380g, the cell pellet was fixed with 500µl of 70% methanol. Another centrifugation step was done and the pellet was lysed with 120µl of 2M KOH. 140µl of DMSO were added and a colour shift to blue was observed. The suspension was then transferred into a 96-well plate and the absorbance of the suspension was measured in the microplate reader GloMaxMulti+ (Promega) at 600nm. The absorbance correlates with the amount of produced superoxide. A mixture of KOH and DMSO was used as a blank.

2.2.3 Determination of phagocytosis by flow cytometry

The phagocytoctic activity of the cells was determined by the usage of the flow cytometry technique. Flow cytometry (fluorescence-activated cell sorting [FACS]) technique is used to investigate the size, granularity and fluorescence intensity of cells in a very short time. Cell surface proteins or intracellular proteins are labelled (after permeabilisation) with fluorescent dyes. The FACS scanner aspirates cells in suspension and scatters and channels them though a laser beam. The laser beam is then deflected by the passing cells which is detected by surrounding photomultipliers. The characteristic light scattering gives information about size and granularity of the cells. The amount of emitted fluorescence correlates with the expression level of the labelled protein. All information was recorded with FACSDiva (BD Bioscience).

In this approach, flow cytometry was used to measure the phagocytotic activity of cells during simulated microgravity and hypergravity. Therefore, 1.5 x 10^6 cells (NR8383) per ml were stimulated with 100µg of FITC-zymosan and exposed to simulated microgravity or 1g in 1ml pipettes within the Pipette-Clinostat (see 2.3.2). Cells phagocytosed the fluorescent labelled zymosan for different amounts of time and samples were transferred into ice-cold PBS. After centrifugation at 300g for 7min, the cells were washed with PBS, centrifuged and the cell pellet was then resuspended in 180µl PBS and transferred into flow cytometry

tubes. The samples were stored on ice, in darkness, until measurement. The FACS analysis was performed with FACS Canto II (BD Bioscience), equipped with a 488nm laser and the data was anlysed with FACS Diva software (BD Bioscience). Morphological properties of the cells and fluorescence intensities of the fluorochrome were displayed in forward scatter (FSC) versus sideward scatter (SSC) density plots and histogram plots, respectively. For the examination of the phagocytotic activity, the percentage of FITC positive cells was determined. 20,000 cells were analysed at each time point.

2.2.4 Protein biochemistry

2.2.4.1 Preparation of cell lysates

The cells (up to $4x10^6$) were harvested and washed twice with ice-cold PBS.

protein extraction buffer
8M urea
1:10 PhosphoSTOP (Roche)
1:10 ProteaseComplete (Roche)

The protein extraction buffer was prepared with 8M urea dissolved in PBS. Stock solutions of one tablet of each PhosSTOP and Protease Complete (both Roche) were diluted 1:10 in the urea extraction buffer. PhosSTOP blocks the activity of phosphatases and ProteaseComplete the activity of proteases. After completely removing the PBS, 80µl of urea lysis buffer was added to the cells. Probes were kept on ice and vortexed regularly. After 15min the cell debris were centrifuged at 16,000g for 10min at 4°C. The supernatant (=cell lysate) was transferred into a new tube and stored at -80°C. The protein amount was analysed by BCA-assay (see below).

2.2.4.2 Determination of protein concentration by the BCA-assay

The protein amount in cell lysate was determined using a standard bicinchoninic acid (BCA) assay. The principle of this assay is the reduction of Cu^+ molecules to Cu^{2+} by proteins. The protein content is proportional to the amount of reduction as Cu^{2+} ions build chelat complexes with a high absorption at about 562nm. This is visualised by a colour-shift from light green to purple. Before measuring the protein content of the probes, a standard bovine serum albumin (BSA) was performed by a serial dilution with urea extraction buffer. 3µl of the standard (0, 0.125, 0.25, 0.5, 1, 2, 4mg/ml BSA) and

protein samples were placed into a 96-well plate as a double determination. BCA reagent B (BioRad) was diluted 1:50 in BCA reagent A (BioRad), and 200µl of this solution was added to each well. After incubation of the plate for 30min at 37°C the plate was read at a wavelength of 590nm in the GloMax Multi+ (Promega) microplate reader. Extraction buffer and BCA solution was used as a blank. Together with the protein standard curve, the protein amount of all samples were calculated.

2.2.4.3 Sodium Dodecyl Sulfate - Polyacrylamide Gel-Electrophoresis (SDS-PAGE)

Sodium dodecyl sulfate (SDS) – polyacrylamide gel-electrophoresis is a technique to separate proteins according to their size. SDS denatures proteins and applies a negative charge to each protein. By using radical polymerisation, acrylamide is formed into a polyacrylamide gel matrix. SDS binds to proteins, prevents folding and gives the proteins a negative charge. This leads to a protein separation in the polyacrylamide gel based only according to their size but not to their charge or folding. In this study, gels of 10% polyacrylamide (resolving part) and 5% polyacrylamide stacking gel were used.

1x Laemmli running buffer	sample buffer
25mM Tris	0.28M Tris-HCl pH 8
200mM Glycin	30 % (m/v) Glycerol
0.1% (w/v) SDS	10 % (m/v) SDS
ad 1l A.bidest	60mM DTT
	0,0012% (v/v) Bromphenolblue

	stacking gel 5%	resolving gel 10%
A. bidest	3.4ml	1.9ml
1.0M Tris-HCl, pH 6.8	630µl	-
1.5M Tris-HCl, pH 8.8	-	1.3ml
30% (v/v) Acrylamide	830µl	1.7ml
10% (v/v) SDS	50µl	50µl
10% (v/v) APS	50µl	50µl
TEMED	5µl	2µl

Equal amounts (20-40µg) of protein were mixed with 5x loadingbuffer and boiled for 5min at 99°C. After 5min on ice, the samples were centrifuged at 16,000g for 5min. The gel was clamped into the electrophoresis chamber which was then filled with 1.2l of 1x Laemmli running buffer. The samples and 7.5µl of a protein standard (BioRad) were pipetted into the gel pockets. The gel was run for approximately 1.5h at 120V until the blue dye front reached the bottom of the gel. Proteins were then blotted to a cellulose membrane (see below).

2.2.4.4 Western blot analysis

The name Western blot derives from the term Southern blot, a technique invented by E. Southern for detection of DNA. Analogous to Southern blot, a Western blot detects specific proteins of cells and tissues. Firstly, the separation of native proteins is made by gel electrophoresis to separate the proteins according to their molecular weight. Secondly, the proteins separated on the gel are transferred to a membrane (nitrocellulose or polyvinylidene difluoride) by electro-blotting. Whatman paper, sponge, blot cassette and nitrocellulose membrane were moistened in 1x transfer buffer. On the black side of the blot cassette a "sandwich" was built using a sponge, Whatman paper, the gel, nitrocellulose membrane, Whatman paper and sponge. The closed cassette was placed into the blotting chamber and filled with 800ml of 1x transfer buffer. The blotting was performed at 80V for 2h. Afterwards, the membrane was washed for 5min in 10ml of Tris buffered saline with Tween (TBST). Blocking of the membrane was carried out for 1h at room temperature in 5% (w/v) milk powder in TBST.

1x Tris buffered saline with Tween (TBST)
0.5M Tris-HCl, pH 7.5
1.5M NaCl
0.06% (v/v) Tween

The primary antibodies phospho-Syk (see section 2.1.5) were diluted in 5ml TBST. The incubation of the membrane was performed at 4°C over night with gentle shaking. On the next day, the membrane was washed 3 times with TBST for 5min. The primary antibodies were then detected by incubating the membrane with the fluorescent secondary antibody (diluted in 10ml 5% milk powder in TBST) IRDye800CW for 1h at room temperature with gentle shaking. After washing the membrane in TBST for 5min for 3 times, the blots were analysed in LI-COR Odyssey Sa Infrared Imaging System. The bands were further analysed and quantified with imageJ according to Miller (2010). To show that equal amounts of proteins were used, the membranes were "stripped off" the antibodies and then blocked in milk powder and incubated once more with primary and secondary antibodies. A ubiquitous protein, Actin, was used to visualise equal amount of proteins.

1x transfer buffer
200mM Glycin
25mM Tris
20% (v/v) Methanol
0.002% (w/v) SDS

"stripping" buffer
0.2M NaOH

2.2.5 Electrophoretic Mobility Shift Assay (EMSA)

The Electrophoretic Mobility Shift Assay (EMSA) is used to study protein/DNA interactions and therefore the corresponding gene regulation. Protein/DNA complexes run more slowly on a polyacrylamide gel compared to free DNA molecules. Here, the presence of NF-κB subunits interacting with DNA, in the isolated nuclear extract were evaluated. 32p labelled DNA fragments were added to the isolated nuclear extract. These bind due to their complementary structure to the NF-κB/DNA complexes and result in a band shift during gelelectrophoresis.

2.2.5.1 Preparation of nuclear extracts

$3x10^6$ cells were stimulated with 625µg/ml opsonied zymosan and subjected to clinorotation for 4h. The reaction was stopped with the addition of ice-cold PBS. Samples were washed twice with ice-cold PBS. The pellet was incubated with buffer A. After 15min, 25µl of buffer B were added and incubated for 1min at 4°C. Nuclei were pelleted by centrifugation with 11,300g at 4°C for 5min. The pellet was resuspended in 50-70µl buffer C and incubated for 20min on ice under constant agitation. The nuclear envelope was pelleted by centrifugation with 11,300g for 5min at 4°C. The supernatants (=nuclear extracts) were collected and stored at -80°C. Protein concentration was determined by a standard BCA-assay (see section 2.2.4.2).

buffer A	buffer B	buffer C
10mM HEPES	10% Igepal	20mM HEPES, pH 7.9
10mM KCL		0.4M NaCl
0.1mM EDTA		1mM EDTA
0.1mM EGTA		1mM EGTA
1mM DTT (freshly added)		1mM DTT (freshly added)
1mM PMSF (freshly added)		

2.2.5.2 Annealing and labelling of NF-κB oligonucleotides

The lyophilised NF-κB oligonucleotides were resuspended in water, and the concentration of 100pM/µl was adjusted. An 1.5ml Eppendorf reaction tube was used to mix 20µg NF-κB sense and 20µg NF-κB antisense strand. 10µl 10x annealing buffer was added and the reaction volume was filled up to 100µl with A. bidest. The incubation of the tube was carried out for min in a heat block at 95°C, which was then turned off, with the samples left in, until it reached room temperature. The cooling to room temperature took up to

45–60min. The annealed oligonucleotides were diluted with A. bidest to a concentration of 25ng/ml. It was either stored at -20°C or directly labelled.

annealing buffer
20mM Tris/HCl, pH 6.7
10mM $MgCl_2$
50mM NaCl
1mM DTT

Annealed oligonucleotides were labelled with a total volume of 50µl.

annealing reaction
1µl NF-κB oligonucleotide (=25ng)
5µl kinase buffer 10x
12µl gamma-32-P-ATP (Perkin Elmer)
2µl T4-kinase (Roche)
30µl A.bidest

The labelling was performed at 37°C for 30min under gentle agitation. Afterwards, the radioactive labelled oligonucleotides were purified using Quant 96 *g*-50 micro columns (GE Healthcare), to remove unincorporated labelled nucleotides from the DNA labeling reaction. The probe was then counted by *LSC (liquid scintillation counting)* and transferred into a radioactive storage box at 4°C until use.

2.2.5.3 EMSA

For the EMSA, nuclear extracts were incubated with the radioactive labelled oligonucleotide probe containing the specific recognition sequence for NF-κB. The binding reaction occurs under specific salt/pH conditions in a binding buffer. *Poly-dIdC* was added to prevent unspecific binding of proteins to the NF-κB oligonucleotide probe in order to reduce background signals.

5x binding buffer
25mM HEPES, pH 7.8
25mM $MgCl_2$
250mM KCl
1mM EDTA
50% Glycerol
25mM DTT

binding mix
2µl poly dldC (1µg/µl)
4µl 5x binding buffer
10µg protein (nuclear extract)
ad. 20µl A.bidest

The binding mix was incubated for 20min at room temperature, before adding 2µl of the radioactive labelled NF-κB oligonucleotide probe. After 7min incubation time, 6x loading buffer was added, and the samples were separated on a non-denaturating gel (20x20cm, 15-well comb) at 200V, for 3-4h in a water-cooled electrophoresis chamber (Peqlab).

non denaturating gel	running buffer
40ml A.bidest	0.25x TBE buffer
1.25ml 10x TBE buffer	
7.5ml Acrylamide 40%	
312.5µl APS 10%	
185.5µl TEMED	

The gel was subsequently dried in a gel dryer (80°C, 2h, under vacuum) and bands were detected by autoradiography, i.e. by exposing the dried gel 24-96h to an autoradiography film at -80°C.

2.3 Simulation of microgravity

Different devices are used world-wide to simulate the conditions of microgravity on earth. The residual gravitational force is usually smaller than $1g$, depending on the device used. The term *microgravity* describes gravitational forces of less than a thousandsth of $1g$ (Albrecht-Buehler 1992). Here, according to the available literature of space research, the term microgravity is used to describe gravity forces of less than $1g$. For a review of the teminology see Herranz et al. (2013).

The two following sections introduce the two different ground-based devices for microgravity simulations used in this study and their adaptation of cell biological assays.

2.3.1 PMT-Clinostat

The Photomultiplier (PMT)-Clinostat (fig. 2.1) was designed by Dr. Astrid Horn and Dr. Jens Hauslage (Horn et al. 2011). The device is placed in an incubator and consists of a motor which rotates a cuvette (3cm long with a diameter of 4mm) along its horizontal axis. A photomultiplier is located at the tip of the cuvette which enhances the light signal, emitted by the cells during the luminol reaction. The light signal is read out by a 3.5GHz frequency counter (BK Precision). The frequency counter is connected to a laptop (Fujitsu Siemens) to record the luminescent output each second with a counter software program. The speed of the cuvette was set at 60rpm which corresponds to a maximal residual acceleration of $0.008g$ calculated according to the centrifugation equation:

$\alpha = \omega^2 * r$

with ω = angular velocity (rotation speed) and r = radius of the cuvette

For further information see Albrecht-Buehler (1992).

The luminol-assay was adapted to the Clinostat environment according to Horn (2011): 792µl cell suspension with a concentration of $7x10^5$ cells/ml, 165µl luminol (10mM), 33µl HRP (500U/ml) and 10µl stimulating substance (e.g. zymosan). Every experiment, unless stated otherwise, was performed in an incubator or heating box (Horn 2011) at 37°C for 60min.

A

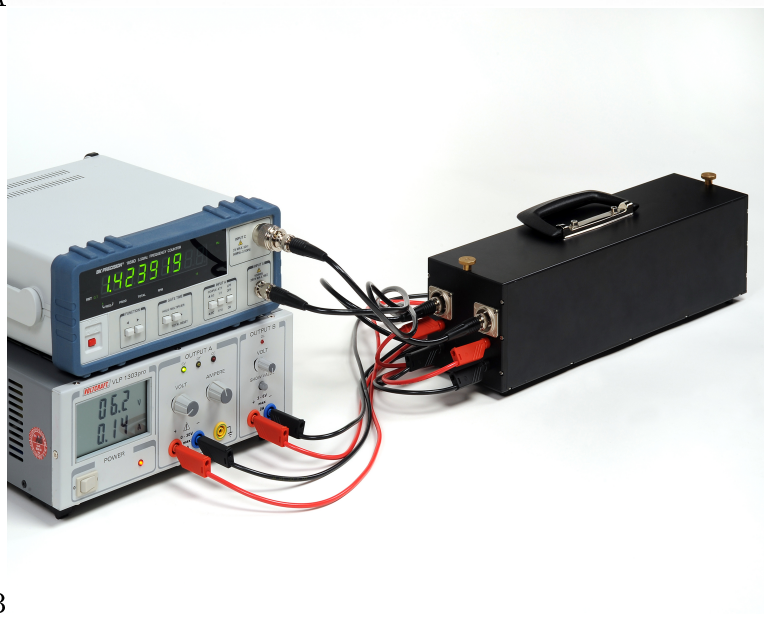

B

Figure 2.1: **PMT-Clinostat**. Design: Jens Hauslage, Astrid Horn
A: Top view of PMT-Clinostat: A: photomultiplier tube B: cuvette C: motor
B: PMT-Clinostat connected to frequency counter and power supply.

2.3.2 2D Pipette-Clinostat

The 2-dimensional Pipette-Clinostat (fig. 2.2) consists of ten 1ml pipette holders which rotate the pipettes along their horizontal axes, with a speed of 60rpm. It works according to the Clinostat principle and has a maximal residual acceleration of $0.008g$. This Clinostat is applicable for non-adherent cell lines and can be placed in an incubator. 15ml Falcon tubes can be used to directly fix the cells without stopping the Clinostat and thereby preventing exposure to $1g$ conditions before termination of the experiment.

Figure 2.2: **2D Pipette-Clinostat at DLR.** Design: Jens Hauslage

For investigations on protein biochemistry, samples of clinorotated cells of the cell line NR8383 were prepared as followed: 3-6x10^6 were fed with 100µg/ml zymosan or 100µg/ml opsonised zymosan. PBS was used for a non-stimulated control. For exposure on the Clinostat, cells were split into 2-3 pipettes (500µl each) and rotated for 15min (protein analysis) or 240min (EMSA). Corresponding $1g$ controls were kept in pipettes on the bottom of the Clinostat. Afterwards, cells were directly transferred into ice-cold PBS and processed to protein extraction or nuclei extraction.

2.4 Hypergravity

Different centrifuges were used to achieve increased gravity conditions. An incubator centrifuge (MuSIC) was used for endpoint measurements. For online-kinetic measurements a human centrifuge (SAHC) was utilised due to its increased amount of space to be able to install the experimental set up.

2.4.1 Multi-Sample Incubator Centrifuge (MuSIC)

This Multi-Sample Incubator Centrifuge (MuSIC, see fig. 2.3) is an incubator with a centrifuge for multiple samples which allows hypergravity experiments under constant temperature, in this case 37°C. This device enables studies in terms of endpoint measurements and has the advantages of continuously adjustable rotation speed as well as exposure of many samples in parallel. Up to 12 Eppendorf cups were installed on the centrifugation plate. $1g$ control samples were placed underneath the rotating plate. The centrifuge was run with a speed of 97rpm which equals $1.8g$ at the tip of the Eppendorf cup on the rotating plate. For investigations under $3g$ conditions, the centrifuge was rotated which a speed of 123rpm. The MuSIC was used to elucidate the amount of superoxide radicals during oxidative burst measured with the NBT-assay (see section 2.2.2.2) according to the protocol of Huber (2007) and Horn (2011).

Figure 2.3: **Multi-Sample Incubator Centrifuge (MuSIC) at DLR.**

2.4.2 Short-Arm Human Centrifuge (SAHC)

The Short-Arm Human Centrifuge (fig. 2.4) is widely utilised to study physiological parameters on humans and to develop countermeasures for human space exploration by using "artificial gravity". However, there is the opportunity to adapt physical or biological experiments to the planar platform of the centrifuge.

Figure 2.4: **Short-Arm Human Centrifuge at DLR in Cologne** (Source: ESA).

For online-kinetic measurements of the oxidative burst, the PMT-Clinostat was adapted to the human short-arm centrifuge. The full PMT-Clinostat hardware with its heating box (Horn 2011) was installed on the planar platform of the centrifuge (see fig. 2.6). The cuvette of the Clinostat hardware was aligned horizontally to the centrifugal force by the centrifuge. The figure shows the centrifugal force of the centrifuge and the gravitational force vector on the Clinostat box during the SAHC experiments. In pilot experiments, the cuvette was aligned in the direction of g-vector of the centrifuge. No differences were observed when compared to the perpendicular installed cuvette. As the centrifugation could result in a aggregation of cells at the tip of the cuvette, which could in turn lead to light signal quenching, the cuvette was installed perpendicularly to the centrifuge's g-vector.

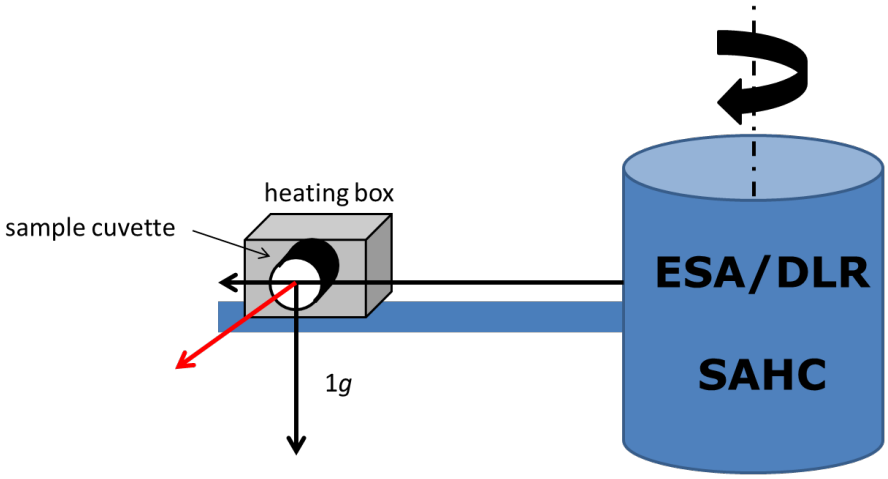

Figure 2.5: **Schematic drawing of the different forces during the SAHC study.**
The Clinostat was installed in a heating box on the centrifuge. The sample cuvette was aligned horizontally to the axis of rotation. The black arrows indicate the centrifugal force and the gravitational force ($1g$) vector, respectively. The resulting force vector of both is indicated in red.

For measuring the oxidative burst of the cell line NR8383, the centrifuge was rotated for 45min with a resultant g-force at the part of cuvette of $1.8g$ and $3g$, respectively.
All experiments were performed at a temperature of 37±1°C. Connection of a relay and a specialised computer program enabled the performance of a parabolic flight mode, consisting of 15 parabolas containing a $1.8g$, "$0g$" (simulated microgravity), $1.8g$ phase, and a $1g$ phase in between the parabolas. During the $1.8g$ phases the centrifuge was in operation mode. During the $1g$ and $0g$ phases the centrifuge operated at $1.1g$. The centrifuge could not be stopped completely due to technical reasons. Simulated microgravity ($0g$) was achieved by rotating the Clinostat cuvette at 60rpm. Parabolic flight profiles were run for approximately one hour. To study the effects of adaption processes to altered gravity, the rotation of the centrifuge was stopped and the measurement was completed at $1g$ conditions or in reverse order.

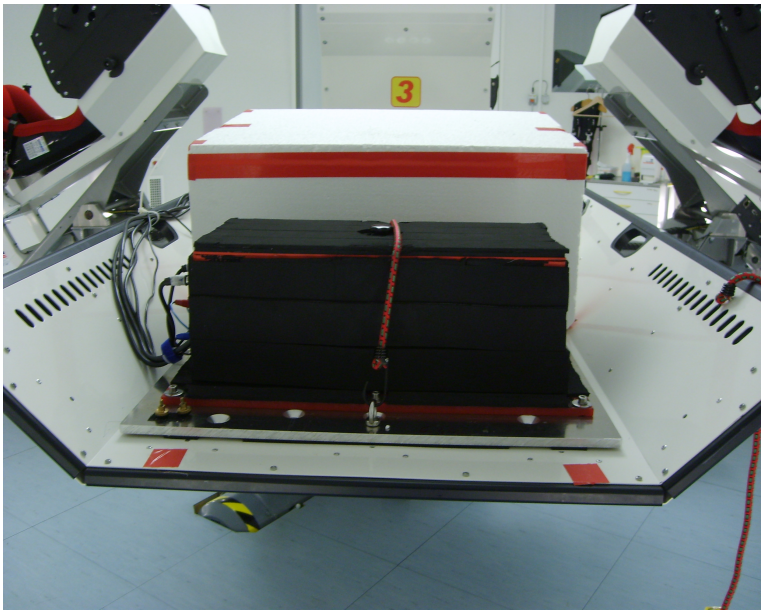

Figure 2.6: **PMT-Clinostat within a heating box installed on the SAHC.**

2.5 Real microgravity

2.5.1 Parabolic flight

During the 56th and 57th ESA parabolic flight campaigns experiments were performed together with the TRIPLE LUX B experiment of Prof. Dr. Peter Hansen from the Technical University of Berlin, entitled: "Immunological and cellular reactions under influence of microgravity and cosmic radiation – The application of a biosensor with phagocytotic cells". The TRIPLE LUX B project is very similar to the research on the ROS production of macrophages, since the ROS production of blue mussel hemocytes is under investigation.

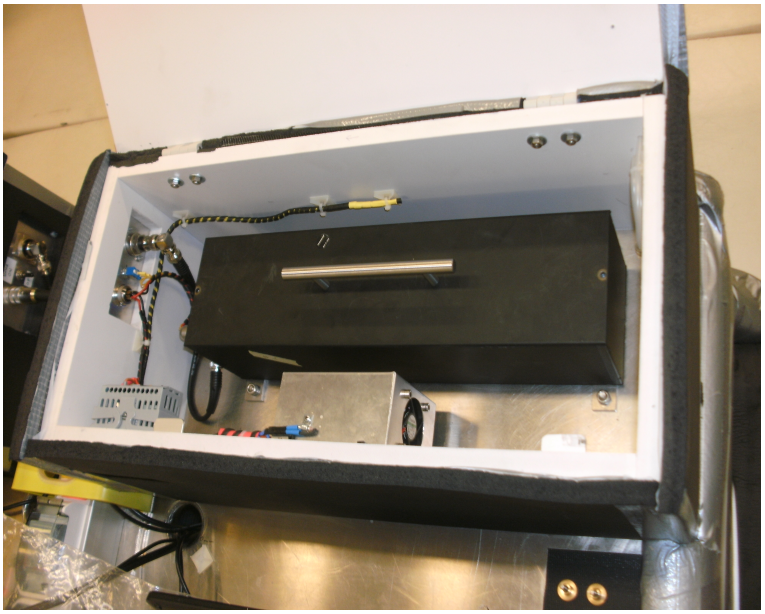

Figure 2.7: **Forex heating box with PMT-Clinostat** (black box). Design: Kai Wasser (DLR, Cologne)

In a comparative approach, the ROS production of blue mussel hemocytes and macrophages of the cell line NR8383 were measured during parabolic flights. To facilitate this, an experimental setup providing two Clinostats within Forex heating boxes (German Aerospace Center) (see fig. 2.7) was built. The Clinostat was in a non-rotating ($1g$) mode in order to keep the results comparable to ground studies using the Clinostat in its operation ($0g$) mode. The PMT-Clinostat was installed in a Forex heating box to keep the cells at 37°C. The frequency counter and a laptop for data recording were fixed on a parabolic flight rack (fig. 2.8).

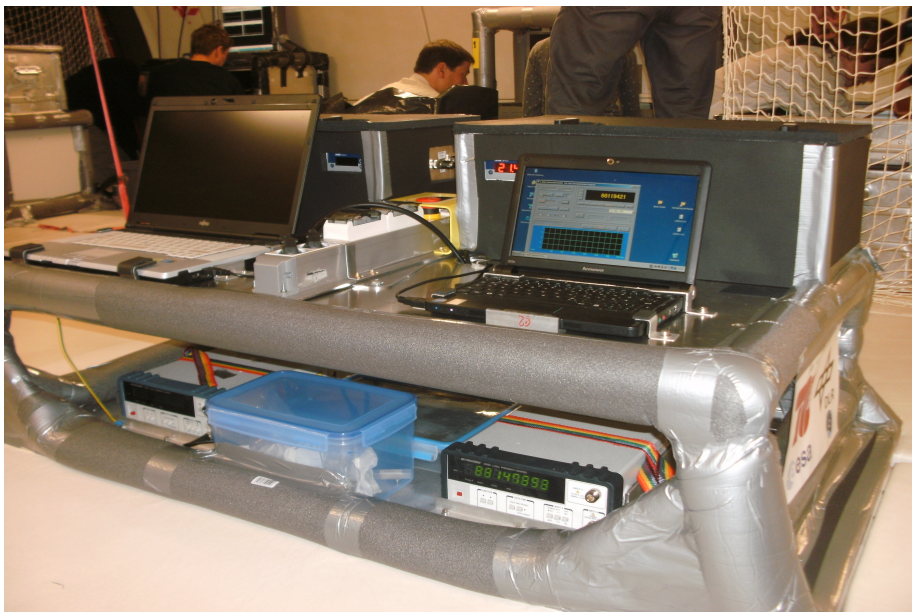

Figure 2.8: **Flight rack for the 56th and 57th parabolic flight campaign**, Bordeaux-Mérignac.

An acceleration sensor (Arduino uno with Tinker acceleration module) was connected to one of the laptops to synchronise the luminescence data with the g-profile of the flight. Two samples were prepared for each of the 3 flight days. The sample cuvettes were kept in the Clinostat box during the aircraft's take-off. 10min before the first parabola, luminol, HRP and a stimulating substance (e.g. zymosan) were added to the cells. The volume of each of the substances was the same as for the ground experiments (see section 2.2.2.1). Nonetheless, the substances were injected with a 1ml syringe, taking the dead volume of the syringes into account. After the addition of luminol, HRP and zymosan/PBS to the cells, the ROS production was measured during flight conditions for 16/15 parabolas. In the 8 minute break between parabolas 16. and 17., the sample was fixed by aspirating the cell liquid into a 3ml syringe filled with 100µl of 37% PFA or 10% SDS. Then, the second sample was prepared and fixed after the last parabola as explained above.

2.6 Statistical analysis

Each experiment was performed at least three times. Control runs were performed with non-stimulated cells (PBS control). These results gained with PBS controls are only shown when they resulted in noticeable variations from the norm. Statistics were based on the Kolmogorov–Smirnov normality-test using the IBM SPSS statistics 19 software. The homogenity of variances was tested with the Levene's test. A Student's t-test or one-way ANOVA (Tukey's post-hoc test) was then performed with a 95% confidence interval, to ascertain if the data was distributed normally. Non-normally distributed data were tested to the level of significance with the Mann-Whitney-U test. The nomenclature used in the figures is: * = significant ($p < 0.05$ - 0.01) ** = very significant ($p < 0.01$ - 0.001), *** = extremely significant ($p < 0.001$). For a clearer graphical chart, the data were normalised and therefore set each $1g$ mean as 1, to be able to compare different data sets obtained on different days.

3 Results

The work here is based on observed changes in ROS production in the rat macrophage cell line NR8383 Horn (2011). Since the changes under simulated and real microgravity had been partly evaluated, the current work mainly concentrates on the characteristics of ROS production during hypergravity. Several studies were performed on the MuSIC and SAHC. To elucidate the role of phagocytosis in the observed changes in ROS production, FACS analysis was performed after exposure to micro- and hypergravity. Due to a discrepancy between the observed ROS production and phagocytosis, it was assumed that signalling might play an important role. To further address signalling, LPS and curdlan were used to stimulate the cells in order to examine an involvement of different distinct pathways in respect to their gravisensivitiy. Furthermore, since the ROS production is a very fast responding mechanism, the phosphorylation of the spleen tyrosine kinase Syk, was under investigation. The activation of the transciption factor NF-$\varkappa$B was assessed in order to examine if signalling steps after ROS production and Syk phosphorylation are affected as well.

3.1 Impact of altered gravity on ROS production in cell line NR8383

3.1.1 Simulated microgravity reduces ROS production after zymosan stimulation

The work of Horn (2011) clearly shows the impact of real and simulated microgravity on the oxidative burst following opsonised zymosan stimulation. Here, the influence of altered gravity on non-opsonised stimulation was under investigation. In contrast to the studies of Horn (2011), non-opsonised zymosan was used to initiate oxidative burst. Figure 3.1 demonstrates the reduced ROS production during simulation of microgravity in the PMT-Clinostat, This is significantly decreased under this condition, compared to $1g$ reference ($p \leq 0.001$).

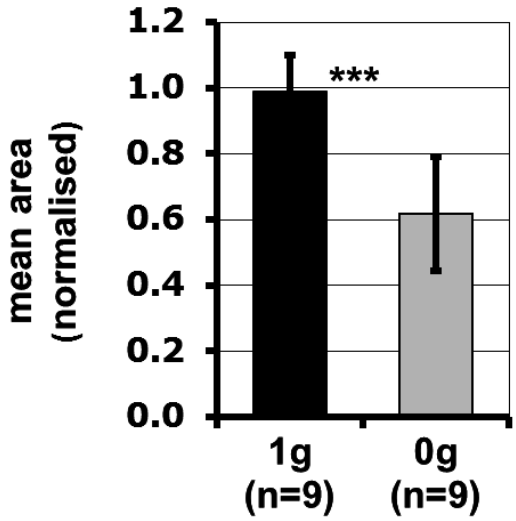

Figure 3.1: **Clinorotation reduces ROS production after stimulation with non-opsonised zymosan.**
Influence of simulated microgravity (PMT-Clinostat) on the entire ROS production (=area under curve) after stimulation with zymosan (100µg/ml), determined by the oxidation of luminol. Normalised data shown with standard deviation. Significance was estimated with student's t-test. (***$p<0.001$).

3.1.2 Increased ROS production under hypergravity conditions

The reduction of the ROS production during the respiratory burst of macrophages under altered gravity has been described in detail in Horn (2011). Parabolic flight data showed an increase in ROS production in the phases of hypergravity after stimulation with opsonised zymosan (see Horn 2011). In this study, the characteristics of the increased ROS production were under investigation. First, the pilot experiments of Astrid Horn (2011) on the SAHC were reproduced and the impact of ROS production was further explored. To narrow the number of involved cell surface receptors, which lead to phagocytosis and ROS production, non-opsonised zymosan particles were used. The luminol-assay is a non-specific indicator for reactive oxygen species intra- and extracellular. Therefore, the NBT-assay was utilised in order to determine the intracellular superoxide production of the NADPH oxidase complex during oxidative burst.

3.1.2.1 ROS production at 1.8g and 3g is increased after stimulation with opsonised zymosan

To reproduce the pilot experiment of Horn (2011), cells were stimulated with opsonised zymosan particles and the ROS production under hypergravity conditions was measured.

The PMT-Clinostat was installed on the SAHC to perform the online-kinetic measurement. With the luminol-assay, the production of ROS under conditions of hypergravity was visualised. Cells were stimulated with approx. 500µg/ml opsonised zymosan and exposed to hypergravity for 45 minutes at $1g$ (non-rotating), $1.8g$ and $3g$. This was analogous to Horn's study (2011). Figure 3.2 shows a set of $1g$, $1.8g$ and $3g$ experimental runs. The figure demonstrates that the ROS production was increased at $1.8g$. Applying $3g$ induced a further increase in the production of ROS. The experiment was repeated three times and figure 3.2 shows one representative experiment.

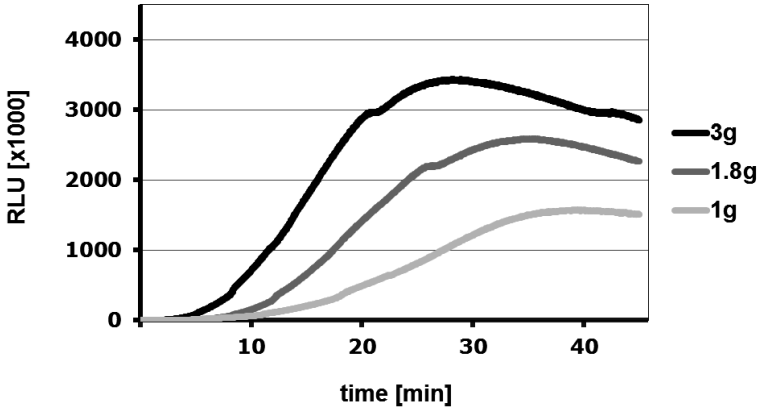

Figure 3.2: **Hypergravity increases ROS production when stimulated with opsonised zymosan.** Influence of hypergravity (SAHC) on the ROS production of the cell line NR8383 after stimulation with approx. 500µg/ml opsonised zymosan, determined by the oxidation of luminol. Data was normalised as the collection of data was made on different days. Data reflects one representative experiment of at least three replicates.

3.1.2.2 Superoxide production is increased at 3g centrifugation

Since the luminol-assay is only able to monitor the overall radical production of cells, the NBT-assay was used to measure the intracellular superoxide production during the oxidative burst. NBT was coupled to opsonised zymosan particles, in order to be taken up by the cells. The measured absorbency after the colour shift due to the reduction of NBT into formazan is shown in figure 3.3. The superoxide production is significantly increased during $3g$ centrifugation ($p=0.013$) compared to the $1g$ control. This assay produces very high standard deviations and was therefore not used for further investigations.

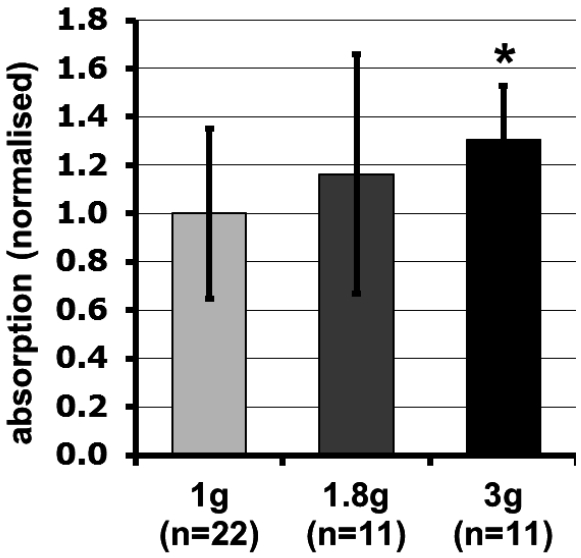

Figure 3.3: **Hypergravity increases the production of superoxide when stimulated with opsonised zymosan.**
Influence of hypergravity (MuSIC) on the intracellular superoxide production of the cell line NR8383 after stimulation with NBT-opsonised zymosan (approx. 500µg/ml), was determined by the reduction of NBT, resulting in a colour shift. Data were normalised and shown with standard deviation. Significance was estimated with student's t-test (* $p<0.05$).

3.1.2.3 ROS production at 1.8*g* and 3*g* after stimulation with non-opsonised zymosan

To further characterise the ROS production under hypergravity and to look at two distinct signalling pathways, the cells were stimulated with non-opsonised zymosan particles at a concentration of 100µg/ml. The production of ROS under 1.8*g* did not differ from the production at normal 1*g* conditions. However, an increase in the ROS production was visible at increased acceleration of 3*g* (fig. 3.4). The production of radicals depends on the acceleration level.

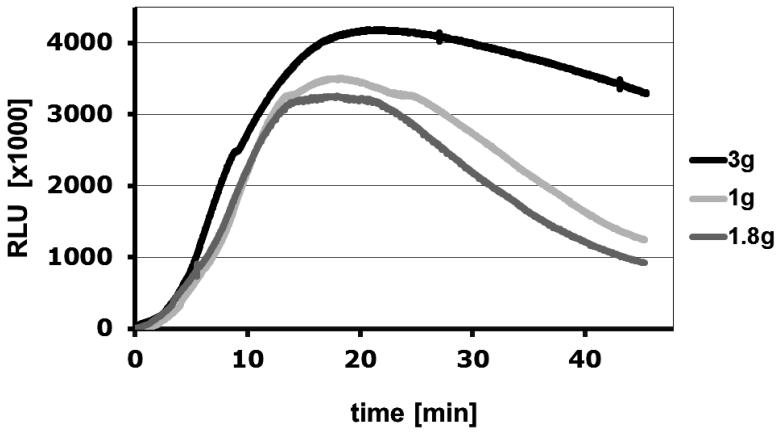

Figure 3.4: **Hypergravity increases ROS production at 3g but not 1.8g, when stimulated with non-opsonised zymosan.**
Influence of hypergravity (SAHC) on the ROS production of the cell line NR8383 after stimulation with 100µg/ml zymosan, determined by the oxidation of luminol. Data represents one experiment out of 9 replicates.

The experiments using non-opsonised zymosan were repeated several times to evaluate the results statistically. Figure 3.5 shows normalised data of the entire ROS production of several experiments on the SAHC. No difference between 1g and 1.8g was observed, Nonetheless, the production of ROS significantly increased at 3g ($p \leq 0.001$) compared to the 1g control. However, figure 3.5 shows normalised data of the area under the curve, the absolute maximum of each curve and the time until the peak of the curves was reached (= lag-time).

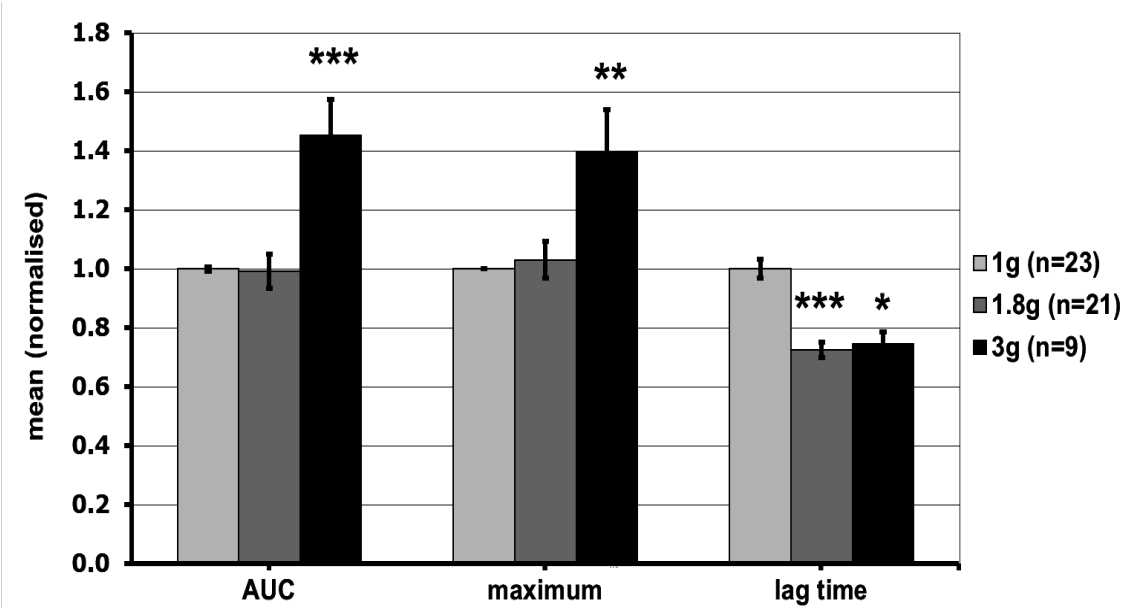

Figure 3.5: **Hypergravity affects different parameters of zymosan induced ROS production.** Influence of hypergravity (SAHC) on the ROS production of the cell line NR8383 measured by the oxidation of luminol. The area under curve (AUC= entire ROS production); maximum of the curves; time until the maximum of the curve was reached (=lag-time) are shown. Normalised data with standard deviation. Significance was estimated with student's t-test (* $p<0.05$, ** $p<0.01$, ***$p<0.001$).

The results indicate that it takes significantly longer to reach the maximum ROS production in hypergravity. $3g$ acceleration affects maximum, the total ROS production (AUC) and the lag-time, whereas the amount of ROS and maximum remains normal under $1.8g$ conditions. Only the time until the maximum is reached is delayed.

3.1.3 Increased ROS production during centrifugation is not stress-induced

Macrophages are capable of producing oxygen radicals without any ligand stimulation due to stress. Since the centrifugation of cells could result in mechanical stress of the cells, the general, non-phagocytic ROS production was examined. Cells were exposed to hypergravity after addition of the ligand solvent PBS. PBS does not have any impact on ROS production itself. In this case it was used to simulate stimulation in terms of the addition of a substance. Two separate stress analysis were performed during the SAHC campaign. The general non-phagocytic ROS production was first analysed in a 96-well luminol-assay in parallel to all SAHC experiments. Subsequent campaign days contained a (hypergravity) PBS experiment to investigate the ROS production due to mechanical stress response. However, no abnormalities in either experimental set-up were detected (see fig. 3.6 and 3.7). Figure 3.6 shows the normalised mean area under curve (equalling the entire ROS production) upon zymosan and PBS "stimulation" under normal $1g$ conditions in the 96-well approach. The non-activated, PBS "stimulated" cells produce a small amount of background ROS.

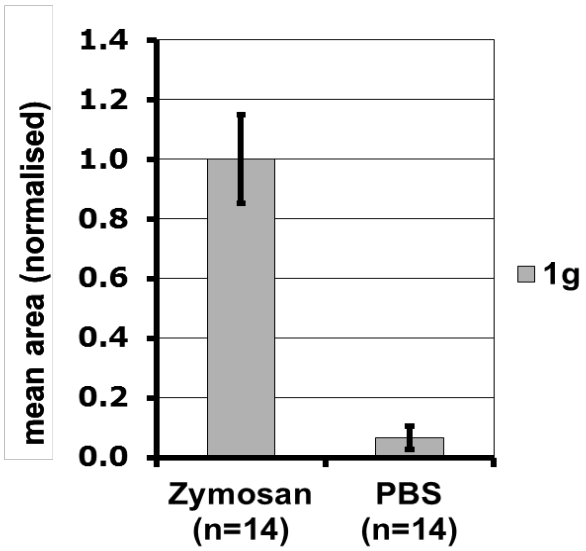

Figure 3.6: **ROS production at 1g (lab control).**
ROS production (determined by luminol-assay) of NR8383 cell line after stimulation with zymosan (100µg/ml) and the ligand solvent PBS as a control substance under 1g conditions in a 96-well format. Normalised data shown with standard deviation.

Figure 3.7 shows the control SAHC experiments using PBS as a "stimulating substance" under 1.8g and 3g compared to the zymosan 1g data. The results clearly show that the increased ROS production under 3g acceleration after zymosan stimulation (see fig. 3.4) is not induced by mechanical stress, because the background ROS production level stays constant under increased gravity conditions.

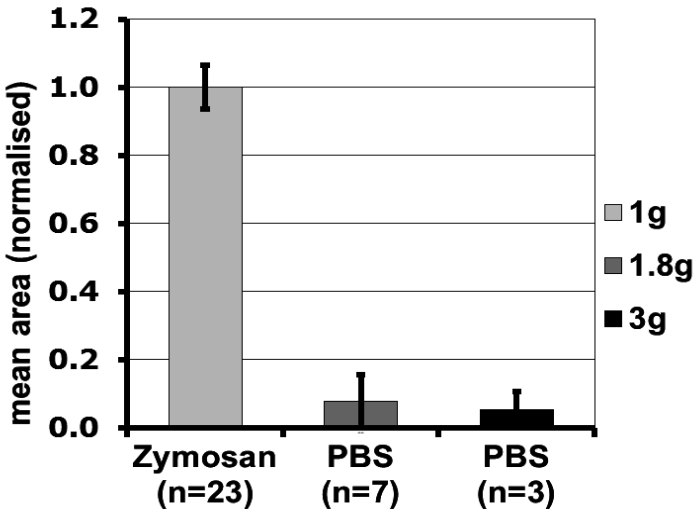

Figure 3.7: **ROS production at different accelerations (PBS controls).**
ROS production (determined by luminol-assay) of NR8383 cell line after stimulation with zymosan (100µg/ml) and the ligand solvent PBS as a control substance under different gravity conditions on SAHC. Normalised data shown with standard deviation.

3.1.4 Macrophages show adaptation to hypergravity conditions

To study the adaptation process of the ROS production to altered gravity, hypergravity was applied for 20 minutes and the centrifuge was stopped and the measurement was continued for further 25 minutes at $1g$ conditions. Figure 3.8 demonstrates the ROS production at $1.8g$ and the transition to $1g$ after 20 minutes. The ROS production at $3g$ and the stop of the centrifuge after 20 minutes is shown in figure 3.9.

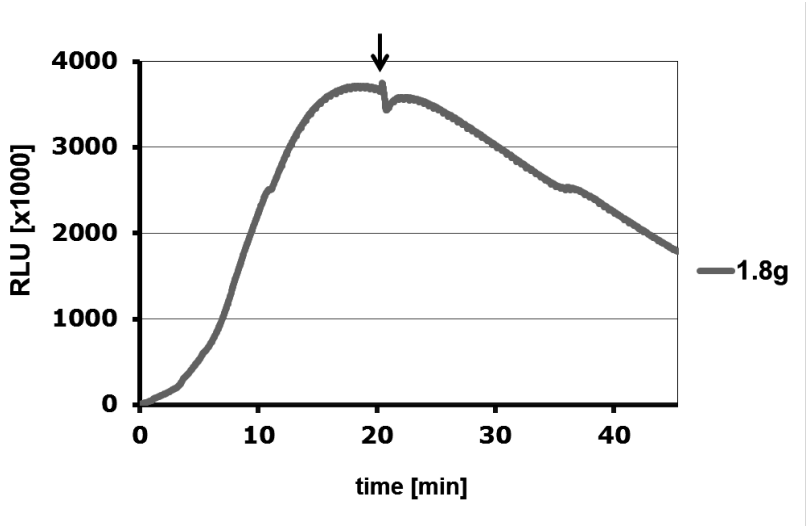

Figure 3.8: **ROS production during 1.8g on SAHC.**
Online-kinetic measurement of oxygen radicals (ROS) in the macrophage cell line NR8383 during centrifugation at 1.8g for 20 minutes and 25 minutes at 1g after stimulation with zymosan (100µg/ml), determined by the oxidation of luminol. Arrow indicates centrifuge stop. Data represents one experiment out of 3 replicates.

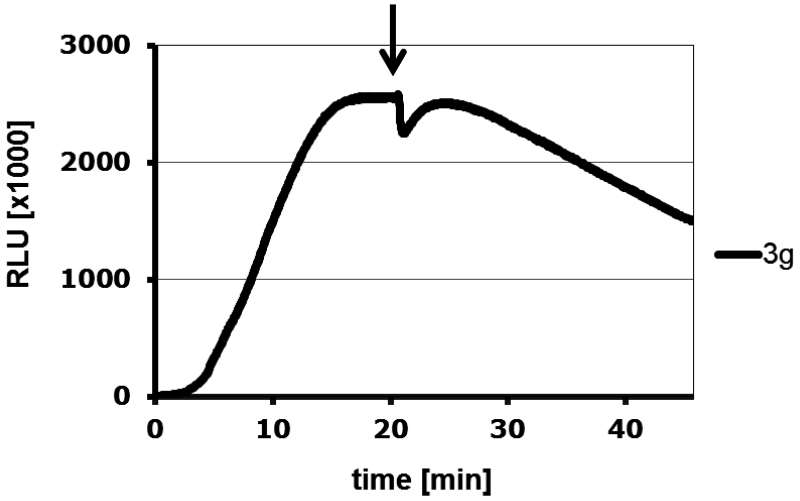

Figure 3.9: **ROS production during 3g on SAHC.**
Measurement of oxygen radicals (ROS) in the macrophage cell line NR8383 during centrifugation at 3g for 20 minutes and 25 minutes at 1g after stimulation with zymosan (100µg/ml), determined by the oxidation of luminol. Arrow indicates centrifuge stop. Data represents one experiment out of 3 replicates.

Under both acceleration conditions, a sudden stop of the centrifuge resulted in a drop in ROS production. After 3-5 minutes the ROS production normalised and continued as under normal gravity conditions.

The sudden start of the centrifuge, acceleration up to 1.8g, did not result in any ROS production changes as shown in figure 3.10. Here, the measurement was started under 1g

conditions (centrifuge standing still). After 20 minutes the centrifuge was started ($1.8g$) and the measurement was continued for further 25 minutes.

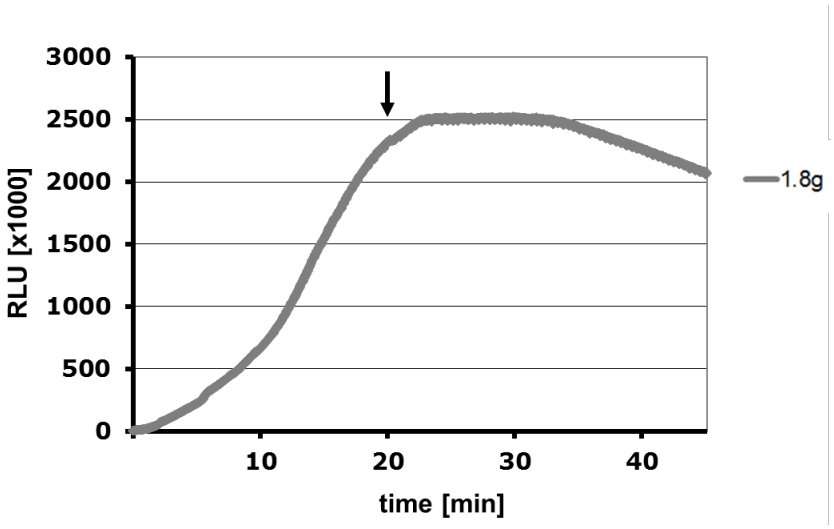

Figure 3.10: **ROS production during $1g$ and $1.8g$ on SAHC.**
Measurement oxygen radicals (ROS) in the macrophage cell line NR8383 determined by the oxidation of luminol, during $1g$ (centrifuge standing still) for 20 minutes and $1.8g$ for 25 minutes after stimulation with zymosan (100µg/ml). Arrow indicates centrifuge start.

3.1.5 Simulation of the parabolic flight-like g-profile

The installation of a Clinostat on a centrifuge enabled the production of a g-profile in a parabolic flight-like fashion. A program and relay allowed the control of the Clinostat from the control room of the SAHC. Figure 3.11 shows the acceleration g-profile, using the Clinostat and the centrifuge consecutively, and the corresponding ROS production during exposure to this specific g-profile. A $1g$ control reference curve was added, to show the normal ROS production in comparison to the parabolic flight g-profile.

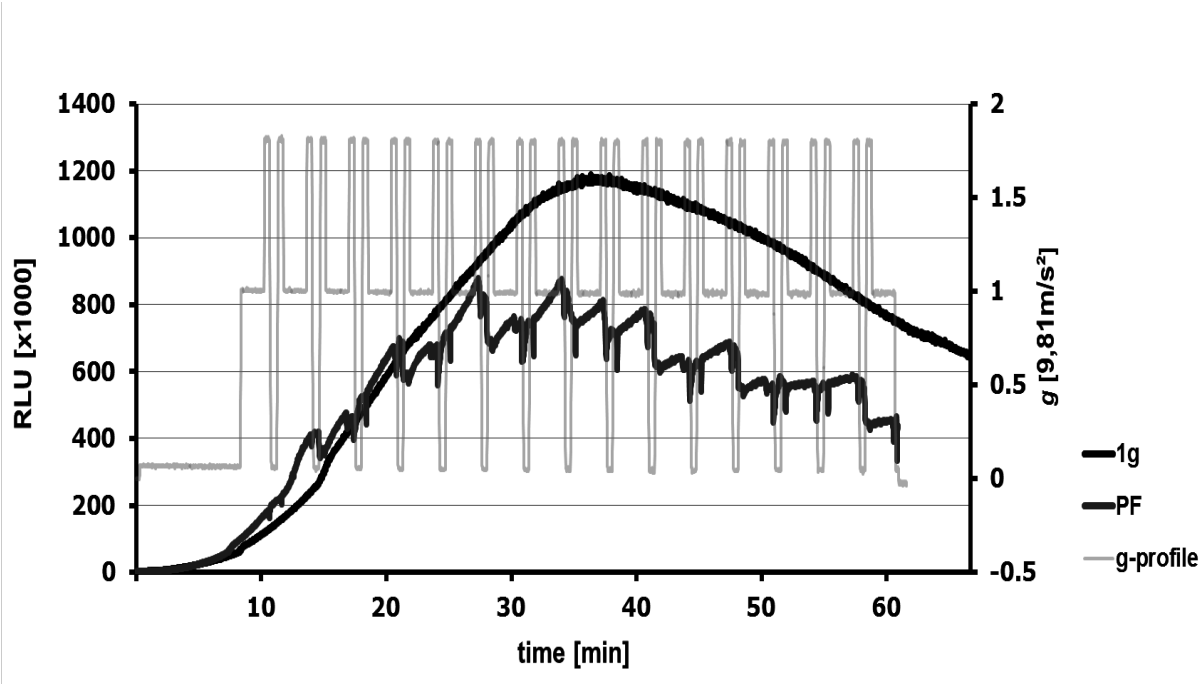

Figure 3.11: **Simulated parabolic flight profile on the SAHC with opsonised zymosan stimulation.**
Cells (NR8383) were stimulated with opsonised zymosan (approximately 500µg/ml). Clinostat and centrifuge were switched on consecutively. After 9 minutes of $1g$, the centrifuge was switched on for 22 seconds ($1.8g$). The centrifuge was then stopped and the clinostat was switched on for 20 seconds and followed by 22 seconds of hypergravity ($1.8g$). The parabolas were separated by 108 seconds of $1.1g$, brought about by a very slow rotating centrifuge due to technical reasons. Data represents one experiment out of 2 replicates.

Figure 3.11 indicates the ROS production upon opsonised zymosan stimulation, whereas figure 3.12 shows the production of ROS after non-opsonised zymosan stimulation. Both figures demonstrate that the cells respond to very fast gravitational changes. Cells seem to respond to each alteration of the g-force, for example to the switch from $1g$ to hypergravity ($1.8g$) and from simulated microgravity ($0g$) to the second hypergravity phase.

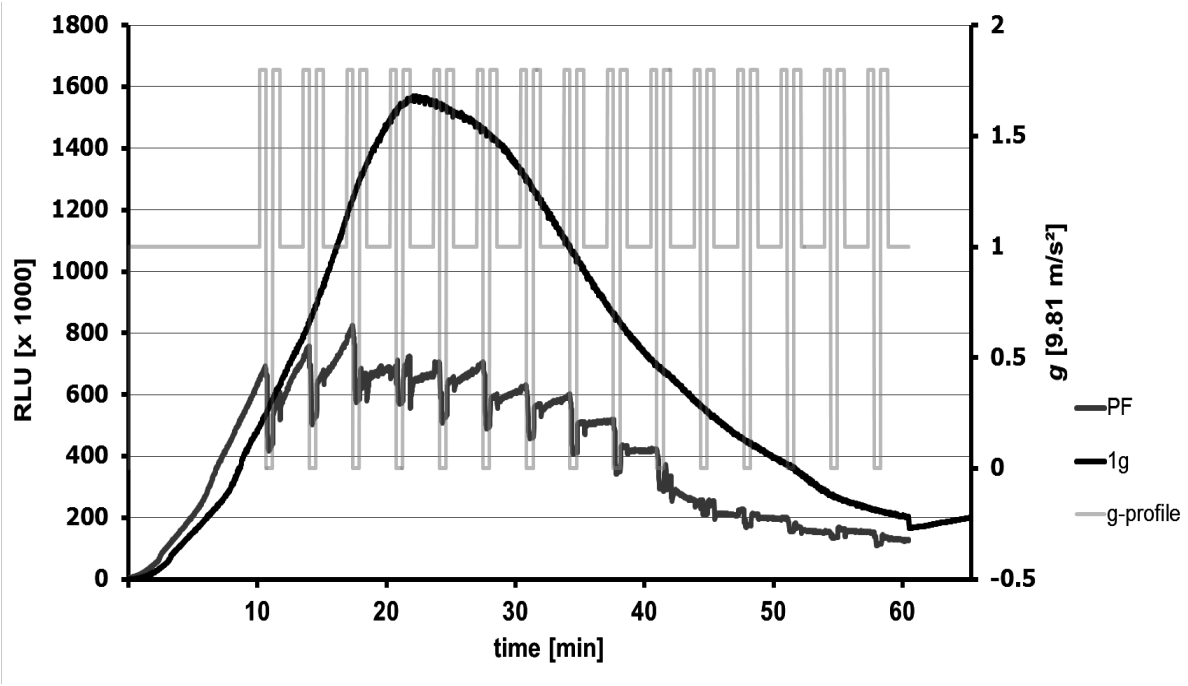

Figure 3.12: **Simulated parabolic flight profile on the SAHC with zymosan stimulation.** Cells (NR8383) were stimulated with non-opsonised zymosan (approximately 100µg/ml). Clinostat and centrifuge were switched on consecutively. After 9 minutes of $1g$, the centrifuge was switched on for 22 seconds ($1.8g$). Then, the centrifuge was stopped and the clinostat was switched on for 20 seconds, followed by 22 seconds of hypergravity ($1.8g$). The parabolas were separated by 108 seconds of $1.1g$, caused by a very slow rotating centrifuge due to technical reasons. Data represents one experiment out of 7 replicates.

Cells stimulated with normal non-opsonised zymosan particles did show a clear response to the simulated microgravity conditions, as seen by the sudden drop in ROS production.

3.2 Impact of real microgravity on ROS production

3.2.1 56th and 57th ESA Parabolic Flight Campaigns verify ground-based experiments

The 56th and 57th ESA parabolic flight campaigns in Bordeaux-Méringnac were used to prove the results gained in the extensive ground-based studies. Figure 3.13 shows a comparative experiment on board the A300 zero-g aircraft. Cells were stimulated with non-opsonised zymosan to study the effects of hypergravity and real microgravity. During the flight, the rat macrophages did not respond to hypergravity but a decrease takes place after the microgravity phase in terms of radical production. The decrease was recorded 20 seconds after the real microgravity phase due to a time-delay in the response.

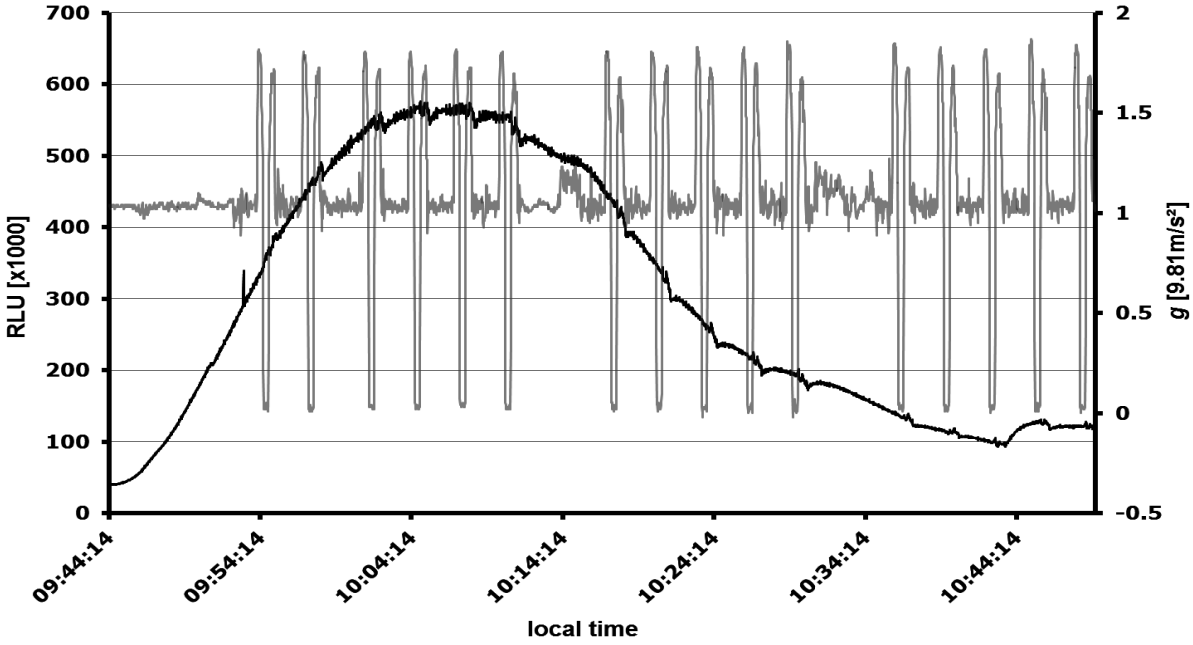

Figure 3.13: **ROS production during parabolic flight after zymosan stimulation.** NR8383 cells were stimulated with non-opsonised zymosan (100µg/ml) during the first 16 parabolas of the first flight day during the 57. ESA parabolic flight campaign. ROS production was visualised with the luminol-assay (black line). g-data were recorded with the Arduino data logger (grey line). Data represents one experiment out of 6 replicates.

3.2.2 Non-stimulated cells show ROS production during parabolic flight in response to stress

In line with all ground-based experiments, the ROS production without stimulation of the cells was monitored during the 56th parabolic flight campaign. Figure 3.14 shows one example of 2 replicates using PBS as a substance to simulate the stimulation e.g. of

zymosan. The cells only respond to the second hypergravity phase with increased ROS production.

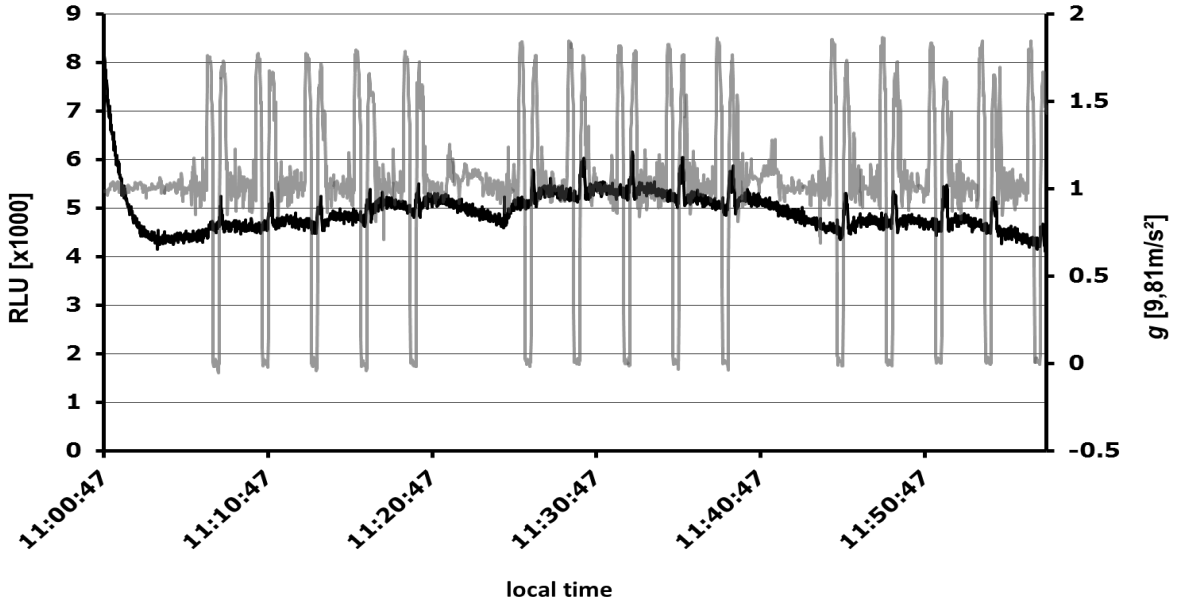

Figure 3.14: **ROS production of non-stimulated cells during parabolic flight.** NR8383 were not stimulated during the second 15 parabolas of the third flight day during the 56th ESA parabolic flight campaign. ROS production was visualised with the luminol-assay (black line) and g-data were recorded by Novespace (grey line). Both data sets were synchronised manually.

3.3 Phagocytosis is changed under altered gravity conditions

3.3.1 Phagocytosis is slightly reduced under simulated microgravity

Phagocytosis of pathogens is the first line of defence of macrophages facing pathogens in the body of its host. Here, the phagocytosic capacity of the macrophage cell line NR3838 was examined.

Cells were fed with FITC-coupled zymosan particles for different periods of time during exposure to simulated microgravity or hypergravity. The FITC-zymosan positive percentage (here called phagocytotic index) of cells were examined with flow cytometry. Simulated microgravity was achieved by exposing cells in the Pipette-Clinostat. Data were normalised to their $1g$ reference. Figure 3.15 shows the results of 5 individual experiments under simulated microgravity conditions in the Pipette-Clinostat. The phagocytosis of the NR8383 cells line was reduced under simulated microgravity conditions, with the lowest amount after 60min ($p \leq 0.001$). The phagocytosis increases again after 90 and 120min but does not reach the level of the control cells under $1g$ conditions.

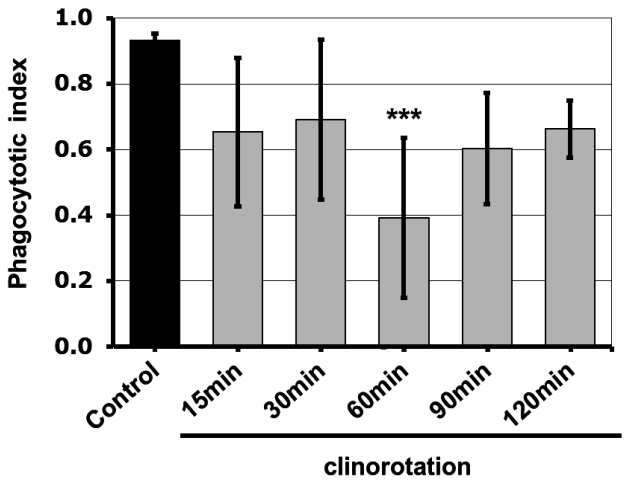

Figure 3.15: **Phagocytotic index during simulated microgravity.**
NR8383 cells were stimulated with 100µg/ml FITC-coupled zymosan particles and exposed to clinorotation for indicated time periods. Phagocytotic index was calculated by measuring the FITC positive cells according to FACS analysis. Normalised data are shown with standard deviation of at least 5 individual experiments. Significance was estimated with one-way ANOVA (***$p<0.001$).

3.3.2 Hypergravity reveals significantly increased phagocytosis

Hypergravity was achieved with the MuSIC and with a maximum acceleration of $3g$. The capability to phagocytose FITC-coupled zymosan particles under hypergravity ($3g$) conditions was increased at all time points compared to their $1g$ reference (Fig. 3.16). After

15min of exposure the phagocytosis rate was increased up to 50% to normal phagocytosis at $1g$ conditions, with a high level of significance ($p \leq 0.001$). The significantly enhanced phagocytosis is most prominent at the early stages of phagocytosis, e.g. after 15 and 30min. After 60, 90 and 120min, the phagocytosis is still enhanced but the level of significance is lower.

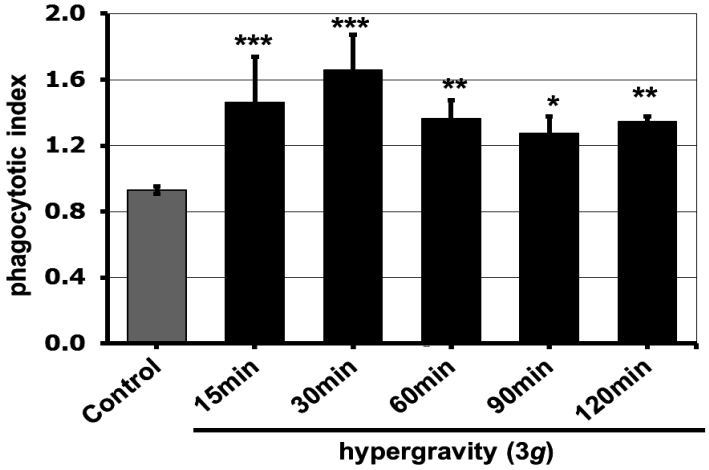

Figure 3.16: **Phagocytotic index during hypergravity.**
NR8383 cells were stimulated with 100µg/ml FITC-coupled zymosan particles and exposed to hypergravity on the MuSIC for indicated time periods. Phagocytotic index was calculated by measuring the FITC positive cells according to FACS analysis. Normalised data are shown with standard deviation of at least 4 individual experiments. Significance was estimated with one-way ANOVA (* $p<0.05$, ** $p<0.01$, ***$p<0.001$).

3.4 Stimulation of different cell surface receptors to evaluate their sensitivity towards simulated microgravity

Different stimuli were used to initiate oxidative burst after activation of different signalling pathways. Firstly, the general ROS production under $1g$ was examined to look for stimuli which lead to a reliable production of ROS. Secondly, the substances which fullfilled these criteria were used to measure ROS production under simulated microgravity conditions within the PMT-Clinostat and using the luminol-assay.

3.4.1 ROS production upon stimulation with different substances

To characterise the cell line NR8383 regarding its ROS production capabilities, different substances were used to initiate oxidative burst upon pattern recognition receptor stimulation. For this purpose, the luminol-assay was utilised in a 96-well approach. NR8383 cells were stimulated with different substances and ROS production was measured at $1g$ conditions. A number of single pattern recognition substance were used, including: Lipopolysaccharide, curdlan, mannan, pam3csk4. Multiple receptor stimulating factors like zymosan and opsonised zymosan were also used.

Figure 3.17 shows the entire ROS production, as the area under curve, after stimulating different cell surface receptors. The yeast cell wall particle zymosan, induced the highest amount of oxygen radicals. Opsonised zymosan, labelled with antibodies and complement factors after washing with blood serum, gained a slightly higher amount of oxygen radicals. Neither the use of the mannose polymer mannan, which is recognised by the Dectin-2 receptor, nor the synthetic bacterial lipopolysaccharide pam3csk4 (TLR2 receptor) resulted in any ROS production. PBS and NaOH were used as a solvent control.

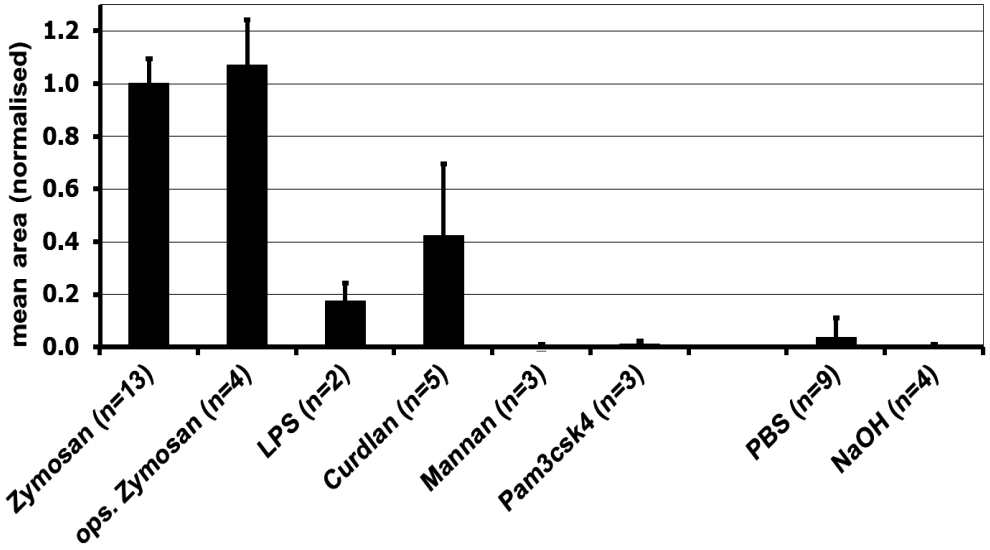

Figure 3.17: **ROS production induced by cell surface receptor stimulation.**
Mean normalised ROS production of NR8383 cell line after stimulation with different substances. Error bars indicate standard deviation.

The stimulation of the cell surface receptors TLR4 with the bacterial lipopolysaccharide (LPS) and the stimulation of Dectin-1 through curdlan (glucose polymer) led to reliable ROS production. The Dectin-1 and the TLR receptor are both activated by zymosan stimulation. Since both TLR 4 and Dectin-1 stimulation showed a reliable ROS production, both signalling pathways were assumed to be useful to study distinct pathways in terms of their gravisensivity.

3.4.2 ROS production after LPS and curdlan stimulation is decreased in simulated microgravity

The distinct stimulation of cell surface receptors leading to ROS production was performed using LPS, a TLR2 agonist, and curdlan, a Dectin-1 agonist. 100ng/ml lipopolysaccharide (LPS) gained a significant loss in ROS production during exposure to simulated microgravity (fig. 3.18).

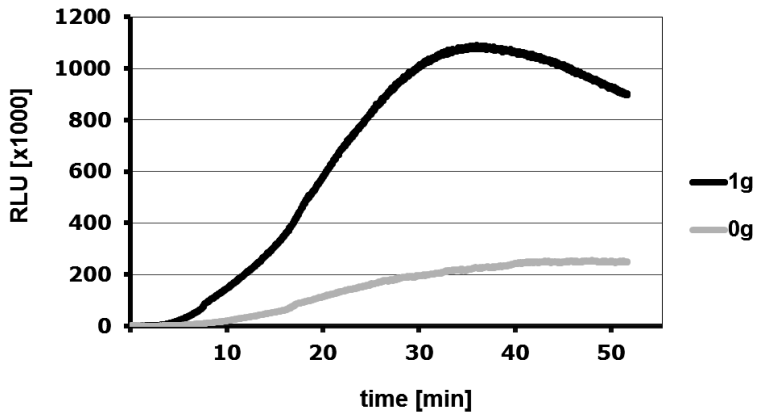

Figure 3.18: **Clinorotation reduces ROS production after LPS stimulation.**
Influence of simulated microgravity (PMT-Clinostat) on the ROS production of the cell line NR8383 after stimulation with 100ng/ml LPS, determined by the oxidation of luminol. Data represents one experiment out of 5 replicates.

Dectin-1 receptor stimulation was achieved with 500µg/ml β 1,4-glucan curdlan. The exposure to simulated microgravity led to a decreased production of oxygen radicals compared to the $1g$ control (fig. 3.19).

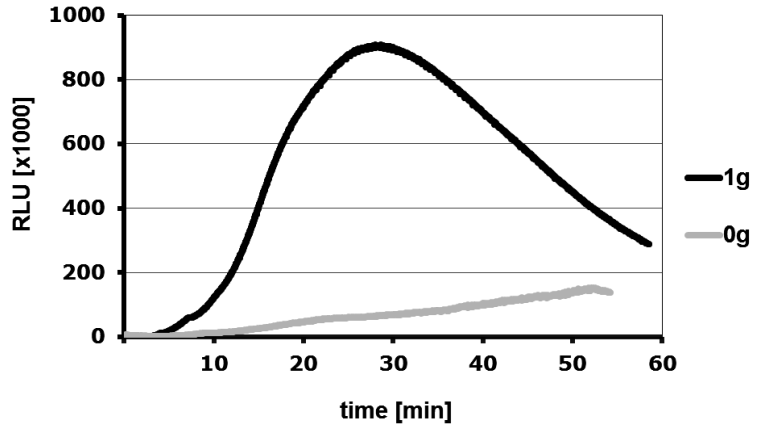

Figure 3.19: **Clinorotation reduces ROS production after curdlan stimulation.**
Influence of simulated microgravity (PMT-Clinostat) on the ROS production of the cell line NR8383 after stimulation with 500µg/ml curdlan, determined by the oxidation of luminol. Data represents one experiment out of 8 replicates.

For a direct comparison between the different stimuli, the area under curve (AUC) and thus the entire ROS amount produced during clinorotation and $1g$ conditions respectively, were calculated. Figure 3.20 shows the AUC of different experiments, stimulating the cells with LPS and curdlan. The amount of oxygen radicals of the oxidative burst during

clinorotation was significantly decreased after stimulation with LPS ($p \leq 0.001$) and curdlan ($p \leq 0.001$) compared to the $1g$ reference.

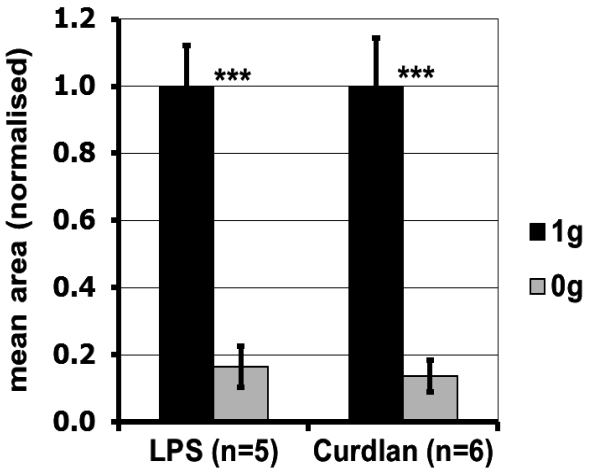

Figure 3.20: **Clinorotation reduces ROS production after stimulation of different cell surface receptors.**
Influence of simulated microgravity (PMT-Clinostat) on the entire ROS production (=area under curve) after stimulation with LPS (100ng/ml) and curdlan (500µg/ml), determined by the oxidation of luminol. Normalised data shown with standard deviation. Significance was estimated with either student's t-test or Mann-Whitney-U test (* $p<0.05$, ** $p<0.01$, ***$p<0.001$).

3.5 Syk phosphorylation under altered gravity conditions

3.5.1 Investigation of the necessity of Syk phosphorylation in ROS production in the NR8383 cell line

The stimulation with different pathogenic substances of the cell line NR8383 in simulated microgravity led to a decreased ROS production. However, all distinct activated pathways upon stimulation with different substances have different signalling steps in common. Here, the role of the spleen tyrosine kinase Syk was under investigation. Syk is an important keyplayer for phagocytosis, actin reorganisation and ROS production. Since the changes in ROS production under altered gravity are very fast, the phosphorylation status of Syk was under investigation. First, the inhibition of Syk was tested by adding piceatannol to characterise the role of Syk in the cell line NR8383. Secondly, the phosphorylation status was examined with Western blot analysis after 15 minutes of clinorotation in the Pipette-Clinostat. Figure 3.21 shows the normal ROS production upon stimulation with different stimuli and after the addition of the Syk inhibitor piceatannol. 100µM piceatannol inhibited the ROS production after zymosan, opsonised zymosan and curdlan more to 80% after inhibited, compared to normal radical production during oxidative burst.

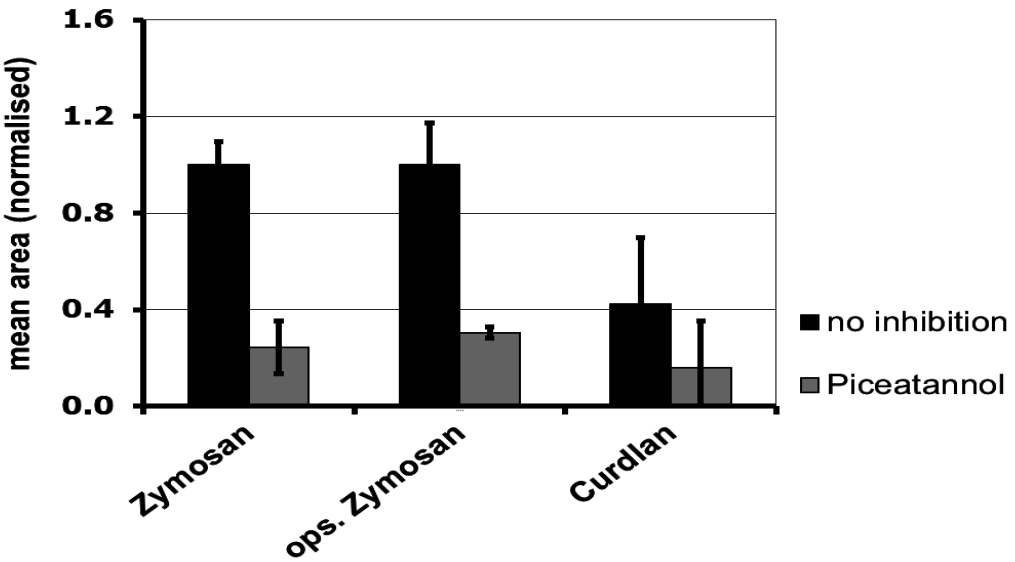

Figure 3.21: **Inhibition of ROS production by piceatannol.**
Mean ROS production of NR8383 cell line after stimulation with different stimuli and inhibition of Syk kinase by addition of 100µM piceatannol. Data were normalised. Error bars indicate standard deviation. At least 3 replicates were carried out.

3.5.2 The phosphorylation of the Syk kinase is significantly reduced in simulated microgravity

Since the macrophages of the cell line NR8383 show a high sensitivity to the inhibition of Syk due to their capability of producing ROS, the phosphorylation status of Syk was evaluated after exposure to simulated microgravity. This was done to examine the role of the Syk kinase in this signalling process. Figure 3.22 A shows the Western blot of clinorotated NR8383 cells. Lysates of non-stimulated cells did not contain phosphorylated Syk protein. Zymosan and opsonised zymosan stimulated cells showed a reliable amount of phosphorylated Syk. After exposure to clinorotation of 15 minutes, the amount of phosphorylated Syk protein was diminished (see fig. 3.22 A). β-actin was used as a loading control for each sample. All bands were normalised to the normal Syk phosphorylation after zymosan stimulation at $1g$ and normalised to the loading control actin. The results are visualised in figure 3.22 B. The difference between $1g$ and simulated microgravity ($0g$) upon zymosan and opsonised zymosan was statistically significant with p=0.024 and p=0.049.

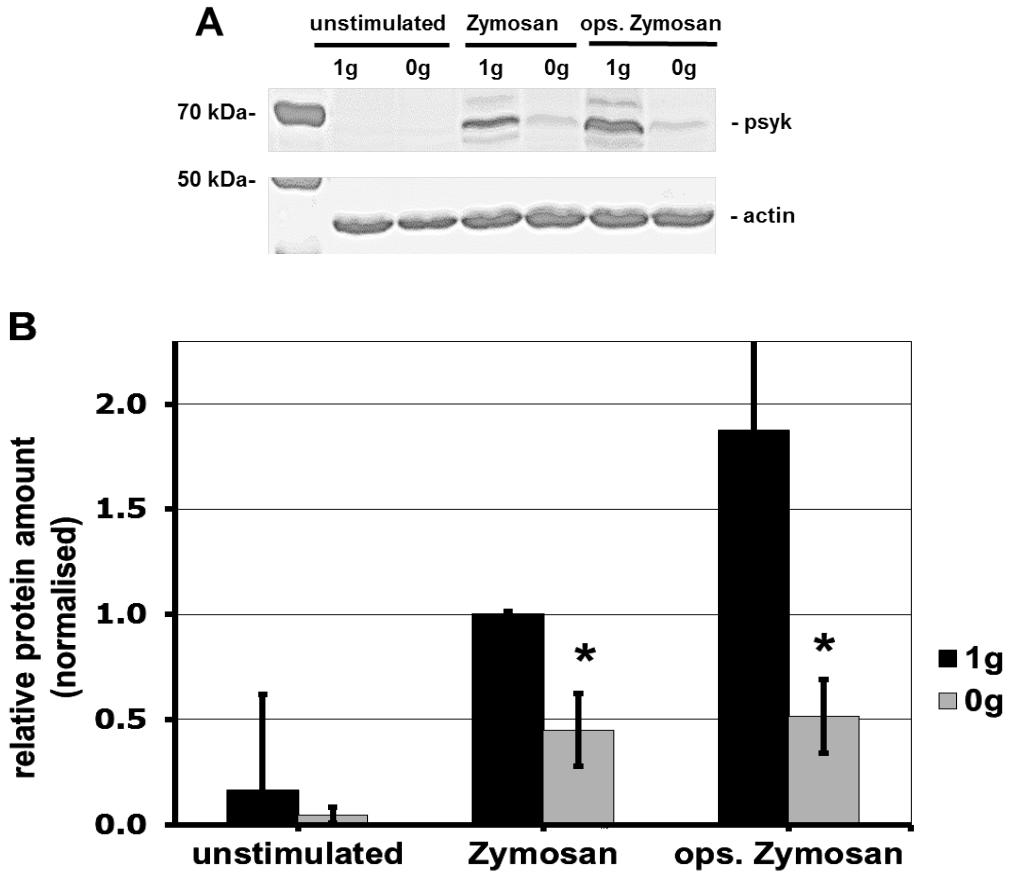

Figure 3.22: **Reduced phosphorylation of Syk in simulated microgravity.**
A: Western blot analysis of phosphorylated Syk protein in NR8383 cells stimulated with 100µg/ml zymosan and opsonised zymosan, respectively, in simulated microgravity and $1g$ controls for 15min.
B: 5 individual experiments were quantified using ImageJ gel analysis software. Mean values of protein amount was determined by normalising means to $1g$ control and loading control bands (β-actin). Error bars indicate standard deviation. Significance was estimated with student's t-test (* $p<0.05$).

3.5.3 Hypergravity does not have a significant influence on Syk phosphorylation

The effects of hypergravity on the ROS production were shown in section 3.1.2. Hypergravity did result in an increased ROS production during zymosan and opsonised zymosan stimulation of NR8383 at $3g$ acceleration. The impact of this acceleration was studied on the Syk phosphorylation. Figure 3.23 demonstrates the effect of hypergravity on the Syk phosphorylation after stimulation with opsonised zymosan. No significant difference was detected between $1g$ and the hypergravity sample ($p=0.182$).

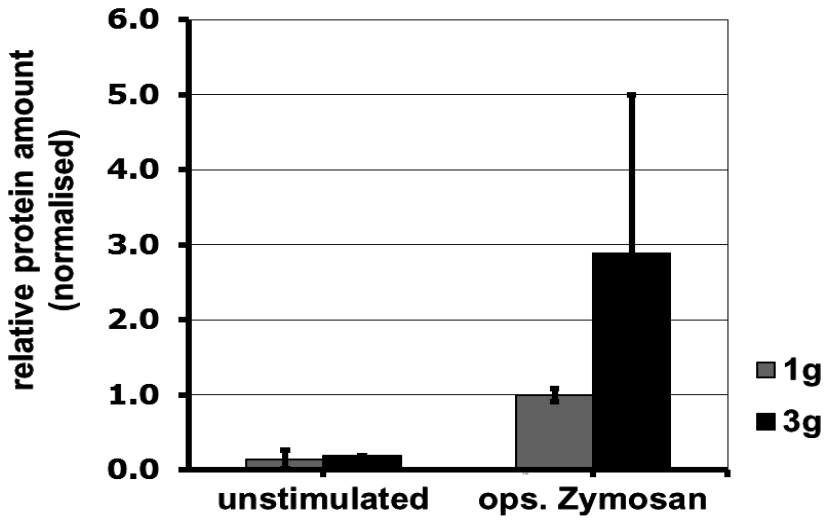

Figure 3.23: **Phosphorylation of Syk in hypergravity (3g).**
Western blot analysis, quantified with ImageJ gel analysis software, of phosphorylated Syk protein in NR8383 cells stimulated with 100µg/ml opsonised zymosan in hypergravity (3g) and 1g controls for 15 min. 6 individual experiments were carried out and analysed. Mean values of protein amount was determined by normalising means to 1g controls and loading control bands (β-actin). Error bars indicate standard deviation. Significance was estimated with student's t-test.

3.6 NF-κB activation remains normal in simulated microgravity conditions

Since fast processes like ROS production and Syk phosphorylation are disturbed and other signalling pathways (TLR4 and Dectin-1) are also impaired by microgravity, a signalling step downstream of Syk, the activation of NF-κB might also be influenced by altered gravity and was therefore under investigation.

NF-κB activation is crucial for macrophage because it is a transcription factor leading to the production of pro-inflammatory chemokine and cytokine production. NF-κB activation requires accomplished upstream signalling e.g. phagocytosis. The protein NF-κB becomes activated in the cytosol, translocates to the nucleus and activates transcription by binding to the specific DNA regions. This protein-DNA interaction was assessed *via* an Electrophoretic Mobility Shift assay (EMSA). EMSA technique is based on the principle that DNA-protein complexes run more slowly on a denaturation polyacrylamide gel, compared to free oligonucleotides. 32P labelled NF-κB recognising oligonucleotides were added to the nuclear extract and run on a non-denaturing gel. The stimulation of cell surface receptors was done by adding opsonised zymosan particles during 4 hours of clinorotation on the Pipette-Clinostat. Figure 3.24 shows the radiographic EMSA gel with the 32P la-

belled NF-kB sequences. The DNA:NF-κB complexes are the first band. The residual free DNA runs further on the gel and shows the EMSA typical pattern. Non-stimulated cells were used as a control and did not show a NF-κB band, whereas zymosan stimulated cells do. There is no visible change in the NF-κB activation due to simulated microgravity.

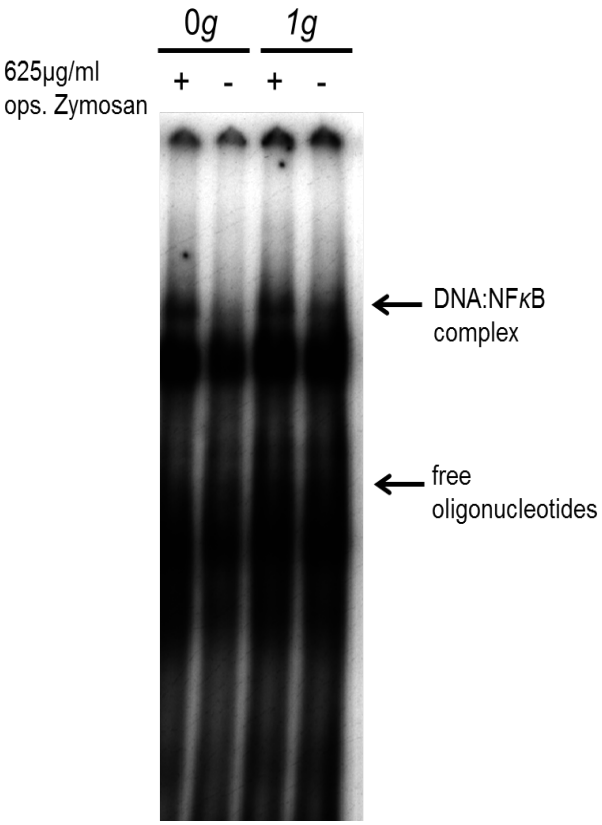

Figure 3.24: **Radiographic EMSA dried gel, labelled with NF-kB recognition sequence.** NR8383 cells were stimulated with opsonised zymosan and exposed to clinorotation for 4 hours. Nuclear lysates were incubated with 32P labelled NF-kB recognition sequences and unravelled upon its mass. Free oligonucelotides run faster compared to NF-κB:DNA complexes. The gel represents one out of 4 individual experiments.

4 Discussion

It is well known that the conditions of spaceflight influence the health of astronauts and the consequences on the innate immune systems are still under investigation. The aim of this study was to further examine the influence of gravity on the functioning, as well as signalling, of macrophages. The ROS production as a measurable indicator for the cell activity was used to ascertain the influence of real and simulated microgravity as well as hypergravity. Here it was shown that both conditions (micro- and hypergravity) have an impact on the ROS production. Further experiments focussd on the underlying mechanism.

The phagocytosis of zymosan particles was monitored to evaluate if the observed changes in ROS production are a side effect of altered phagocytosis or a direct effect on signalling The latter was postulated as phagocytosis in microgravity was nearly unchanged, but the ROS production was diminished. To demonstrate an impaired signalling, Syk phosphorylation and NF-$\varkappa$B activation were examined. Syk phosphorylation, which is required for ROS production in macrophages, is highly impaired by simulated microgravity, indicating this signalling step as a gravisensitive process and a potential reason of disturbed ROS production in microgravity. As NF-$\varkappa$B was not affected by simulated microgravity, it indicates that fast processes are impaired, rather than long-term signalling.

The work presented here can be divided into three major parts: ROS production, phagocytosis and signalling. Each of the parts will be discussed in respect to the effects of microgravity and hypergravity. In the later sections of this discussion, parts of the results from the beginning will be reincorporated, and discussed in a more depth.

The discussion begins with the characterisation of the ROS production under altered gravity conditions.

4.1 Oxidative burst as a gravisensitive process in macrophages

Earlier studies have shown (Horn 2011; Hughes & Long 2001; Huber 2007), that ROS production is a gravity sensitive process. Here, the ROS capacity under altered gravity conditions was further elucidated using the stimulus zymosan, which is a yeast cell wall component recognised by CR1/3, TLR 2/6 and Dectin 1 receptors. However, I wanted to further narrow down the signalling pathways, which are involved in the oxidative burst, to

get insight on the underlying mechanism. Thus, experiments under simulated microgravity, hypergravity and real microgravity were conducted to characterise the response to altered gravity.

4.1.1 The impact of microgravity on the ROS production

Clinorotation in the PMT-Clinostat showed significantly reduced ROS production after zymosan stimulation (see fig. 3.1), which is fully in line with the observations of Horn (2011) and Huber (2007), using opsonised zymosan as a stimulus. Stimulation with non-opsonised zymosan resulted here in significantly decreased ROS production. This however, was less powerful compared to the data gained with opsonised zymosan (Horn 2011), indicating that opsonification seems to make a difference in gravisensivity.

Hughes & Long (2001) have investigated the impact of Wall-Vessel rotation, which is used as a microgravity simulation (Schwarz et al. 1992), on the oxidative burst of promyelocytic (HL-60), indicating that this simulation technique also reduces the ROS production. Studies on monocytes and neutrophils of spaceflown astronauts reveal a high susceptibility to microgravity: Kaur et al. (2008) demonstrated that neutrophils from spaceflown astronauts have a depleted oxidative burst when challenged with LPS, a TLR 4 agonist. Furthermore, the interleukin production of monocytes was changed in astronauts, indicating the high impact of spaceflight on monocyte signalling (Kaur et al. 2004). Taken together, the results of this study on the radical production in microgravity are in line with data from ground-based studies and spaceflown samples of other investigators, identifying the oxidative burst as a fast responding, gravity-sensitive process in pathogen defence of macrophages.

4.1.2 The impact of hypergravity on the ROS production

The stimulation with non-opsonised zymosan particles under hypergravity conditions on the centrifuge, was used to monitor the ROS production under hypergravity. The gained data (see fig. 3.4) exhibit an increase in ROS production at $3g$ acceleration. Interestingly, compared to the pilot study of Horn (2011), the non-opsonised zymosan particles here used, which are recognised by cell surface receptor CR1/3, TLR2/6 and Dectin-1, did not show an increased ROS production at $1.8g$. Seemingly, the threshold of response to increased gravity is above $1.8g$. This might be due to the activation of different signalling pathways: opsonised zymosan is recognised by four distinct pattern recognition receptors (Fcγ, CR1/3, TLR2/6 and Dectin-1), whereas normal zymosan is only recognised by CR1/3, TLR2/6

and Dectin-1. So it can be assumed therefore, that the increased number of involved surface receptors lead to an increased susceptibility to hypergravity.

The luminol-assay used is relatively unspecific because it detects intracellular and extracellular ROS species. The intracellular production of superoxide was measured and proved that the finding of the luminol-assay since the amount of superoxide was significantly increased at $3g$. Therefore, the data gained with the luminol-assay are reliable and it can be excluded that it detects only extracellular radicals which are of a non-phagocytotic origin, e.g oxidative stress. Macrophages produce reactive oxygen species in terms of oxidative stress (Babior 2000; Finkel 2003) a process which can be detected by the luminol-assay used here as well. However, this study also shows that the increase in ROS production is not caused by stress. All controls performed without a stimulating substances leading to the release of oxygen radicals, did not show any changes due to the gravitational conditions. Nevertheless, a little stress response was visible during the non-phagocytosis PBS control on the parabolic flight, where each of the second $1.8g$ phase of each parabola showed a small increase in ROS production (see fig. 3.14). This is a clear stress response to the conditions during parabolic flight. The transition between $0g$ and the $1.8g$ phase results in an absolute g-value of $2.8g$ which could be the reason for this stress response. Furthermore, the constant change of acceleration might stress the cells. Above all, each cell batch was freshly thawed prior to the flight, a process which is also a stressor for the cells.

It is already known that among the immune cells, lymphocytes increase their activity (Lorenzi et al. 1986) and proliferation (Tschopp & Cogoli 1983) during hypergravity but the effects on the oxidative burst have not been addressed so far.

The result gained here, along with the results of Tschopp & Cogoli (1983), demonstrate that hypergravity has a stimulating effect on the cells. It can be assumed that this is caused by the forces acting on the cells under hypergravity conditions. Macrophages and other cells are always exposed to shear foces and might need these conditions for normal behaviour. *In vitro*, cells are kept in cell culture flasks, a condition which does not provide any shear forces. Mechanical stimulation of cells is caused by increased forces acting on the cells, which can, in turn, lead to altered signalling due to force transmittance, a phenomenon which will be further discussed in section 4.2.4. In general, the underlying mechanism which lead to the changes in ROS production remain unclear. To further elucidate possible signalling steps, which could display a gravisensivity, the phagocytosis was investigated. This was also required to be able to uncouple the gained results from ROS production studies, since changes in ROS production could be simply caused by changed phagocytosis.

4.2 Effects of altered gravity on phagocytosis

4.2.1 Microgravity

The phagocytosis rate under simulated microgravity is slightly reduced (see fig. 3.15) and this was also shown in the study of Horn (2011) and Huber (2007). In this study, the phagocytosis was monitored by FACS analysis, a technique where the occurrence of phagocytosis was measured but not the amount of phagocytosed particles. Huber (2007) discovered a reduced phagocytosis of opsonised zymosan particles after 30 minutes of clinorotation. Here, the maximal reduction was observed after 60 minutes, using non-opsonised zymosan.

Huber's study also shows that the phagocytosis rate normalises after 180 minutes, which is in line with the data presented here, revealing no significant differences after 120 minutes of phagocytosis during clinorotation compared to $1g$ controls (see fig. 3.15). As described in Horn (2011), the reduced phagocytosis can be a result of the restricted particle availability: during clinorotation, the suspended cells are forced into small circular paths, as well as the zymosan particles which in turn, could lead to the diminished availability to phagocytise zymosan.

4.2.2 Reduced phagocytosis due to morphological changes

Microgravity diminishes the forces acting on a cell and it is well-known that according to these changes, the cytoskeleton is rearranged. This phenomenon is clearly visible when looking at the cells. Eiermann et al. (2013) showed that the morphology of adherent melanoma cells change under simulated microgravity. Figure 4.1 shows, how RAW 264.7 macrophages decrease in size and become more rounded. After approximately 1 hour the cells start to gain in size. This rounding of the cells could be a reason why the macrophages in this study decrease their capability to phagocytose, since cells which round up (e.g. during mitosis) stop phagocytosis and endocytosis (Berlin et al. 1978; Raucher & Sheetz 1999). Furthermore, cell membrane tension is increased when cells are rounded during mitosis (Sheetz & Dai 1996; Raucher & Sheetz 1999), which in turn, could lead to a disturbance in phagocytosis. It can be assumed, that an increased membrane tension requires more energy to take up particles during phagocytosis. The study of Kopp (2011) showed that the cell shape changes in microgravity within the first 60 minutes but readapt afterwards, This maybe also the case in this study, because the cells reduced their phagocytosis between 30-60 minutes significantly, but show only a small reduction at later time points (fig. 4.1).

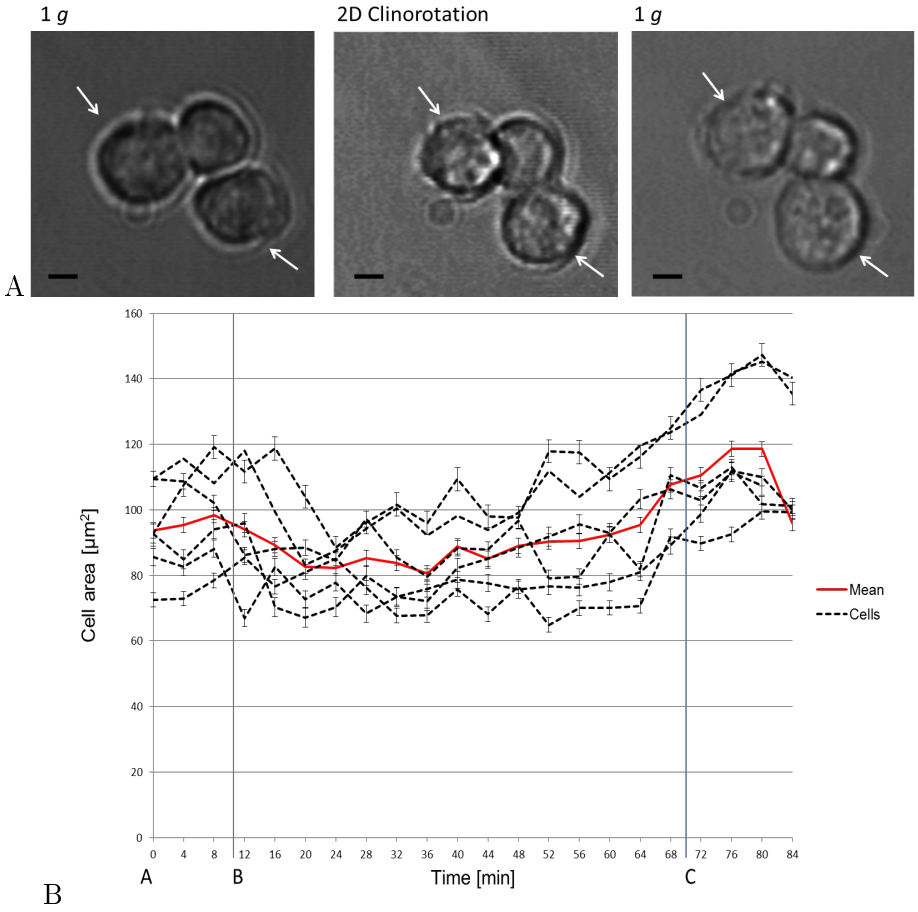

Figure 4.1: **Cell shape during clinorotation.**
A. Shape of RAW264.7 macrophages before during and after clinorotation. White arrows indicate cells with clear changes in cell morphology. Scale bar: 10µm.
B. Area measurement over time: Impact of clinorotation on cell areas. Five cells were measured (black lines) and the mean (red line) was determined. AB: 1 g; BC: clinorotation; C: 1 g. Cell shape during clinorotation. Arrow indicate the changes in morphology. Scale bar: 10µm.
Taken from Kopp (2011) bachelor thesis.

The role of the cytoskeleton in force transmitting due to altered gravity is currently under discussion. The tensegrity model of Ingber (Ingber 1997a,b, 1993) shows that the major mechanotransducer in cells is the cytoskeleton, which transduces forces acting passively or directly on the cells. The tensegrity model decribes the cell under continuos tension, which is required for intact signalling. Cells respond to mechanical changes with the reorganisation of the cytoskeleton. This phenomenon is observed when cells are exposed to microgravity conditions: Crawford-Young (2006); Uva et al. (2002); Schatten et al. (2001); Moes et al. (2007) show that the cytoskeleton, especially the actin cytoskeleton, is initially disturbed and rearranged in microgravity. A functional actin cytoskeleton is required for a successful phagocytosis and an impairment in the cytoskeleton might result in an impaired phagocytosis. It was demonstrated that the cells lose their ability to migrate due to actin-dependent mechanisms which constrains the impact of microgavity to the cytoskeleton (Meloni et al. 2006). However, this study indicates that macrophages are still capable of

phagocytosis, which means the actin filaments are not seriously broken down.

In suspended cells, where the force transmittance is not made *via* the connections between extracellular matrix and actin cytoskeleton *via* integrins, mechanotransduction is not very well understood and still under discussion. Thus, the integrins remain "unstimulated" in simulated microgravity. This lack of force-dependent stimulation on integrins and therefore the cytoskeleton, could lead to a diminished phagocytosis and ROS production. However, the semi-adherent rat macrophages used in this study, are still capable of phagocytosis of zymosan particles. It can, therefore, assumed that the connection of the cytoskeleton to extracellular matrix *via* focal adhesion sites is not indispensable for phagocytosis. Since the cells in this study remain capable of phagocytosing zymosan particles, the observed dimished ROS production is not caused by the slightly and generally reduced phagocytosis during clinorotation. Furthermore, as discussed in section 4.1.2, the alterations in ROS production are very fast and might therefore be a phagocytosis independent phenomenon.

4.2.3 Hypergravity

In contrast to microgravity, hypergravity has an effect on phagocytosis after 15 minutes of hypergravity ($3g$), the macrophages show a significantly increased particle uptake (see fig. 3.16). This strong phagocytosis remains constant over all time points of measurement. Two major reasons could lead to the increased phagocytosis under hypergravity:

1. The increased gravitational force might enhance (passive) particle binding to the cells, accompanied by increased phagocytosis.

2. The mechanical (gravitational) force acting on the cells could have a stimulating effect and thus an active effect on the cells.

Both points will be adressed in the following sections together with a discussion on the effects of microgravity on phagocytosis and ROS production.

4.2.4 Mechanical stimulation of cells

The adherence of a cell to a surface, itself causes tension due to cell membrane and cytoskeleton (Davies 1995) even at normal gravity conditions. Hypergravity might increase this tension due to the increased gravitational force acting on the cells. The non-adherent NR8383 cell line, used here, is pressed to the bottom of the cuvette during exposure to hypergravity which could result in an increased tension within the cell. In general, every

cell *in vivo* is exposed to physical forces, like gravity, which can be a mechanical stressor to a cell. Therefore, cells are highly adapted to forces, since different types of cells are exposed to different extracellular, physical forces. Shear stress is one of the major forces endothelial cells have to cope with, and which can, in turn, modulate the gen-expression of these cells (Chien et al. 1998). The review of Davies (1995) depicts how mechanical forces acting on cells always occur and that the response to forces is an ancient evolutionary mechanism. Furthermore, the hypergravity conditions might reflect the conditions *in vivo*, in terms of a force environment which is required for cell functioning. Leukocytes need shear forces (from blood flow) for rolling and adhesion in the tissue. The most important proteins in this adhesion process are integrins. These transmit forces to the cytoskeleton and modulate the actin cytoskeleton to respond to inflammation, in terms of phagocytosis and oxidative burst (Schymeinsky et al. 2009). Linker proteins, existing between integrins and cytoskeleton, play an important role in adhesion and migration. One of them is the mammalian actin binding protein (mABP1) which connects integrin and actin fibres and is involved in adhesion, phagocytosis and oxidative burst (Schymeinsky et al. 2011, 2009). Here, the increased phagocytosis in macrophages could be a result of force-dependent activation of the cells, modulating the integrin and cytoskeleton connection *via* linker proteins, which in turn lead to an increased phagocytosis and ROS production.

4.2.5 Impact of altered phagocytosis on ROS production

There is, however, a discrepancy between the slightly reduced phagocytosis and the highly impaired oxidative burst of the cells in simulated microgravity: Phagocytosis is not significantly changed after 15 minutes of clinorotation, whereas the impairment of ROS production is visible right at the beginning of the measurement. Seemingly, reduced ROS production is not caused by reduced phagocytosis. In hypergravity, the cells show a higher phagocytotic activity as well as a higher amount of radicals, which leads to the assumption, that this is in relation to each other. Nevertheless, it remains to be elucidated, whether the findings in ROS production arise from changes in phagocytosis or gravisensitive signalling. The work of Horn (2011) supports the idea of gravisensitive signalling, because it has revealed that the gravi-dependent changes in ROS production are very fast. After taking up zymosan particles, ROS production is accomplished in quick steps e.g. protein phosphorylation and NADPH oxidase subunit assembly. These are fast processes compared to particle uptake in terms of phagocytosis, which is a relatively slow process. Hence, it can be assumed that the particle uptake remains normal but the initiated signalling responds rapidly to the lack of gravity.

Furthermore, it is well-known that oxygen radicals serve as second messengers which can, in turn, modulate the involved receptors and signalling steps during phagocytosis and so

may lead to the observed reduction of phagocytosis after 60min of clinorotation (see fig. 3.15).

4.3 Altered gravity influences fast processes like ROS production

To further explore the speed of the responses in ROS production to altered gravity, experiments with different g-profiles were conducted. During the performed parabolic flights in this study, the macrophages responded rapidly to the microgravity phase with a decrease in ROS production (see fig. 3.13). The real parabolic flight and simulated parabolic flight profile, as well as the $1.8g$ studies on the SAHC using non-opsonised zymosan, did not show an increase in radical production (compare fig. 3.13, 3.12 and 3.4). These results are in contrast to the studies of Horn (2011) which showed an increase in the $1.8g$ phases of each parabola upon stimulation of opsonised zymosan (fig. 4.2).

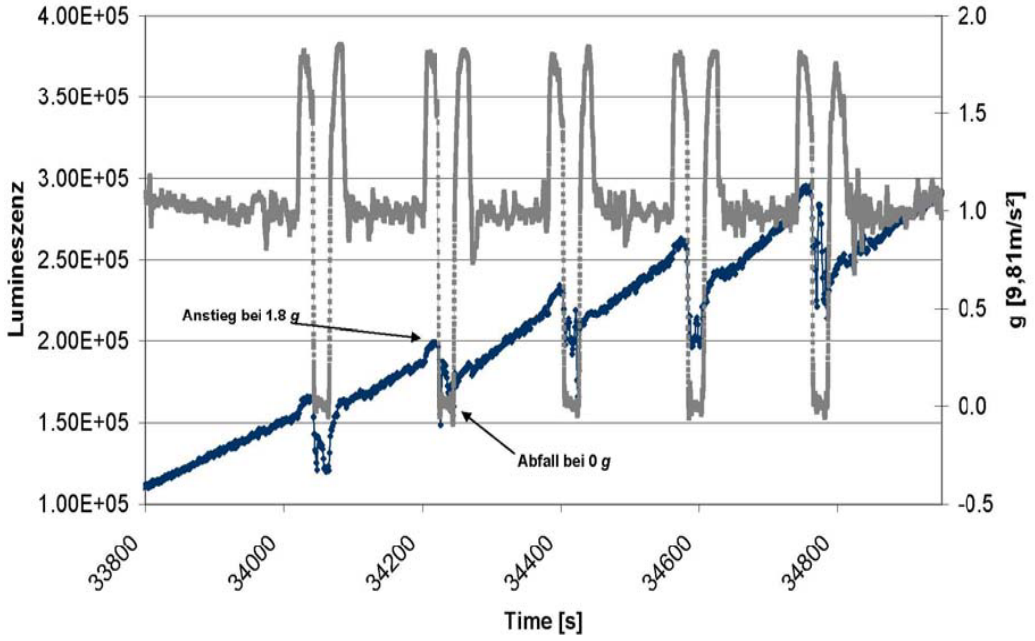

Figure 4.2: **ROS production during parabolic flight after opsonised zymosan stimulation.** ROS production (blue line) after opsonised zymosan stimulation during parabolic flight with g-profile (grey line). In the phase of microgravity, the ROS production is diminished, whereas the first hypergravity phase of each parabola slighly increases the ROS production. Taken from Horn (2011)

The artificial parabolic flight profile on the SAHC showed how quickly the cells respond to altered gravity although the results differed from those of the real parabolic flight. This was probably due to technical issues for it took several seconds to fully stop the centrifuge,

therefore, the transitions between the different g-phases were not as smoothly as during a real parabolic flight. Consequently, it has to be considered that the different phases during a parabolic flight can overlay responses to either hyper- or microgravity. Measuring the g-data and ROS production with the same laptop during the 57^{th} ESA parabolic flight campaign visualised the time-delay between the alterations of these two parameters. Interestingly, it takes approximately 20 seconds until the reactive oxygen species production responds to the changed gravity condition. This delay was not observed after opsonised zymosan stimulation (compare Horn 2011, fig. 4.2) but this could also derive from technical differences between both studies (Astrid Horn, personal communication). However, this time-delay could be a result of different phagocytosis mechanisms of the various zymosan types. Lee et al. (2010) showed that there are differences in respect to time and mechanism between opsonised particles and zymosan particles.

Furthermore, the studies on the SAHC, e.g. stopping the centrifuge, are very important, since they show that the cells respond very quickly to altered gravity conditions and that the oxidative burst continues normally after stopping (see fig. 3.8 and 3.9) the centrifuge. The sudden stop of the centrifuge causes very fast changes in the physical forces and thus mechanical stress on the cells. Resulting intracellular changes might lead to an altered ROS production. A few seconds after the stop of the centrifuge, the cells readapt to the normal $1g$ conditions and continue the ROS production in a normal manner. The alteration in ROS production during a parabolic flight (see Horn 2011, fig. 4.2) emphasises the assumption that the cells respond almost immediately (within seconds) to altered gravity. This is probably based on a cytoskeleton distortion and an altered signalling due to mechanical activation. Taken together, the results clearly show that the ROS response to altered gravity must be a result of very fast signalling processes, rather than phagocytosis.

4.4 Differences in activation of distinct pathways

Macrophages have a huge variety of cell surface receptors to recognise different pathogen patterns (Abbas et al. 2010). The pathogen pattern recognition, followed by phagocytosis, leads to the oxidative burst and the production of reactive oxygen species (fig. 4.3). In this study, different pathogen analogues were used to initiate oxidative burst under altered gravity to distinguish the influence of altered gravity on ROS production.

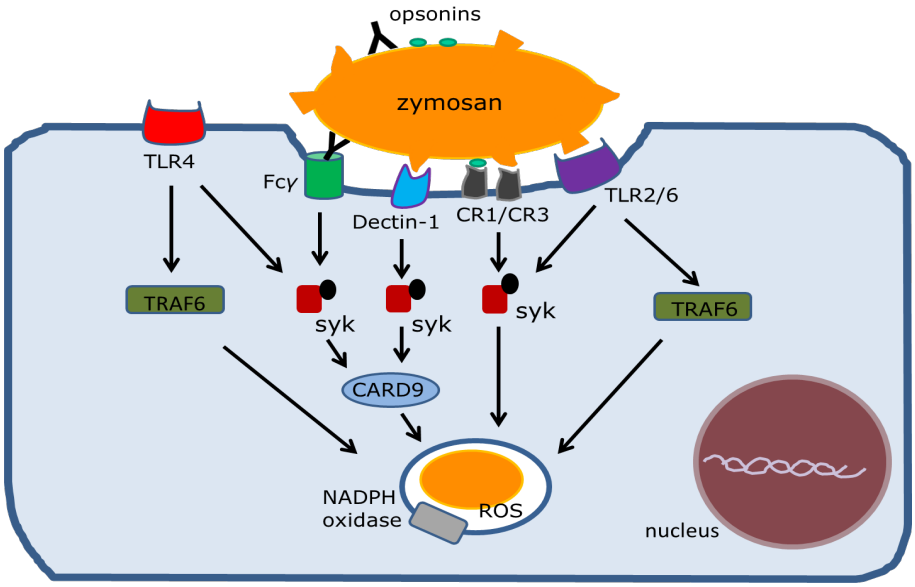

Figure 4.3: **ROS signalling pathway**.
Pattern recognition receptor signalling resulting in the production of ROS. Different cell surface pattern recognition receptors are activated upon opsonised zymosan stimulation. The Fcγ, complement 3, Dectin-1, TLR2/6 and TLR4 receptors require the phosphorylation of Syk for ROS production in the phagosome. In contrast, non-opsonised zymosan is just recognised by partly complement 3 (upon β-glucan), TLR2/6 and Dectin-1.

Horn (2011) has characterised the ROS production under simulated and real microgravity following opsonised zymosan stimulation. This study completes the work of Horn (2011) by reproducing the use of opsonised zymosan in hypergravity and demonstrates an increase in ROS during $1.8g$ and $3g$ (see fig. 3.2). Furthermore, the non-opsonised zymosan was used to narrow down the involved pathways. Zymosan is recognised by CR1/3, TLR 2/6 and Dectin-1 receptors. Opsonification promotes binding of antibodies and complement factors to particles and increases the number of recognition receptors. The Fcγ receptors recognise the Fc fragment of antibodies which have labelled the zymosan particles. Complement factors, which are bound to zymosan are recognised by the integrin receptor CR3/CD18. The use of non-opsonised zymosan showed differences in ROS production during altered gravity compared to the opsonised version. The $1.8g$ hypergravity did not lead to an increase in ROS production which is in contrast to opsonised zymosan (see fig. 3.2). The difference may be due to the number of involved receptors, suggesting that a higher number in activated pathways leads to a higher response, and therefore an increased susceptibility to altered gravity conditions. The more receptors are involved, the more forces that can be transduced into the cell, resulting in an increased response to hypergravity. It can be also stated that a single pathway for example the Fcγ receptor pathway, could be more compromised by hypergravity than other receptors.

The stimulation of single pattern recognition receptors, for example Dectin-1 by β-1,3-glucan curdlan led to a severe impairment of oxidative burst in simulated microgravity. LPS was used to initiate oxidative burst through TLR4 receptor activation and as an

analogon to the TLR2/6 receptor which is activated by zymosan stimulation. Here, both curdlan and LPS stimulation under simulated microgravity reveal a significantly decreased ROS production (see fig. 3.18 and 3.19). It can be concluded, that besides activation of several pathways at once (opsonised and non-opsonised zymosan), single pathways are highly affected by microgravity. Surprisingly, the stimulation of Dectin-1 and a TLR 2/6 receptor at once by zymosan resulted in a less prominently impaired ROS production under simulated microgravity, compared to distinct pathway activation by curdlan and LPS (compare fig 3.1 with 3.20). This effect is similar to that observed when ITAM based PRR (Dectin-1 and Fcγ) dampen TLR receptor responses, e.g. cytokine production (Ivashkiv 2009), and similarily effect ROS production. Cell surface receptors are known for their collaboration with each other, resulting in a synergistic effect. Dectin-1 collaborates with TLR 2 and 4 when stimulated with zymosan and leads to a stronger cytokine and ROS production (Gantner et al. 2003) in murine macrophages as well as human macrophages (Ferwerda et al. 2008). The cross-talks between these receptors are important for the immune response against *C. albicans* infections (Ferwerda et al. 2008). Ortiz-Stern & Rosales (2003) reported that the Fcγ receptor cross-talks bidirectionally with integrins. This interaction between different PRR could be the reason for different susceptability to altered gravity but the impact of cross-talk on ROS production and downstream signalling is not well understood.

Furthermore, the observation of differences in zymosan versus opsonised zymosan speaks in favour of the model by Ingber, since the CR3 integrins are involved here, which are known to be the transmitter between extracellular forces to signalling (Schwartz 2001; Ingber 1991). Here, it is postulated that the strong response of the ROS production to altered gravity after stimulation with opsonised zymosan is due to the connection of the involved cell surface receptors (complement and Fcγ) to integrins, and therefore the adapter molecule between mechanical stress and intracellular signalling.

4.5 Syk phosphorylation is a gravisensitive process

Until recently, the underlying mechanism of the observed changes in ROS production upon stimulation of different cell surface receptors remained to be clarified. To examine if the signalling is impaired by altered gravity, the Syk phosphorylation was analysed. Syk is a common signalling step of pattern recognition receptors Fcγ, CR3/CD18, TLR2/6 and Dectin-1. As shown in figure 4.3, all of the cell surface receptors activate the tyrosine kinase Syk. This could be a keyplayer leading to the altered ROS production observed under microgravity conditions.

Studies with Syk knock-out mice showed the requirement of this kinase for ROS production and underlines the necessity of Syk (Underhill et al. 2005). The importance of Syk in the

ROS signalling of NR8383 macrophages was shown by inhibiting it with piceatannol during ROS measurement (see fig. 3.21). Here, it was also shown that Syk plays an important role during microgravity, since its phosphorylation during clinorotation was impaired (see fig. 3.22). This clearly demonstrates that the impaired phosphorylation of Syk is the reason for diminished ROS production. Syk phosphorylation is required for ROS production and the phosphorylation is strongly impaired upon opsonised and non-opsonised zymosan stimulation.

Under hypergravity conditions the Syk phosphorylation shows a trend towards an increased phosphorylation (see fig. 3.23). From the ROS production data and the phagocytosis activity under hypergravity, it can be assumed that the increased Syk phosphorylation derives from increased phagocytosis, rather than altered signalling. Since hypergravity has an activating effect on macrophages (Tschopp & Cogoli 1983), we can conclude that phagocytosis and Syk phosphorylation, as well as ROS production are increased due to the mechanical loading of the cells. However, other signalling steps are assumed to be the reason for diminished ROS production, occurring downstream of Syk: The NADPH oxidase is a potential candidate to show gravisensivity. The production of ROS is mainly done by the NADPH oxidase complex in the phagosome membrane. The oxidase complex pumps O_2^- radicals into the phagosome lumen to digest engulfed pathogens (Babior 1999; DeLeo et al. 2011; El-Benna et al. 2005). This enzyme consists of 6 subunits which are assembled during phagocytosis. For a successful assembly, phosphoylation of the subunits is required to transfer them into their active form (DeLeo et al. 2011; Nauseef 2004). This assembly is crucial for superoxide production and could be affected by altered gravity, due to impaired phosphorylation steps during assembly. This is in a similar manner to the Syk phosphorylation. Babior, in his review article (1999), discusses the connection between NADPH oxidase subunits with the cytoskeleton, where adherence, an integrin and cytoskeleon based phenomen, modulates superoxide production faster, compared to suspended cells.

Nevertheless, a key step in ROS signalling, the phosphorylation of the Syk kinase, was detected as being highly sensitive to microgravity, and is one of several reasons for diminished ROS production in macrophages. The Syk kinase itself is important for phosphorylation of different effector proteins in pathogen defence. Crescio (2013) showed that the activity of the Syk kinase is increased under "simulated microgravity" (on Random Positioning Machine). This study is in contrast to the results presented here for the impaired phosphorylation of Syk observed here, will most likely result in a decreased kinase activity. In fact, the study of Crescio (2013) concentrated on the RPM as a microgravity simulator, a device which is still under discussion concerning the quality of its microgravity simulation (Herranz et al. 2013). It has to be taken into consideration that different ground-based facilities might produce diverse results and are not always comparable.

Paulsen et al. (2010) demonstrated an increased tyrosine phosphorylation in monocytes during a parabolic flight, whereas a diminished tyrosine phosphorylation was measured in

T lymphocytes. These results are in contrast to those shown here but each model system, or cell type, requires a different methological set-up (Herranz et al. 2013) and may not be in accordance to each other. Further discrepancies may be due to the use of different cell types. Paulsen et al. (2010) reported increased tyrosine phosphorylation in monocytes, which are progenitors of macrophages and occur in the blood stream, whereas macrophages are mostly present in the tissue (Abbas et al. 2010). Differences in responsibilites and localisations of cell types can result in differences concerning tyrosine phosphorylation under microgravity conditions.

In addition, Syk is connected to the cytoskeleton and integrin signalling (Laroux et al. 2005; Mócsai et al. 2002) and neutrophils from Syk-deficient mice display impaired adhesion and migration (Schymeinsky et al. 2006). Syk, therefore, could be a gravisensitive link between force integration to intracellular signalling as found in Ingber's model. Vogel & Sheetz (2006) review how forces are transduced to cytoskeleton associated proteins, when force alters protein folding and functioning. Due to the connection of Syk to the cytoskeleton, it is a candidate for mechanosensation in terms of transducing extracellular forces (or the lack of forces) to the intracellular signalling, in this case ROS production.

The kinase Syk is also able to phosphorylate the IκBα (Takada et al. 2003) subunit to initiate translocation of the transcription factor NF-κB to mediate transcription, leading to the production of TNF and/or interleukins (Tripathi & Aggarwal 2006). It was assumed, therefore, that an impaired Syk phosphorylation could lead to an impaired downstream signalling, e.g. NF-κB activation.

4.6 Long-term effects on signalling- NF-κB translocation

The transcription factor NF-κB is crucial for mediating inflammation in macrophages and other immune cells upon pathogen recognition (fig. 4.4). The expression of chemokines and cytokines is very important for the innate immunity (Abbas et al. 2010; Tripathi & Aggarwal 2006). Since the Syk kinase is less phosphorylated it can be assumed that the downstream target of Syk, NF-κB will also be impaired under microgravity conditions.

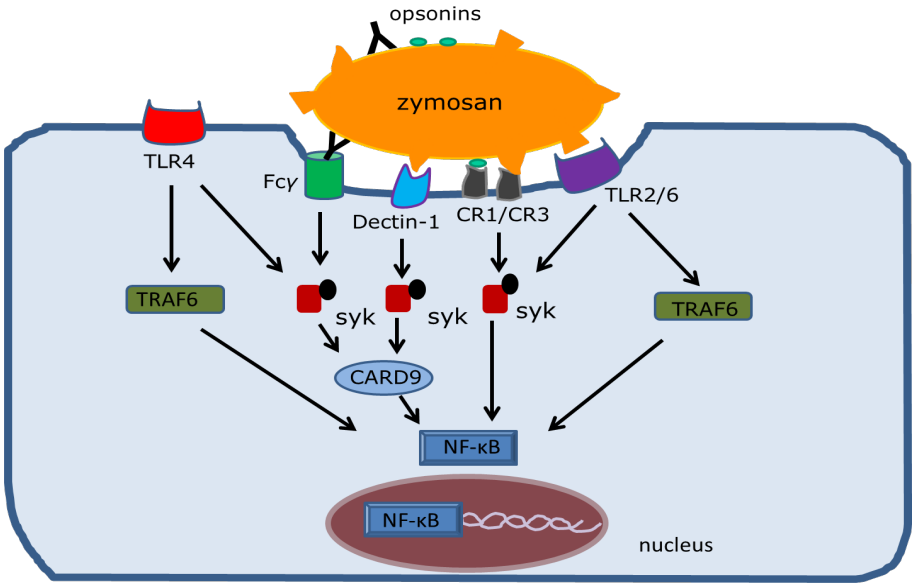

Figure 4.4: **NF-κB signalling pathways**.
Pattern recognition receptor signalling resulting in the activation of the transcription factor NF-κB. Different cell surface pattern recognition receptors are activated upon opsonised zymosan stimulation. The Fcγ, Complement 3, Dectin-1, TLR2/6 and TLR4 receptor stimulation lead to the activation of NF-κB.

In NR8383 cells the translocation of NF-κB to the nucleus remains normal (see fig. 3.24), expecting that the phosphorylation through Syk continues. However, the two molecules are acting at different time points during signalling. Syk phosphorylation is fast and indispensable for ROS production, whereas NF-κB activation and translocation to the nucleus might take longer. The analysis of NF-κB showed that the translocation stays normal up to 4 hours. This result is in contrast to the depleted activation of transcription factors AP-1 and NFAT of T-lymphocytes under simulated microgravity (Morrow 2006). It can be assumed that the ROS production normalises within 4 hours or the amount of ROS is sufficient to activate of NF-κB in a normal manner.

In addition, besides a highly impaired Syk phosphorylation, the Syk kinase seems to be still capable of activating IκBα subunits and therefore, NF-κB translocation. Taken together, ROS production and Syk phosphorylation are required for NF-κB activation and are both impaired under microgravity but the NF-κB translocation remains functional. Therefore, it can be assumed that gravity, or mechanical loading, has an impact on early and fast signalling steps. Adherent cells show disorder in cell shape but are able to adapt to the lack of gravity (Eiermann et al. 2013). It follows that early signalling might be profoundly impaired but later steps may be still functional due to an adaptation process.

Paulsen et al. (2010) demonstrated how T cells and monocytes display impaired signalling during 15 minutes of clinorotation. In T cells, MAP kinase pathway was activated but returned to normal level whereas NF-κB translocation to the nucleus was disturbed. Counter to this, monocytes did not show any of these impairements but an increased ty-rosine phosporylation. Taken together, the data in support of this thesis and other studies show,

that different cell types respond individually to altered gravity and altered signalling in microgravity is not yet well understood.

4.7 Impact of spaceflight on human health

The findings of an intact NF-κB activation, but impaired oxidative burst, may explain why astronauts show a higher susceptibility to infections, but are not seriously affected by diseases in space. So far, astronauts suffer from impaired wound-healing and slight infections, which are not life-threatening. It can be assumed that the lack of gravity has a disturbing influence on integrin signalling, which might in turn be a reason for impaired wound-healing in space, since integrin signalling is crucial for cell adhesion and migration.

The transferability of the result gained *in vitro* to the *in vivo* situation is difficult to estimate. Furthermore, the immune system shows huge individual differences among the astronauts, a fact which has always to be taken into account. Whether the impairment of oxidative burst is a key element in the impaired immune system of astronauts has to be elucidated. The study presented here gives insight into the altered macrophage functioning *in vitro*. However, one has to consider that there are many additional factors *in vivo,* like the hormonal status or external stressors which alter immune functions. This is especially so, since the cultivation of the cell lines in the laboratory differs greatly from the conditions *in vivo*.

Infection of mice during spaceflight and analysis of the ROS production capacity of macrophages of spaceflown mice or astronauts, might help to analyse the effects of altered gravity on the immune system.

4.8 Conclusion and outlook

The work presented here clearly demonstrates that macrophages are highly susceptible to altered gravity conditions and respond very speedily. An early signalling step (Syk phosphorylation) is impaired whereas activation of transcription factor (NF-κB) is not changed. The results show early and fast responding steps to be altered by the lack of gravity. Furthermore, the results point to an adaptation process, because later steps (transcription factor activation) are not altered and suggest that studies on the adaptation processes should be conducted.

Another promising gravisensitive step, besides Syk phosphorylation, could be the enzyme which actually produces superoxide, the NADPH oxidase. An impaired assembly could be another reason for the characteristically impaired ROS production under microgravity conditions.

Syk is involved in all of the pathogen pattern recognition associated signalling pathways adressed here. The use of zymosan does not give insight into the gravisensitivity of single pathways due to its multiple receptor engagement properties. It might be useful to monitor Syk phosphorylation when single receptors are stimulated by using e.g. LPS or curdlan to evaluate their participation in this phenomenon.

The existence of a mechanism for gravity sensing is still unknown, but under discussion today in terms of different models of graviperception. The results gained in this study are in favour of the model postulated by Ingber, but the physiological effects of mechanical forces like gravity on cells are still elusive and remain to be further analysed. Linker proteins between integrins and cytoskeleton are candidates which can be highly susceptible to altered force/gravity conditions. The Syk analysed here is a protein with a connection to integrins (*via* the complement receptor CR3/CD18; Schymeinsky et al. 2006; Mócsai et al. 2002) and the cytoskeleton (Mócsai et al. 2010; Laroux et al. 2005) and shows a sensivity concerning the absence of gravity. The mammalian actin binding protein (mABP1) is a linker protein between integrin and cytoskeleton and is very important for adhesion, as well as oxidative burst (Schymeinsky et al. 2009, 2011). The mABP1 is phosphorylated by the Syk kinase and is able to positively regulate the ROS production. Mice with a mABP1 knockout show higher susceptibility to *Candida albicans* infections but NF-κB activation is not changed (Felix Tolksdorf, personal communication). This protein, therefore, shows similarities to Syk and could also be affected by altered gravity, presenting an interesting subject of investigation for further studies.

Understanding the general force transmittance, and therefore the gravity "sensing", could give further insight into how spaceflight affects human health. Since different types of cells are affected by the lack of gravity, it can be assumed that the mechanism leading to impaired signalling must be something that different cell types have in common. Taken together, the study suggests that the changes in signalling in the cells, is not altered due

to the microgravity environment. It is more likely that they respond to the changes force conditions due to mechanical "stress".

Hence, it can be recommended that further investigations of this integrin-cytoskeleton connection with respect to force transmittance in order to gain further knowledge which can, in turn, be the basic principle for all observed cellular changes during spaceflight.

5 Summary

The recognition of pathogen patterns followed by the production of reactive oxygen species (ROS) during oxidative burst is one of the major functions in macrophages. This process is the first line of defence which is crucial for prevention of pathogen associated diseases. The immune system of astronauts is impaired during spaceflight, resulting in an increased susceptibility to infections. Several studies have shown that the oxidative burst of macrophages is highly impaired after spaceflight, but the underlying mechanism remained to be elucidated. Here, we investigated the characteristics of the reactive oxygen species production during oxidative burst after pathogen pattern recognition in hypergravity (Short-Arm Human Centrifuge) and microgravity (parabolic flight and ground-based Clinostat). Furthermore, the spleen tyrosine kinase Syk phosphorylation, which is required for ROS production, and the translocation of the transcription factor NF-$\varkappa$B to the nucleus were monitored to elucidate the influence of altered gravity on macrophage signalling. Hypergravity reveals an increase, whereas real and simulated microgravity leads to a significantly diminished ROS production upon zymosan recognition. The corresponding phagocytosis rate during altered gravity was only slightly reduced in microgravity, whereas hypergravity increased the phagocytosis drastically. Since the changes in ROS production occur within seconds and uncoupled of phagocytosis, the phosphorylation of Syk was examined, showing a significantly reduced phosphorylation in simulated microgravity. To address later signalling steps, the translocation of NF-$\varkappa$B to the nucleus was measured and remains normal. The results show that the ROS production in macrophages is a highly gravisensitive process which is caused by the diminished Syk phosphorylation. However, besides the impaired ROS production, the NF-$\varkappa$B signalling remains constant under simulated microgravity conditions, showing that early and fast responding steps are affected, whereas long-term signalling continues unaffected, indicating adaptation processes. Hypergravity seems to have an activating and stimulating effect on macrophages due to an increased force environment, indicating that immune cells require certain force conditions to be fully functional. Taken together, the study clearly demonstrates that macrophages display impaired signalling upon pattern recognition, when exposed to reduced gravity conditions, which can be a reason why astronauts display a higher susceptibility to infections.

6 Zusammenfassung

Die Hauptaufgabe von Makrophagen besteht in der Erkennung und Verdauung aufgenommener Pathogene durch die Produktion von reaktiven Sauerstoff Spezies (ROS) innerhalb des oxidativen Burst. Dieser Prozess stellt die erste Immunantwort dar und verhindert den Ausbruch von Erkrankungen durch Bakterien und Viren. Astronauten leiden unter einem beeinträchtigten Immunsystem, welches zu einer erhöhten Anfälligkeit für Erkrankungen im Weltraum führen kann. Einige Studien weisen darauf hin, dass der oxidative Burst von Makrophagen durch Weltraumbedingungen stark beeinträchtigt ist, jedoch ist molekulare Mechanismus noch unbekannt ist. In der vorliegenden Studie wurden die Charakteristika des Pathogen-induzierten oxidativen Bursts unter veränderten Schwerkraftbedingungen, Hypergravitation (humane Kurzarmzentrifuge) und Mikrogravitation (Parabelflug und Klinostat) untersucht. Des Weiteren wurde die Phosphorylierung des für die ROS Produktion wichtigen Proteins Syk und die Aktivierung des Transkriptionsfaktors NF-$\varkappa$B untersucht, um den Einfluss veränderter Schwerkraft auf die Signalwege innerhalb von Makrophagen aufzuklären. Hypergravitation führt zu einer Zunahme, Mikrogravitation zur einer signifikanten Abnahme der radikalen Sauerstoff-Produktion, nach Stimulation durch Zymosan. Die damit verbundene Phagozytose-Rate war in Mikrogravitation leicht reduziert, jedoch in Hypergravitation signifikant erhöht. Die Veränderungen in der ROS Produktion verlaufen sehr schnell (innerhalb von Sekunden), wodurch eine Kopplung mit der Phagozytose ausgeschlossen werden kann. Aufgrund dessen wurde ein schneller Prozess, die Syk Phosphorylierung, untersucht, die eine signifikante Verringerung in simulierter Mikrogravitation zeigte. Ein späterer Schritt innerhalb der Signalkaskade, die Aktivierung des Transkriptionsfaktors NF-$\varkappa$B, zeigte keine Veränderung in simulierter Mikrogravitation. Die Ergebnisse zeigen, dass die ROS Produktion in Makrophagen ein gravisensitiver Prozess ist, bei dem die verringerte Syk Phosphorylierung eine Rolle spielt. Jedoch bleibt die Aktivierung des Transkriptionsfaktors NF-$\varkappa$B erhalten, was darauf hindeutet, dass Gravitation lediglich schnelle und frühe Prozesse beeinflusst, aber keinen Einfluss auf spätere Signalschritte ausübt. Hypergravitation hat einen stimulierenden Effekt auf die Zellen, offensichtlich ausgelöst durch die Erhöhung der Kräfte die auf die Zellen wirken und zeigt, dass Immunzellen nur unter gewissen Kräfteverhältnissen vollständige Funktionalität zeigen. Daraus lässt sich schließen, dass Makrophagen bei der Stimulation mit einem Pathogen-Analogon unter reduzierter Schwerkraft Veränderung in den Signalwegen zeigen, was ein Grund für die Beeinträchtigungen des Immunsystems von Astronauten sein kann.

List of Figures

Bibliography

Abbas, A., Lichtman, A., & Pillai, S. (2010). *Cellular and Molecular Immunology*. Elsevier, 6 edition.

Albrecht-Buehler, G. (1992). The simulation of microgravity conditions on the ground. *ASGSB Bulletin*, 5(2), 3–10.

Alenghat, F. J. & Ingber, D. E. (2002). Mechanotransduction: all signals point to cytoskeleton, matrix, and integrins. *Science Signalling*, 119, 2–6.

Allen, R. (1986). Phagocytic leukocyte oxygenation activities and chemiluminescence: a kinetic approach to analysis. *Methods Enzymology*, 133, 449–493.

Anken, R. & Rahmann, H. (2002). Gravitational zoology: how animals use and cope with gravity. In G. Horneck & C. Baumstark-Khan (Eds.), *Astrobiology* (pp. 315–333). Springer Berlin Heidelberg.

Babior, B. (1999). Nadph-oxidase: an update. *Blood*, 93, 1464–1476.

Babior, B. (2000). Phagocytes and oxidative stress. *The American Journal of Medicine*, 109, 33–44.

Berlin, R. D., Oliver, J. M., & Walter, R. J. (1978). Surface functions during mitosis i: phagocytosis, pinocytosis and mobility of surface-bound cona. *Cell*, 15, 327–341.

Brown, G. D. (2005). Dectin-1: a signalling non-tlr pattern-recognition receptor. *Nature Reviews Immunology*, 6(1), 33–43.

Brown, G. D. & Gordon, S. (2001). Immune recognition: a new receptor for β-glucans. *Nature*, 413, 36–37.

Brown, G. D., Herre, J., Williams, D. L., Willment, J. A., Marshall, A. S. J., & Gordon, S. (2003). Dectin-1 mediates the biological effects of β-glucans. *Journal of Experimental Medicine*, 197(9), 1119–1124.

Buravkova, L. & Romanov, Y. (2001). The role of cytoskeleton in cell changes under conditions of simulated microgravity. *Acta Astronautica*, 48(5-12), 647–650.

Chien, S., Li, S., & Shyy, J. Y.-J. (1998). Effects of mechanical forces on signal transduction and gene expression in endothelial cells. *Hypertension*, 31(1), 162–169.

Clément, G. (2005). *Fundamentals of Space Medicine*. Springer.

Cogoli, A. (1993). The effect of hypogravity and hypergravity on cells of the immune system. *Journal of Leukocyte Biology*, (54), 259–268.

Cox, D., Chang, P., & Kurosaki, T. (1996). Syk tyrosine kinase is required for immunoreceptor tyrosine activation motif-dependent actin assembly. *Journal of Biological Chemistry*, 271(28), 16597–16602.

Crawford-Young, S. J. (2006). Effects of microgravity on cell cytoskeleton and embryogenesis. *The International Journal of Developmental Biology*, 50(2-3), 183–191.

Crescio, C. (2013). *Effects of microgravity and oxidative stress on the human T lymphocytes: different approaches to study their protein expression and post-translational modifications*. PhD thesis, University of Sassari, Sassari.

Crowley, M., Costello, S., Fitzer-Attas, C., Turner, M., Meng, F., Lowell, C., Tybulewicz, V., & DeFranco, A. (1997). A critical role for syk in signal transduction and phagocytosis mediated by fcγ receptors on macrophages. *Journal of Experimental Medicine*, 186, 1027–1039.

Crucian, B., Stowe, R., Quiriarte, H., Pierson, D., & Sams, C. (2011). Monocyte phenotype and cytokine production profiles are dysregulated by short-duration spaceflight. *Aviation, Space, and Environmental Medicine*, 82(9), 857–862.

Crucian, B. E., Stowe, R. P., Pierson, D. L., & Sams, C. F. (2008). Immune system dysregulation following short- vs long-duration spaceflight. *Aviation, Space, and Environmental Medicine*, 79(9), 835–843.

Davies, P. (1995). Flow-mediated endothelial mechanotransduction. *Physiological Reviews*, 75(3), 519–560.

DeLeo, F., Allen, L.-A., Apicella, M., & William, N. (2011). Nadph oxidase activation and assembly during phagocytosis. *Journal of Immunology*, 163, 6732–6740.

Dennehy, K. M., Ferwerda, G., Faro-Trinidade, I., Pyz, E., Willment, J., Taylor, P., Kerrigan, A., Tsoni, S., Gordon, S., Meyer-Wentrup, F., Adema, G. J., Kullberg, B. J., Schweighoffer, E., Tybulewicz, V., Mora-Montes, H.M., Gow, N. A. R., Williams, D. L., Netea, M. G., & Brown, G. D. (2008). Syk kinase is required for collaborative cytokine production induced through dectin-1 and toll-like receptors. *European Journal of Immunology*, (38), 500–506.

Ehlers, M. R. (2000). Cr3: a general purpose adhesion-recognition receptor essential for innate immunity. *Microbes and Infection*, 2, 289–294.

Eiermann, P., Kopp, S., Hauslage, J., Hemmersbach, R., Gerzer, R., & Ivanova, K. (2013). Adaptation of a 2-d clinostat for simulated microgravity experiments with adherent cells. *Microgravity Science and Technology*, 25(3), 153–159.

El-Benna, J., My-Chan, P., Gougerot-Pocidalo, M.-A., & Elbin, C. (2005). Phagocyte nadph oxidase: a multicomponent enzyme essential for host defenses. *Archivum Immunologiae et Therapiae Experimentalis*, 53, 199–206.

Fenchel, T. & Finlay, B. J. (1986). The structure and function of müller vesicles in loxodid ciliates. *Journal of Protozoology*, 33(1), 69–76.

Ferwerda, G., Meyer-Wentrup, F., Kullberg, B.-J., Netea, M. G., & Adema, G. J. (2008). Dectin-1 synergizes with tlr2 and tlr4 for cytokine production in human primary monocytes and macrophages. *Cellular Microbiology*, 10(10), 2058–2066.

Finkel, T. (2003). Oxidant signals and oxidative stress. *Current Opinion in Cell Biology*, 15(2), 247–254.

Finkel, T. & Holbrook, N. J. (2000). Oxidants, oxidative stress and the biology of ageing. *Nature*, 408, 239–247.

Forman, H. J. & Torres, M. (2001). Signaling by the respiratory burst in macrophages. *International Union of Biochemistry and Molecular Biology Life*, 51, 365–371.

Gantner, B. N., Simmons, R. M., Canavera, S. J., Akira, S., & Underhill, D. M. (2003). Collaborative induction of inflammatory responses by dectin-1 and toll-like receptor 2. *Journal of Experimental Medicine*, 197(9), 1107–1117.

Gersuk, G., Underhill, D. M., Zhu, L., & Marr, K. (2006). Dectin-1 and tlrs permit macrophages to distinguish between different aspergillus fumigatus cellular stress. *Journal of Immunology*, 176, 3717–3724.

Gerzer, R., Hemmersbach, R., & Horneck, G. (2006). Life science. In B. Feuerbacher & H. Stoewer (Eds.), *Utilization of Space* (pp. 341–373). Spinger.

Giancotti, F. G. R. E. (1999). Integrin signaling. *Science*, 285(5430), 1028–1033.

Goodridge, H., Simmons, R., & Underhill, D. (2007). Dectin-1 stimulation by candida albicans yeast or zymosan triggers nfat activation in macrophages and dendritic cells. *Journal of Immunology*, 178, 3107–3115.

Gross, O., Gewies, A., Finger, K., Schäfer, M., Sparwasser, T., Peschel, C., Förster, I., & Ruland, J. (2006). Card9 controls a non-tlr signalling pathway for innate anti-fungal immunity. *Nature*, 442(7103), 651–656.

Gueguinou, N., Huin-Schohn, C., Bascove, M., Bueb, J.-L., Tschirhart, E., Legrand-Frossi, C., & Frippiat, J.-P. (2009). Could spaceflight-associated immune system weakening preclude the expansion of human presence beyond earth's orbit? *Journal of Leukocyte Biology*, 86(5), 1027–1038.

Häder, D.-P. (1999). Gravitaxis in unicellular organisms. *Advances in Space Research*, 24(6), 843–850.

Hemmersbach, R., Bromeis, B., Block, I., Bräucker, R., Krause, M., Freiberger, N., Stieber, C., & Wilczek, M. (2001). Paramecium- a model system for studying cellular graviperception. *Advances in Space Research*, 27(5), 893–898.

Herranz, R., Anken, R., Boonstra, J., Braun, M., Christianen, P. C., Geest, M. d., Hauslage, J., Hilbig, R., Hill, R. J., Lebert, M., Medina, F. J., Vagt, N., Ullrich, O., van Loon,

J. J., & Hemmersbach, R. (2013). Ground-based facilities for simulation of microgravity: organism-specific recommendations for their use, and recommended terminology. *Astrobiology*, 13(1), 1–17.

Holland, S. M. (2010). Chronic granulomatous disease. *Clinical Reviews in Allergy & Immunology*, 38(1), 3–10.

Horn, A. (2011). *Vorbereitungen für das Biolab Experiment TRIPLE LUX A Hardwareentwicklung, Kalibrierung und biologische Bodenkontrollen.* PhD thesis, Otto-von-Guericke-Universität, Magdeburg.

Horn, A., Ullrich, O., Huber, K., & Hemmersbach, R. (2011). Pmt (photomultiplier) clinostat. *Microgravity Science and Technology*, 23(1), 67–71.

Huber, K. (2007). *Phagozytose und oxidativer Burst als Biomarker für Immuntoxizität.* PhD thesis, Technischen Universität, München.

Hughes, J. & Long, J. (2001). Simulated microgravity impairs respiratory burst activity in human promyelocytic cells. *In Vitro Cellular & Developmental Biology - Animal*, 37, 209–215.

Iles, K. E. & Forman, H. J. (2002). Macrophage signaling and respiratory burst. *Immunologic Research*, 26(1), 95–105.

Ingber, D. E. (1991). Integrins as mechanochemical transducers. *Current Opinion in Cell Biology*, 3, 841–848.

Ingber, D. E. (1993). Cellular tensegrity: defining new rules of biological design that govern the cytoskeleton. *Journal of Cell Science*, (104), 613–627.

Ingber, D. E. (1997a). Integrins, tensegrity and mechanotransduction. *Gravitational and Space Biology Bulletin*, 10(2), 49–55.

Ingber, D. E. (1997b). Tensegrity: the architectural basis of cellular mechanotransduction. *Annual Review of Physiology*, 59, 575–599.

Ingber, D. E. (1999). How cells (might) sense microgravity. *The FASEB Journal*, 13, 3–15.

Ingber, D. E. (2006). Cellular mechanotransduction: putting all the pieces together again. *The FASEB Journal*, 20(7), 811–827.

Ivashkiv, L. B. (2009). Cross-regulation of signaling by itam-associated receptors. *Nature Immunology*, 10(4), 340–347.

Kaur, I., Simons, E. R., Castro, V. A., Mark Ott, C., & Pierson, D. L. (2004). Changes in neutrophil functions in astronauts. *Brain, Behavior, and Immunity*, 18(5), 443–450.

Kaur, I., Simons, E. R., Kapadia, A. S., Ott, C. M., & Pierson, D. L. (2008). Effect of spaceflight on ability of monocytes to respond to endotoxins of gram-negative bacteria. *Clinical and Vaccine Immunology*, 15(10), 1523–1528.

Kopp, S. (2011). Impact of gravity on the actin filament system of the macrophage cell line raw 264.7. bachelor thesis, university of applied science, bonn-rhein-sieg.

Larbolette, O., Wollscheid, B., Schweikert, J., Nielsen, P. J., & Wienands, J. (1999). Sh3p7 is a cytoskeleton adapter protein and is coupled to signal transduction from lymphocyte antigen receptors. *Molecular and Cellular Biology*, 19(2), 1539–1546.

Laroux, S., Romero, X., Wetzler, L., Engel, P., & Cox, T. (2005). Cutting edge: Myd88 controls phagocyte nadph oxidase function and killing of gram-negative bacteria. *Journal of Immunology*, 175, 5596–5600.

Lee, C.-Y., Herant, M., & Heinrich, V. (2010). Target-specific mechanics of phagocytosis: protrusive neutrophil response to zymosan differs from the uptake of antibody-tagged pathogens. *Journal of Cell Science*, 124, 1106–1114.

Lewis, M. L., Reynolds, J. L., Cubano, L. A., Hatton, J. P., Lawless, B. D., & Piepmeier, E. H. (1998). Spaceflight alters microtubules and increases apoptosis. *The FASEB Journal*, 12, 1007–1018.

Lorenzi, G., Fuchs-Bislin, P., & Cogoli, A. (1986). Effects of hypergravity on 'whole-blood' cultures of human lymphocytes. *Aviation, Space, and Environmental Medicine*, 57(12(1)), 1131–1135.

Majeed, M., Caveggion, E., Lowell, C. A., & Berton, G. (2001). Role of src kinases and syk in fcγ receptor-mediated phagocytosis and phagosome-lysosome fusion. *Journal of Leukocyte Biology*, 70, 801–811.

Martin, K. R. & Barrett, J. C. (2002). Reactive oxygen species as double-edged swords in cellular processes: low-dose cell signaling versus high-dose toxicity. *Human & Experimental Toxicology*, 21(2), 71–75.

Medzhitov, R. (2001). Toll-like receptors and innate immunity. *Nature Reviews Immunology*, 1, 135–145.

Meloni, M. A., Galleri, G., Pippia, P., & Cogoli-Greuter, M. (2006). Cytoskeleton changes and impaired motility of monocytes at modelled low gravity. *Protoplasma*, 229(2-4), 243–249.

Miller, L. (2010). Imagej gel analysis: http://rsb.info.nih.gov/ij/docs/menus/analyze.html#gels.

Mócsai, A., Abram, C. L., Jakus, Z., Hu, Y., Lanier, L. L., & Lowell, C. A. (2006). Integrin signaling in neutrophils and macrophages uses adaptors containing immunoreceptor tyrosine-based activation motifs. *Nature Immunology*, 7(12), 1326–1333.

Mócsai, A., Humphrey, M. B., van Ziffle, J. A., Hu, Y., Burkhardt, A., Spusta, S. C., Majumdar, S., Lanier, L. L., Lowell, C. A., & Nakamura, M. C. (2004). The immunomodulatory adapter proteins dap12 and fc receptor γ chain (fcrγ) regulate development of functional osteoclasts through the syk tyrosine kinase. *Proceedings of the National Academy of Sciences*, 101(16), 6158–6163.

Mócsai, A., Ruland, J., & Tybulewicz, V. L. J. (2010). The syk tyrosine kinase: a crucial player in diverse biological functions. *Nature Reviews Immunology*, 10(6), 387–402.

Mócsai, A., Zhou, M., Meng, F., Tybulewicz, V. L. J., & Lowell, C. A. (2002). Syk is required for integrin signaling in neutrophils. *Immunity*, (16), 547–558.

Moes, M. J. A., Bijvelt, J. J., & Boonstra, J. (2007). Actin dynamics in mouse fibroblasts in microgravity. *Microgravity Science and Technology*, 19, 180–183.

Morrow, M. (2006). Clinorotation differentially inhibits t-lymphocyte transcription factor activation. *In Vitro Cellular & Developmental Biology - Animal*, 42, 153–158.

Nauseef, W. M. (2004). Assembly of the phagocyte nadph oxidase. *Histochemistry and Cell Biology*, 122(4), 277–291.

Nickerson, C. A., Ott, C. M., Wilson, J. W., Ramamurthy, R., & Pierson, D. L. (2004). Microbial responses to microgravity and other low-shear environments. *Microbiology and Molecular Biology Reviews*, 68(2), 345–361.

Ortiz-Stern, A. & Rosales, C. (2003). Cross-talk between fc receptors and integrins. *Immunology Letters*, 90(2-3), 137–143.

Owan, I., Burr, D., Turner C.H., Qui, J., Tu, Y., Onyia, J., & Duncan, R. (1997). Mechanotransduction in bone: osteoblasts are more responsive to fluid shear forces than mechnical strain. *American Journal of Physiology and Cell Physiology*, 273, 810–815.

Papaseit, C., Pochon, N., & Tabony, J. (2000). Microtubule self-organization is gravity-dependent. *Proceedings of the National Academy of Sciences*, 97(15), 8364–8368.

Paulsen, K., Thiel, C., Timm, J., Schmidt, P. M., Huber, K., Tauber, S., Hemmersbach, R., Seibt, D., Kroll, H., Grote, K.-H., Zipp, F., Schneider-Stock, R., Cogoli, A., Hilliger, A., Engelmann, F., & Ullrich, O. (2010). Microgravity-induced alterations in signal transduction in cells of the immune system. *Acta Astronautica*, 67(9-10), 1116–1125.

Raucher, D. & Sheetz, M. (1999). Membrane expansion increases endocytosis rate during mitosis. *Journal of Cell Biology*, 144(3), 497–506.

Ravetch, J. V. (1997). Fc receptors. *Current Opinion in Immunology*, 9, 121–125.

Ross, G. (1989). Complement and complement receptors. *Current Opinion in Immunology*, 2, 50–62.

Sarkar, D., Nagaya, T., Koga, K. N. Y., Gruener, R., & Seo, H. (2000). Culture in vector-averaged gravity under clinostat rotation results in apoptosis of osteoblastic ros 17/2.8 cells. *Journal of Bone and Mineral Research*, 15(3), 489–498.

Schatten, H., Lewis, M. L., & Chakrabarti, A. (2001). Spaceflight and clinorotation cause cytoskeleton and mitochondria changes and increases in apoptosis in cultured cells. *Acta Astronautica*, 49(3-10), 399–418.

Schwartz, M. A. (2001). Integrin signaling revisited. *Trends in Cell Biology*, 11(12), 466–470.

Schwarz, R. P., Goodwin, T. J., & Wolf, D. A. (1992). Cell culture for three-dimensional modeling in rotating-wall vessels: An application of simulated microgravity. *Journal of Tissue Culture Methods*, 14, 51–58.

Schymeinsky, J., Gerstl, R., Mannigel, I., Niedung, K., Frommhold, D., Panthel, K., Heesemann, J., Sixt, M., Quast, T., Kolanus, W., Mocsai, A., Wienands, J., Sperandio, M., & Walzog, B. (2009). A fundamental role of mabp1 in neutrophils: impact on β2 integrin-mediated phagocytosis and adhesion in vivo. *Blood*, 114(19), 4209–4220.

Schymeinsky, J., Sindrilaru, A., Frommhold, D., Sperandio, M., Gerstl, R., Then, C., Mocsai, A., Scharffetter-Kochanek, K., & Walzog, B. (2006). The vav binding site of the non-receptor tyrosine kinase syk at tyr 348 is critical for β2 integrin (cd11/cd18)-mediated neutrophil migration. *Blood*, 108(12), 3919–3927.

Schymeinsky, J., Sperandio, M., & Walzog, B. (2011). The mammalian actin-binding protein 1 (mabp1): a novel molecular player in leukocyte biology. *Trends in Cell Biology*, 21(4), 247–255.

Sciola, L., Cogoli-Greuter, M., Cogoli, A., Spano, A., & Pippia, P. (1999). Influence of microgravity on mitogen binding and cytoskeleton in jurkat cells. *Advances in Space Research*, 24(6), 801–805.

Sheetz, M. P. & Dai, J. (1996). Modulation of membrane dynamics and cell motility by membrane tension. *Trends in Cell Biology*, 6, 85–89.

Shi, Y., Tohyama, Y., Kadono, T., He, J., Miah, S., Hazama, R., Tanaka, C., Tohyama, K., & Yamamura, H. (2006). Protein-tyrosine kinase syk is required for pathogen engulfment in complement-mediated phagocytosis. *Blood*, 107(11), 4554–4562.

Sierra, C., Lascurain, R., Pereyrab, A., Guevarac, J., Martinez, G., Agundis, C., Zenteno, E., & Vazquez, L. (2005). Participation of serum and membrane lectins on the oxidative burst regulation in macrobrachium rosenbergii hemocytes. *Developmental & Comparative Immunology*, 29(2), 113–121.

Smits, G. J., Kapteyn, J. C., van der Ende, H., & Klis, F. M. (1999). Cell wall dynamics in yeast. *Current Opinion in Microbiology*, 2, 348–352.

Stowe, R., Mehta, S., Ferrando, A., & Pierson, D. (2001). Immune responses and latent herpesvirus reactivation in spaceflight. *Aviation, Space, and Environmental Medicine*, 72(10), 884–891.

Sundaresan, A., Risin, D., & Pellis, N. (2002). Loss of signal transduction and inhibition of lymphocyte locomotion in a ground-based model of microgravity. *In Vitro Cellular & Developmental Biology - Animal*, 38(2), 118–122.

Takada, Y., Mukhopadhyay, A., Kundu, G. C., Mahabeleshwar, G. H., Singh, S., & Aggarwal, B. B. (2003). Hydrogen peroxide activates nf-κb through tyrosine phosphorylation of iκbα and serine phosphorylation of p65: evidence for the involvement of iκbα kinase and syk protein-tyrosine kinase. *Journal of Biological Chemistry*, 278(26), 24233–24241.

Tripathi, P. & Aggarwal, A. (2006). Nf-κb transcription factor: a key player in the generation of immune response. *Current Science*, 90(4), 519–531.

Tschopp, A. & Cogoli, A. (1983). Hypergravity promotes cell proliferation. *Experientia*, 39(2), 1323–1438.

Ullrich, O., Bolshakova, O., & Paulsen, K. (2011). Funktion des immunsystems in schwerelosigkeit: Vom astronauten für die erde lernen. *Raumfahrtmedizin*, 18(3), 118–122.

Ullrich, O., Huber, K., & Lang, K. (2008). Signal transduction in cells of the immune system in microgravity. *Cell Communication and Signaling*, 6(9), 1–6.

Underhill, D. M. (2003). Macrophage recognition of zymosan particles. *Journal of Endotoxin Research*, 9(3), 176–180.

Underhill, D. M., Rossnagle, E., Lowell, C. A., & Simmons, R. M. (2005). Dectin-1 activates syk tyrosine kinase in a dynamic subset of macrophages for reactive oxygen production. *Blood*, 106(7), 2543–2550.

Uva, B. M., Masini, M. A., Sturla, M., Prato, P., Passalacqua, M., Giuliani, M., Taggliafierro, G., & Strollo, F. (2002). Clinorotation-induced weightlessness influences the cytoskeleton of glial cells in culture. *Brain Research*, 934, 132–139.

Vassy, J., Portet, S., Beil, M., Millot, G., Fauvel-Lafeve, F., Gasset, G., & Schoevaert, D. (2003). Weightlessness acts on human breast cancer cell line mcf-7. *Advances in Space Research*, 32(8), 1595–1603.

Vogel, V. & Sheetz, M. (2006). Local force and geometry sensing regulate cell functions. *Nature Reviews Molecular Cell Biology*, 7(4), 265–275.

Wise, K., Manna, S., Yamauchi, K., Ramesch, V., Wilson, B., Thomas, R., Sarkar, S., Kulkarni, A., Pellis, N., & Ramesh, G. (2005). Activation of nuclear transcription factor-κb in mouse brain induced by a simulated microgravity environment. *In Vitro Cellular & Developmental Biology - Animal*, 41, 118–123.

Zou, W., Kitaura, H., Reeve, J., Long, F., Tybulewicz, V. L., Shattil, S. J., Ginsberg, M. H., Ross, F. P., & Teitelbaum, S. L. (2007). Syk, c-src, the αvβ 3 integrin, and itam immunoreceptors, in concert, regulate osteoclastic bone resorption. *The Journal of Cell Biology*, 176(6), 877–888.

Internet

wikipedia: http://en.wikipedia.org/wiki/Tensegrity

www.spaceflight.esa.int:

http://www.spaceflight.esa.int/impress/text/education/Microgravity/Producing_Microgravity.html

Abbreviations

α	alpha
µ	micro
A. bidest	aqua bidest
APS	ammonium persulfate
ATP	adenosintriphosphate
AUC	*area under curve* (integral)
β	beta
BCA	bicinchoninic acid assay
BSA	bovine serum albumin
°C	degree Celsius
$CaCl_2$	calcium chloride
CARD9	*caspase-associated recruitment domain 9*
CO_2	carbondioxide
CR1/CR3	*complement receptor* 1/3
CNES	Centre National d´Ètudes Spatiales
Da	Dalton
DAG	diacylglycerol
dIdC	2´-deoxyinosinic-2´-deoxycytidylic acid
DLR	Deutsches Zentrum für Luft- und Raumfahrt (German Aerospace Center)
DMSO	dimethylsulfoxide
DNA	deoxyribonucleic acid
DTT	dithiotreithol
ECL	electrochemiluminescent
EDTA	ethylene diamine tetraacetic acid
e.g.	lat.: exempli gratia (for example)
EGTA	ethylene glycol tetraacetic acid
EMSA	*Electrophoretic Mobility Shift Assay*
ESA	*European Space Agency*
et al.	lat.: et alteres (and other)
EtOH	ethanol
F	Farad
FACS	*fluorescent activated cell sorting*
FCS	*fetal calf serum*
FITC	*fluorescein isothiocyanat*

g	gram
g	gravity ($9.81 m/s^2$)
GDP	*guanosine diphosphate*
GEF	*guanine nucleotide exchange factors*
GFP	*green fluorescent protein*
GTP	*Guanosine-5´-triphosphate*
h	hour
H_3BO_3	boracic acid
HRP	*horseradish peroxidase*
HCl	hydrocloric acid
ICAM	*intercellular adhesion molecule*
Ig	immunoglobulin
IL	interleukin
IMDM	*Iscove's Modified Dulbecco's Medium*
IP_3	inositol-1,4,5-trisphosphat
ITAM	*immunoreceptor tyrosine-based activation motif*
ITIM	*immunoreceptor tyrosine-based inhibition motif*
IκB	inhibitor of κB
ISS	*International Space Station*
k	kilo
κ	kappa
KCl	potassium chloride
KOH	potassium hydroxide
l	litre
LSC	*liquid scintillation counting*
LPS	lipopolysaccharide
m	metre; milli
M	molarity (mol/l)
mABP1	*mammalian actin binding protein 1*
MAP	*mitogen-activated protein*
MeOH	methanol
$MgCl_2$	magnesium dichloride
$MgSO_4$	magnesium sulfate
MHC	*major histocompatibility complex*
min	minute
mol	Mol
MPO	*myeloidperoxidase*
MuSIC	*Multi Sample Incubator Centrifuge*
m/v	mass per volume
n	nano; number n of experiments
$Na_2B_4O_7$ x H_2O	di-sodiumtetraborat-decahydrate

$Na_2 2CO_3$	sodium carbonate
NaCl	sodium chloride
NADPH	*nicotinamide adenine dinucleotide phosphate*
NaOH	sodium hydroxide
NBT	nitrobluetetrazolium chloride
NFAT	*nuclear factor of activated* T cells
NF-$\varkappa$B	*nuclear factor kappa-light-chain-enhancer of activated B cells*
NK	*natural killer*
p	pico
P	phosphate
PAGE	*polyacrylamide gelelectrophoresis*
PAMPs	*pathogen -associated molecular patterns*
PBS	phosphate buffered saline
PFA	paraformaldehyde
pH	negative decimal logarithm of the hydrogen ion activity
PHOX	phagocytic oxidase
PMA	phorbol 12-myristate 13-acetat
PMSF	phenylmethanesulphonylfluoride
PMT	photomultiplier tube
PRR	*pattern recognition receptor*
RLU	*relative light unit*
RNA	ribonucleoid acid
RNAi	RNA-interference
rpm	*revolutions per minute*
RPM	*Random Positioning Machine*
RPMI	*Roswell Park Memorial Institute*
RT	room temperature
s	second
SAHC	*Short-Arm Human Centrifuge*
SDS	*sodium dodecyl sulfate*
siRNA	*small interfering RNA*
SOD	*superoxid dismutase*
TBST	*tris-buffered saline tween-20*
TEMED	tetramethylethyldiamin
TLR	*Toll-like receptor*
TNF	*tumor necrosis factor*
Tris	tris[hydroxymethyl]aminomethan
UV	ultraviolett
V	Volt
VLE	*very low endotoxin*
v/v	volume per volume

WB	Western blot
WT	wild-type
γ	gamma
ZAP-70	*Zeta-chain-associated protein kinase 70*